ALLOSTERIC INTERACTIONS BETWEEN THE TYPE 1 (CB_1) AND TYPE 2 (CB_2) CANNABINOID RECEPTORS MODIFY β-ARRESTIN2 RECRUITMENT

by

Shawn J. Adderley

Submitted in partial fulfilment of the requirements
for the degree of Masters of Science

at

Dalhousie University
Halifax, Nova Scotia
June 2021

DEDICATION

I dedicate this thesis to my Grandparents Fran and Norton: To my Nana and Grandpa. For always taking the time to let me stop and poke in the dirt, collect rocks, and ask questions. I would not be who I am today without your unwavering support towards my curiosities, your boundless stories, and for your unconditional love and support. I am so lucky to be your Grandson.

TABLE OF CONTENTS

LIST OF TABLES

LIST OF FIGURES

ABSTRACT

Type 1 (CB_1) and Type 2 (CB_2) Cannabinoid receptors form heteromers with unique pharmacology compared to CB_1 or CB_2 alone. We wanted to determine if the Tango β-arrestin2 *luc* reporter assay could measure heteromer-dependant allosteric modulation of β-arrestin2 recruitment to CB_1 and CB_2 following non-selective agonism with CP 55,940 and antagonism using AM251 or AM630. We determined that the Tango assay could detect allostery between CB_1 and CB_2, but the sensitivity of this assay depended on the transfection reagent being used. CP 55,940 agonism in cells expressing CB_1 and CB_2 resulted in ~25% less β-arrestin2 recruitment to both CB_1 and CB_2, and these differences were dependant on receptor stoichiometry. Antagonism of CB_1 or CB_2 increased CP 55,940-induced β-arrestin2 recruitment to the heteromer partner. Thus, the CB_1/CB_2 heteromer negatively modulates β-arrestin2 recruitment following non-selective agonism, and positively modulates β-arrestin2 recruitment following antagonism with AM251 or AM630.

LIST OF ABBREVIATIONS USED

2-AG	2-Arachidonoylglycerol
$5HT_{1A}$	Serotonin 1A Receptor
$5HT_{2A}$	Serotonin 2A Receptor
7TM	7 Transmembrane
A_{2A}	Adenosine 2A Receptor
ABS	Absorbance
AC	Adenylyl Cyclase
ACEA	Arachidonyl-2'-chloroethylamide
AD	Alzheimer's Disease
AEA	Anandamide
Akt	PI3K-Akt signaling pathway
ANOVA	Analysis of Variance
AT1R	Angiotensin II Receptor Type 1
BRET	Bioluminescence Resonance Energy Transfer
Btk	Bruton's Tyrosine Kinase
cAMP	Cyclic adenosine monophosphate
CB_1	Type 1 Cannabinoid Receptor
CB_2	Type 2 Cannabinoid Receptor
CBD	Cannabidiol
cDNA	Complementary DNA
CI	Confidence interval
CMV	Cytomegalovirus
CNR1	Human type 1 cannabinoid receptor gene
CNR2	Human type 2 cannabinoid receptor gene
CNS	Central nervous system
CP 55,940	5-(1,1-dimethylheptyl)-2-[(1R,2R,5R)-5-hydroxy-2-(3-hydroxypropyl) cyclohexyl]-phenol
C-terminus	Carboxy-terminus
D_2	Dopamine 2 receptor
D_{2L}	Dopamine 2 long receptor
DAGL	Diacylglycerol lipase
dH2O	De-ionized water
DMEM	Dulbecco's Modified Eagle Medium
DMSO	Dimethyl sulfoxide
DNA	Deoxyribonucleic acid
EC50	Half maximal effective concentration
eCBs	Endocannabinoids

ECS	Endocannabinoid System
EMAX	Maximal effective concentration
EMIN	Minimal effective concentration
ERK 1/2	Extracellularly regulated kinase 1/2
EtOH	Ethanol
FAAH	Fatty-acid amide hydrolase
Fab2	Antigen-binding fragment 2
FBS	Fetal bovine serum
FRET	Fluorescence resonance energy transfer
GABA	Gamma-Aminobutyric acid
GDP	Guanosine diphosphate
GPCR	G-protein coupled receptor
GPR55	G protein-coupled receptor 55
GRK	G protein-coupled receptor kinase
GTP	Guanosine triphosphate
HA	Human influenza hemagglutinin
HD	Huntingon's Disease
HEK	Human embryonic kidney cell
HU308	4-[4-(1,1-Dimethylheptyl)-2,6-dimethoxyphenyl]-6,6-dimethylbicyclo [3.1.1]hept-2-ene-2-methanol
IC50	Half maximal inhibitory concentration
IgG	Imunoglobulin
IL-6	Interleukin 6
iNOS	Inducible nitric oxide
JNK3	c-Jun N-terminal kinase 3
K_i	Inhibitor constant
LacZ	β-galactosidase gene
luc	Luciferase gene
M1	Pro-inflammatory microglia phenotype
MAPK	Mitogen-activated protein kinase
MeOH	Methanol
MAGL	Monoacylglycerol lipase
mRNA	Messenger ribonucleic acid
NAPE-PLD	N-acyl phosphatidylethanolamine-specific phospholipase D
NEAA	Non-essential amino acid
NF-κB	Nuclear factor kappa beta
N-terminus	Amino terminus
pAkt	Phosphorylated Akt
PBS	Phosphate buffered saline
PD	Parkinson's Disease
PDE	Phosphodiesterase

PDL	Poly-d-lysine
PEI	Polyethyleneimine
pERK1/2	Phosphorylated Extracellular signal regulated kinase 1/2
PFA	Paraformaldehyde
PLA	Proximity Ligation Assay
PLC-β	Phospholipase C
RLU	Relative luminescence units
SD	Standard deviation
TBS	Tris-buffered saline
TCS	TEV protease cleavage site
TEV	Tobacco etch virus protease
THC	Delta-9-tetrahydrocannabinol
TNF-α	Tumor necrosis factor alpha
tTA	Tetracycline-controlled transactivator
V2	Vasopressin 2 receptor
β_2-AR	Beta 2 adrenergic receptor
βgal	Beta-galactosidase
ΔOR	Delta opioid receptor
μOR	Mu opioid receptor

ACKNOWLEDGEMENTS

First and foremost, to my supervisors Dr. Eileen Denovan-Wright for her mentorship, constant support, and friendship; and to Dr. Melanie Kelly, for her support and encouragement – thank you both for this opportunity. To Alexander Young for his teamwork, constant help, and companionship. To Dr. Chris Sinal for his technical support; and Nicole McMullen for her constant help and hard work, I truly would not have made it this far without her guidance. Thanks to my advisory committee: Drs. Jason MacDougall and George Robertson, for your knowledge and encouragement. To my friends in the faculty of Pharmacology for your companionship, especially Stefan Heinz-Milne who offered his friendship and his rare passion for statistics - your help was significant. I am particularly thankful for my family. I cannot express how fortunate I feel to be surrounded by such loving and supportive people - I love and appreciate you all more than you know. Finally, thank you to my partner Dominique, for being my sounding board, my confidante, and for her unwavering love and confidence in me. I would also like to acknowledge Dalhousie University, and The Natural Sciences and Engineering Research Council of Canada (NSERC) for their financial support, without which I could not have completed this degree.

CHAPTER 1: INTRODUCTION

1.1 G-Protein Coupled Receptors

G-Protein Coupled Receptors (GPCR) are a superfamily of plasma-membrane bound proteins named for their interactions with heterotrimeric guanine triphosphate (GTP)-binding proteins (G-proteins). There are 6 Classes of GPCR that are differentiated by structure and function: 1) Class A - rhodopsin-like receptors, 2) Class B -secretin family receptors, 3) Class C- metabotropic glutamate receptors, 4) Class D - fungal mating pheromone receptors, 5) Class E – cyclic adenosine monophosphate (cAMP) receptors, and 6) Class F-frizzled and smoothened receptors (Lee *et al.*, 2018). Of these six Classes, the Class A GPCRs represent the largest and most diverse group (Pierce *et al.* 2002). GPCRs are key targets for pharmacotherapy in the mammalian body due in part to their widespread distribution, vital roles in cellular and physiological function, and extracellular ligand binding region (Hopkins and Groom 2002; Sriram and Insel 2018).

Class A GPCRs have a common structure composed of seven plasma membrane-embedded α-helical transmembrane domains (7TM), three outer membrane loops, three inner membrane loops, an extracellular amino terminus (N-terminus), and an intracellular carboxy terminus (C-terminus). The 7TM domain forms a ligand binding pocket. Ligand binding transduces extracellular stimuli (neurotransmitters; hormones; chemo-attractants; odorants; and exogenous biological or synthetic compounds) into interactions with intracellular proteins including heterotrimeric G-proteins (composed of Gα and Gβγ subunits), β-arrestins, and kinases (Gilman 1987; Iiri *et al.* 1998; Gurevich and Gurevich 2019).

1.1.1 GPCR Signaling

Agonist binding to GPCRs initiates a conformational change involving outward movement of transmembrane regions V and VI. This conformation favors an active receptor state and opens the GPCR to interact with other intracellular proteins to facilitate signal transduction (Farrens *et al.* 1996). In this form, GPCRs act as guanine nucleotide exchange factors for their cognate G-protein partners (Sorkin and Zastrow 2002) and exchange guanine diphosphate (GDP) for guanine triphosphate (GTP) on the Gα subunit of the G-protein. Of note, agonist binding is not always necessary to cause receptor activation, and constitutively active GPCR are not uncommon (Seifert and Wenzel-Seifert 2002)

GPCR are so-named for their interaction with G-protein partners. G-proteins are heterotrimeric signal transduction proteins, composed of Gα and Gβγ subunits, which are divided into four families with distinct signaling patterns. G-proteins are classified by the actions of the Gα subunit: Gαs, Gαi, Gαq, and Gα12 (Wettschureck and Offermanns 2005; Syrovatkina *et al.* 2016; Liu *et al.* 2019) (Fig. 1.1). Gαs are stimulatory G-proteins and Gαi are inhibitory; their activation stimulates or inhibits adenylyl cyclase (AC), respectively, which in turn promotes or inhibits the conversion of intracellular adenosine triphosphate into cAMP (Masters *et al.* 1989; Taussig *et al.* 1993). $G\alpha_q$ dissociation leads to activation of Phospholipase C-*β* (PLC-*β*) (Harden *et al.* 2011), and the $G\alpha_{12}$ subunit interacts with a variety of proteins such as Btk-family of tyrosine kinases (Suzuki *et al.* 2009). GPCR activation results in the dissociation of the heterotrimer from the active GPCR (Fig. 1.1). Once freed, the free Gβγ complex separates from the Gα subunit and interacts with G-protein coupled receptor kinases (GRKs) to act as an independent

signalling molecule (Eishingdrelo and Kongsamut 2013; Syrovatkina *et al.* 2016). Specifically, Gβγ guides GRKs to the plasma membrane to phosphorylate the C-terminal tail of the active GPCR, priming the receptor for desensitization and internalization by β-arrestin molecules (Haga and Haga 1992; Gurevich and Gurevich 2019).

β-arrestin molecules are the primary proteins responsible for stopping G-protein-dependant signaling cascades (Gurevich and Gurevich 2019). There are four types of arrestin molecules, two are expressed exclusively in the rods and cones of the eye and are known as visual arrestins, and the remaining two, β-arrestin1 and β-arrestin2, are ubiquitously expressed (Noor *et al.* 2011). GRKs act as the signaling molecule to initiate β-arrestin mobilization to the C-terminal of the GPCR. β-arrestin competes with G-proteins for intracellular binding to guide the GPCR into clathrin-coated pits destined for internalisation. Their binding creates a steric hinderance for new G-protein binding and prevents new G-protein binding and signal transduction (Lefkowitz and Whalen 2004). In addition, arrestins recruit enzymes such as phosphodiesterase (PDE) which degrade any remaining second messengers created by G-protein signalling (Perry *et al.* 2002). Both β-arrestin1 and 2 interact with Class A GPCR to regulate signaling and internalization (Kohout *et al.* 2001; Pierce and Lefkowitz 2001) (Fig. 1.1). Recent research has revealed that GRKs can phosphorylate the C-terminal tails of GPCR in different ways, and the specific pattern of GRK-dependant phosphorylation affects the way in which β-arrestin1/2 interacts with the GPCR (Yang *et al.* 2017). In addition to receptor desensitization and internalization, β-arrestin1/2 act as G-protein-independent signal transducers. For example, chemical inhibition of the clathrin-mediated endocytosis of chemokine receptors leads to a reduction in phosphorylation and signaling

through the extracellular regulated kinase (ERK 1/2) pathway (García Lopez *et al.* 2009). Likewise, β-arrestin1/2-mediated GPCR endocytosis has been linked to activation of the c-Jun N-terminal Kinase3 (JNK3) and Tyrosine kinases, the PI3-Akt pathway, and the regulation of transcription factors such as NF-κB (Luttrell *et al.* 1997; Ahn *et al.* 2004; Lefkowitz and Shenoy 2005) (Fig. 1.1).

The balance of G-protein dependant and independent signaling is heavily influenced by ligand type, and the presence of different proteins (Ferré and Franco 2010; Seyedabadi *et al.* 2019). Testing the effect of different drugs which target the same receptor has led researchers to better understand the relative ligand-dependant signaling profiles. Moreover, these unique signaling profiles may lead to different physiological significance, and may be exploited to create or choose certain drugs which minimize undesirable side effects (Wisler *et al.* 2018). For example, it has been proposed that creating μ-opioid receptor agonists which cause preferential signaling through G-proteins and away from β-arrestins, may allow for analgesic actions while reducing harmful side effects such as respiratory depression and drug tolerance (Mafi *et al.* 2020). In a similar way, GPCRs can form complexes with other receptors of the same, or different types to modulate their pharmacology. The coupling of two receptors of the same type is called a homomer, while the coupling of two distinct GPCR types is called a heteromer (Ferré and Franco 2010).

1.1.2 Class A GCPR Heteromers

Class A GPCR can interact with one another to form receptor complexes called homomers, or heteromers. Heteromers may be composed of two individual receptors (monomers) or of two homomers, making a higher-order oligomer (Franco *et al.* 2016).

A heteromer is a protein complex made up of at least two receptor partners (protomers) which may exhibit allosteric interactions to display unique biochemical properties relative to the protomers alone (Gomes *et al.* 2016a). While Class C GPCR, such as the $GABA_B$ receptor, have long been known to act as obligate heteromers (White *et al.* 1998), Class A heteromerization is considered a dynamic state which is influenced by the cellular and chemical environment (Franco *et al.* 2016; Gomes *et al.* 2016b).

The phenomenon of receptor-receptor allostery in Class A GPCR was first proposed in 1983 but was not linked to the occurrence of heteromers for over a decade through co-immuno-precipitation and western blotting experiments with opioid receptors (Fuxe *et al.* 1983; Jordan and Devi 1999; Gomes *et al.* 2000). The advent of biophysical methods to detect heteromers such as fluorescence (FRET) and bioluminescence resonance energy transfer (BRET) have since led to significant breakthroughs in the field of heteromer research. This technology relies on the transient expression of fluorescent and luminescent protein-linked receptors which emit a fluorescent signal when the receptors are in complex (El Khamlichi *et al.*, 2019). While heterologous detection of heteromers adds the benefit of control, research into heterologous expression systems may not correspond to patterns observed *in vivo*, and advancements in immunofluorescence methods such as *in situ* proximity ligation assay (PLA) now allow for identification of heteromers in native tissues (Trifilieff *et al.* 2011). By combining transient transfection in heterologous systems, and antibody-based detection of heteromers *in vivo,* researchers can first determine the conditions and effects of specific heteromer formation, regions where they are likely to form, and better understand their biological significance (Fuxe *et al.* 1983; Ayoub and Pfleger 2010; Gomes *et al.* 2016b).

Heteromer formation affects nearly every aspect of GPCR function including biosynthesis, trafficking, ligand binding, signal transduction, arrestin recruitment and receptor internalization (Jordan and Devi 1999; Margeta-Mitrovic *et al.* 2000; Rozenfeld and Devi 2007; Franco *et al.* 2016; Gomes *et al.* 2016b; Liu *et al.* 2016; Bagher *et al.* 2017). These allosteric protein-protein interactions can lead to preferential signaling through one receptor partner, or the adoption of an entirely new signaling pathway (Fig. 1.2). Heteromer-dependant signaling paradigms have been linked to interactions with different G-protein partners and changes in β-arrestin-dependant interactions (Fig. 1.3) (White *et al.* 1998; Lavoie *et al.* 2002; Albizu *et al.* 2010; Bagher 2017; Gao *et al.* 2018). Heteromer signaling is complex, and agonism of one, or both receptors in complex may yield very different outcomes (Vischer *et al.* 2011). On the other hand, antagonism of one protomer of the heteromer may block (cross antagonism) or potentiate the activation of the partner receptor (Fig. 1.2/1.3) (Parenty *et al.* 2008; Haack and McCarty 2011; Bagher *et al.* 2017; Gao *et al.* 2018).

The discovery of heteromers in neuronal and non-neuronal cells important to central nervous system (CNS) pathology - including psychosis, Parkinson's Disease, Alzheimer's Disease, and Huntington's Disease – has led researchers to better understand their biological significance (Canals *et al.* 2003; Bagher *et al.* 2017; Borroto-Escuela *et al.* 2017; Gaitonde and González-Maeso 2017; Navarro *et al.* 2018a). Further research is still needed to determine instances where GPCR heteromers are beneficial or deleterious, and if they represent viable therapeutic targets.

1.2 The Endocannabinoid System

The Endocannabinoid system (ECS) is ubiquitously expressed peripherally and centrally in the mammalian body (Marzo *et al.* 2004). The physiological and neurochemical effects of the ECS occur primarily through the actions of the cannabinoid 1 (CB_1) and cannabinoid 2 (CB_2) receptors via the endogenous ligands, endocannabinoids (eCBs) N-arachidonoylethanolamide (Anandamide or AEA) and 2-arachidonoylglycerol (2-AG) (Devane *et al.* 1992; Sugiura *et al.* 1995; Stella *et al.* 1997), and the enzymes that synthesize and degrade these ligands**.** The ECS plays vital roles in major biological process including memory, learning, motor activity, emesis, nociception, and immune function (Barrie and Manolios, 2017; Kruk-Slomka *et al.*, 2017; Pandey *et al.*, 2009; Sharkey *et al.*, 2014; El Manira & Kyriakatos, 2010). Endocannabinoid signaling and alterations in receptor expression have been implicated in the pathology of neurodegenerative illnesses such as Alzheimer's and Huntington's Disease, which has prompted research into the ECS as a potential therapeutic target for CNS disorders (Di Marzo 2008; Bari *et al.* 2013; Navarro *et al.* 2016; Kendall and Yudowski 2017; Schurman and Lichtman 2017).

1.2.1 Signaling via the Endocannabinoid System

CB_1 and CB_2 receptors are Class A GPCRs that share 44% overall amino acid identity (Munro *et al.* 1993). The amino acid identity between CB_1 and CB_2 increases to 68% within the transmembrane helices that include the hydrophobic ligand binding pocket (Lutz 2002; McAllister *et al.* 2003; Hua *et al.* 2017; Li *et al.* 2019). CB_1 and CB_2 both couple and signal through Gαi leading to the inhibition of AC and prevention of cAMP accumulation (Howlett 2002; Pertwee *et al.* 2010; Castillo *et al.* 2012).

Cannabinoid receptors undergo rapid desensitization and internalization following agonist binding, which is primarily mediated by the actions of β-arrestin2 (Jin *et al.* 1999; van der Lee *et al.* 2009; Chen *et al.* 2014).

ECS signaling is unique compared to most receptor-neurotransmitter signalling systems. While most classical neurotransmitters and neuropeptides remain stored in vesicles until release following depolarization, AEA and 2-AG are synthesized "on-demand" by the enzymes *N*-acyl phosphatidylethanolamine-phospholipase D (NAPE-PLD) and diacylglycerol lipase (DAGL), respectively. More specifically, depolarization of post-synaptic axons results in an increase in intracellular [Ca^{2+}], prompting the synthesis of endocannabinoids from plasma membrane-bound lipid precursors (Fig. 1.4) (Fonseca *et al.* 2013). Release of endocannabinoids results primarily in retrograde neurotransmission, diffusing across the synaptic cleft to target pre-synaptic cannabinoid receptors (Cadas *et al.* 1996; Stella *et al.* 1997; Howlett 2002; Di Marzo 2006). Endocannabinoids are highly lipophilic, allowing them to enter the lipophilic ligand binding pocket of cannabinoid receptors which is embedded within the plasma membrane region (Howlett 2002; Pertwee *et al.* 2010; Castillo *et al.* 2012; Fowler 2013; Hua *et al.* 2016; Hua *et al.* 2017; Li *et al.* 2019). Upon binding to cannabinoid receptors, both endocannabinoids have been reported to display different properties. Generally speaking, AEA is a partial agonist of cannabinoid receptors with higher affinity for CB_1 (K_i≈89nM) relative to CB_2 (Ki≈371nM), while 2-AG is a full agonist with roughly equal affinity for both CB_1 (K_i≈58.3nM) and CB_2 (K_i≈145nM) at both receptors (Pertwee *et al.* 2010; Pertwee 2015). While these general statements are commonly noted, it is important to remember that these characteristics are relative to the ligands they are being compared to,

as well as the signaling parameters being tested (Ibsen *et al.* 2017). AEA and 2-AG signaling is, in part, regulated by enzymatic degradation through fatty-acid amide hydrolase (FAAH) and monoacylglycerol lipase (MAGL), respectively (Cravatt *et al.* 1996; Dinh *et al.* 2002; Bari *et al.* 2006). In addition to endocannabinoids, CB_1 and CB_2 are activated by other groups of natural (phytocannabinoids) and synthetic cannabinoid ligands. Early research into the phytocannabinoid Δ^9-Tetrohydracannabinol (THC) derived from the plant *Cannabis sativa* was integral to the discovery of the ECS (Matsuda *et al.* 1990). THC is a partial agonist for CB_1 (K_i≈40.7 nM) and CB_2 (≈36.4 nM) receptors (Pertwee 1999; Howlett 2002; Pertwee 2005; Pertwee *et al.* 2010; Paronis *et al.* 2012). The synthetic non-selective agonist CP 55,940 has become the predominate reference ligand in cannabinoid research due to its maximal efficacy at both CB_1 (K_i≈0.58 nM) and CB_2 (K_i≈0.69 nM) receptors (Showalter *et al.* 1996; Pertwee 2006; Pertwee *et al.* 2010). On the other hand, synthetic ligands such as ACEA and HU308 act as potent and selective agonists for CB_1 (K_i>1400-fold CB_1>CB_2) and CB_2 (K_i>500-fold CB_2>CB_1), respectively (Pertwee 1999; Hanuš *et al.* 1999; Hillard *et al.* 1999). Inverse agonists such as AM251 and AM630 which are selective for CB_1 (K_i≈7.49 nM; 306-fold selectivity CB_1>CB_2) and CB_2 (K_i≈31.2 nM; 165-fold selectivity CB_2>CB_1), respectively, allow researchers to further isolate specific actions of CB_1 and CB_2 in endogenous and heterologous expression systems (Pertwee *et al.* 1995; Ross *et al.* 1999; de Oliveira Alvares *et al.* 2006; Murphy and Le Foll 2020).

1.2.2 CB_1 and CB_2 Distribution and Actions in the CNS

CB_1 is the most abundant receptor in the CNS with high densities in the hippocampus, cerebellum, cortex, and basal ganglia (Herkenham *et al.* 1991; Glass *et al.* 1997; Mato *et al.* 2003). CB_2 is expressed in the CNS at lower levels relative to CB_1, but CB_2 mRNA and protein immunoreactivity has been isolated in the brainstem, globus pallidus, cortex, striatum, hippocampus, amygdala, brainstem, cerebellum and ventral tegmental area (VTA) (Van Sickle 2005; Viscomi *et al.* 2009; García-Gutiérrez *et al.* 2012; Navarrete *et al.* 2012; Stempel *et al.* 2016; Chen *et al.* 2017). In neurons, CB_1 and CB_2 receptors are expressed on both pre- and postsynaptic neurons, although CB_1 is commonly located presynaptically, whereas CB_2 is more common on post-synaptic neurons. (Szabo *et al.* 2002; Lovinger 2008; Sierra *et al.* 2015; Albayram *et al.* 2016; Sánchez-Zavaleta *et al.* 2018). CB_1 and CB_2 receptor activation in neurons has been linked to the modulation of glutamatergic, GABAergic, dopaminergic, cholinergic, noradrenergic, and serotonergic neurotransmission (Wallmichrath and Szabo 2002; Tzavara *et al.* 2003; Lau and Schloss 2008; Hoffman *et al.* 2010; Kirilly *et al.* 2013). In non-neuronal cells of the CNS, CB_1 and CB_2 expression in microglia function to regulate the brains innate immune system (Mecha *et al.* 2016). Agonism of CB_1 and CB_2 in microglia may dampen the chronic pro-inflammatory response to neurological insult by inhibiting the production of inducible nitric oxide (iNOS) and pro-inflammatory cytokines such as TNF-α and IL-6 (Waksman *et al.* 1999; Ramírez *et al.* 2005; Navarro *et al.* 2018a).

Changes in cannabinoid receptor mRNA and protein expression have been measured during neurological disease and targeting cannabinoid receptors during certain neuropathological states may infer therapeutic benefit (Blázquez *et al.*, 2011; Facchinetti

et al., 2003; Fernández-Ruiz *et al.*, 2011; Palazuelos *et al.*, 2009; Ramírez *et al.*, 2005; Tanveer *et al.*, 2012; Van Laere *et al.*, 2012). In Huntington's disease (HD), neuronal loss of CB_1 receptor mRNA and protein expression in the basal ganglia is considered an early hallmark of disease pathology, occurring before symptomatic onset (Denovan-Wright and Robertson 2000; Blázquez *et al.* 2011). Selective agonism of CB_1 receptors in a cell culture model of HD lead to a significant upregulation in CB_1 mRNA expression, and improved cell viability (Laprairie *et al.* 2013). In Alzheimer's disease (AD), chronic pro-inflammatory activation (M1) of microglia leads to neuronal deterioration (Ramírez *et al.* 2005). Microglia express cannabinoid receptors, and CB_2 mRNA and protein expression are upregulated in pro-inflammatory microglia (M1) (Komorowska-Müller and Schmöle 2020). Treating M1 microglia with cannabinoids can decrease iNOS and pro-inflammatory cytokine release and dampen chronic M1 microglial phenotype generation (Waksman *et al.* 1999; Ramírez *et al.* 2005; Mecha *et al.* 2016; Navarro *et al.* 2018a).

1.2.3 Cannabinoid Receptor/Class A GPCR Heteromers

CB_1 and CB_2 receptors can form heteromers when expressed with other Class A GPCR. To date, CB_1 is known to form heteromers in the CNS with β_2-AR (Hudson *et al.* 2010); AT1R (Rozenfeld *et al.* 2011); A_{2A} (Carriba *et al.* 2007; Navarro *et al.* 2008; Moreno *et al.* 2018); D_2 (Navarro *et al.* 2008; Przybyla and Watts 2010); D_{2L} (Kearn 2005; Bagher *et al.* 2016; Bagher *et al.* 2017); δOR (Bushlin *et al.* 2012; Sierra *et al.* 2019); μOR (Rodríguez *et al.* 2001; Hojo *et al.* 2008; Rios *et al.* 2009); GPR55 (Kargl *et al.* 2012; Martínez-Pinilla *et al.* 2014); Orexin1 (Ellis *et al.* 2006; Ward *et al.* 2011); SSTR5 (Zou *et al.* 2017); and $5HT_{2A}$ (Viñals *et al.* 2015). While fewer studies have been published concerning CB_2 heteromerization, there is evidence of CB_2 forming heteromers

in vivo with other Class A GPCR including GPR55 (Balenga *et al.* 2014) and $5HT_{1A}$ (Franco *et al.* 2019).

Heteromerization of both the CB_1 and CB_2 receptors with other Class A GPCR has been implicated in diverse and complex signaling paradigms. Within the CB_1/D_{2L} heteromer, for example, agonism of either CB_1 or D_2 leads to signaling through canonical inhibitory Gαi proteins (Krishna Kumar *et al.* 2019; Yin *et al.* 2020). However, agonising both CB_1 and D_2 simultaneously results in a G-protein switch to signal through stimulatory Gαs partners (Glass and Felder 1997; Bagher *et al.* 2017). The use of selective blocking peptides, which inhibit the association of CB_1 and D_2, reverts either protomer back to their canonical Gαi signaling (Bagher *et al.* 2017). In addition, co-agonism of CB_1 and D_{2L} resulted in increased β-arrestin translocation to the heteromer complex - leading to increased rates of dimer internalization relative to either receptor alone (Bagher *et al.* 2017). Conversely, selective antagonism of either receptor was able to decrease arrestin mobilization to the partner receptor and reduce heteromer internalization (Bagher *et al.* 2016; Bagher *et al.* 2017).

1.2.4 CB_1 and CB_2 Co-Expression & Heteromerization

CB_1 and CB_2 are co-expressed in the central nervous system, and form heteromers in neurons of the pineal gland (Callén *et al.* 2012), basal ganglia (Sierra *et al.* 2015), and activated striatal microglia (Navarro *et al.* 2018a). CB_1/CB_2 heteromer formation is a dynamic process influenced by pathological state, cell type, and drug treatment. For example, in microglia there is a significant increase in CB_1/CB_2 heteromer immunofluorescence in M1 cells, relative to their resting state (Navarro *et al.* 2018a). Increases in CBr heteromer formation are likewise observed in striatal sections from 6-hydroxydopamine lesioned rats in a rodent model of Parkinson's disease (PD), which

appear to further increase with the onset of dyskinesia following levodopa treatment (Navarro *et al.* 2018a). Interestingly, these results are reversed in pallado-thalamic projection neurons where chronic levodopa and Benserazide treatment in 6-hydroxydopamine lesioned macaques resulted in significant decreases in CB_1/CB_2 heteromer-dependant immunofluorescence (Sierra *et al.* 2015). Moreover, evidence of heteromer-dependant signaling has been noted (Callén *et al.* 2012; Navarro *et al.* 2018a). For instance, non-selective agonism of CB_1 and CB_2 in heteromer-positive cells was shown to reduce signaling in cAMP and pERK1/2 pathways compared to selective agonism of either receptor alone (Callén *et al.* 2012; Navarro *et al.* 2018a). Interestingly, in M1 microglia, co-activation of CB_1 and CB_2 lead to increases in cAMP and pERK1/2 activity, indicating that this interaction may depend on the cell state, or relative expression of CB_1/CB_2 (Navarro *et al.* 2018a). On the other hand, antagonism of CB_2 with the selective inverse agonist AM630 was shown to inhibit CB_1-dependant activation of pERK1/2 in globus pallidus slices (Callén *et al.* 2012). Similarly, in resting and M1 microglia, antagonising either CB_1 or CB_2 leads to cross antagonism of the partner receptor in cAMP and pERK1/2 pathways (Navarro *et al.* 2018a). Biophysical methods such as bioluminescence resonance energy transfer (BRET) have likewise detected CB_1/CB_2 heteromer formation in transiently transfected cells (Navarro *et al.* 2008; Callén *et al.* 2012). While there are inherent limitations to the use of heterologous expression systems to interpret biological significance, the added benefit of experimental control in profiling heteromer behaviour and signaling should not be overlooked. Non-selective agonism of CB_1 and CB_2 in SH-SY5Y neuroblastoma cells endogenously expressing CB_1 and transiently transfected with CB_2 leads to a significant decrease in Akt

phosphorylation in a similar manner to resting microglia (Callén *et al.* 2012; Navarro *et al.* 2018a). CB_1- or CB_2-dependant Akt phosphorylation in SH-SY5Y can also be inhibited through cross antagonism of the partner receptor. CB_1/CB_2 heteromer dependant reductions in Akt activity in SH-SY5Y were mirrored by reductions in neurite outgrowth, where selective agonism of either receptor induced a modest increase in neurite outgrowth (Callén *et al.* 2012). To date, two studies from the Navarro group have sought to quantify arrestin recruitment to the CB_1/CB_2 heteromer following treatment with a variety of phytocannabinoids including THC and cannabidiol (CBD) (Navarro *et al.* 2018b; Navarro *et al.* 2020). These studies were more focused on differences in signaling bias between ligands in cells expressing CB_1 or CB_2, or CB_1 and CB_2, and did not address effects of full agonism, or selective antagonism on arrestin recruitment to the heteromer. Furthermore, these studies only tested differences in arrestin recruitment to CB_2 following co-expression with CB_1 and did not publish data outlining the inverse relationship. In brief, the CB_1/CB_2 heteromer has been observed in both heterologous and endogenous expression systems, and there is evidence of unique pharmacology indicating protein-protein allostery. However, there has been no published data measuring arrestin recruitment following non-selective agonism in cells co-expressing CB_1 and CB_2, nor do we know how selective antagonism effects arrestin recruitment to the CB_1/CB_2 heteromer.

1.3 Research Objectives

CB_1 and CB_2 receptor heteromers have been detected in neurons of the rat pineal gland (Callén *et al.* 2012), basal ganglia (Sierra *et al.* 2015), and activated striatal microglia (Navarro *et al.* 2018a). While there is evidence of protein-protein allostery between CB_1 and CB_2 when co-expressed, heteromer-dependant changes in arrestin translocation following co-agonism and selective antagonism have not been quantified. We hypothesized that co-transfection of CB_1 and CB_2 would alter β-arrestin2 recruitment to CB_1 and CB_2 following non-selective agonism, relative to cells transfected either receptor alone. Furthermore, we hypothesized that co-transfected cells would exhibit patterns of cross antagonism. To test these hypotheses, we have 5 main objectives.

Objectives

1) Validate the use of the Tango β-arrestin2 recruitment assay to study CB_1/CB_2 heteromer interactions.
2) Detect co-localization of CB_1 and CB_2 through Immunostaining in transiently transfected cells.
3) Compare the effect of non-selective CP 55,940 agonism on β-Arrestin2 recruitment in cells transfected with CB_1 or CB_2 alone, relative to cells co-transfected with both receptors.
4) Measure the effect of receptor stoichiometry on heteromer-dependant changes in CP 55,940-induced β-Arrestin2 recruitment.
5) Measure the effect of selective antagonism on CP 55,940-dependant β-Arrestin2 recruitment in cells transfected with CB_1 or CB_2 and cells co-transfected with both receptors.

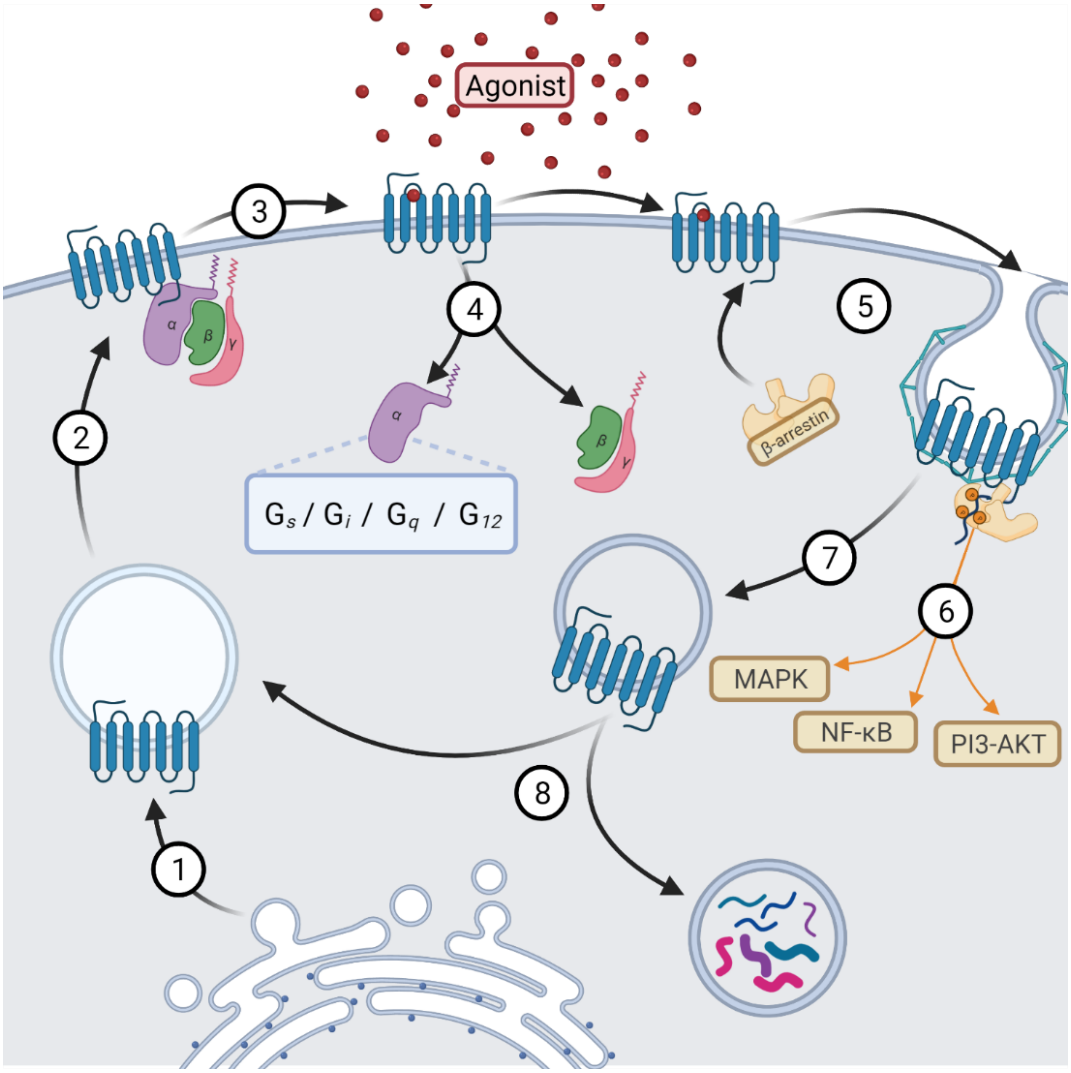

Figure 1.1. The Lifecyle of a GPCR

(1) Receptor buds in vesicle from endoplasmic reticulum (ER) following synthesis from ribosomes; **(2)** Vesicular transport of GPCR to the plasma membrane; **(3)** GPCR binds agonist, leading to conformational change and receptor activation; **(4)** Following activation, Gα and Gβγ dissociate from the receptor and signal based on Gα subtype and Gβγ activity ; **(5)** β-arrestin is recruited to the receptor, initiating endocytosis via clathrin-coated pits; **(6)** β-arrestin may lead to G-protein independent signaling cascades including mitogen activated protein kinase *(*MAPK*)* or JNK3 activation, and effects on nuclear factor activity; **(7)** GPCR becomes fully enveloped in intracellular vesicle following endocytosis β-arrestin dissociates from the receptor; **(8)** GPCR may be recycled to the plasma membrane, or endosome becomes lysosome and the receptor is degraded.

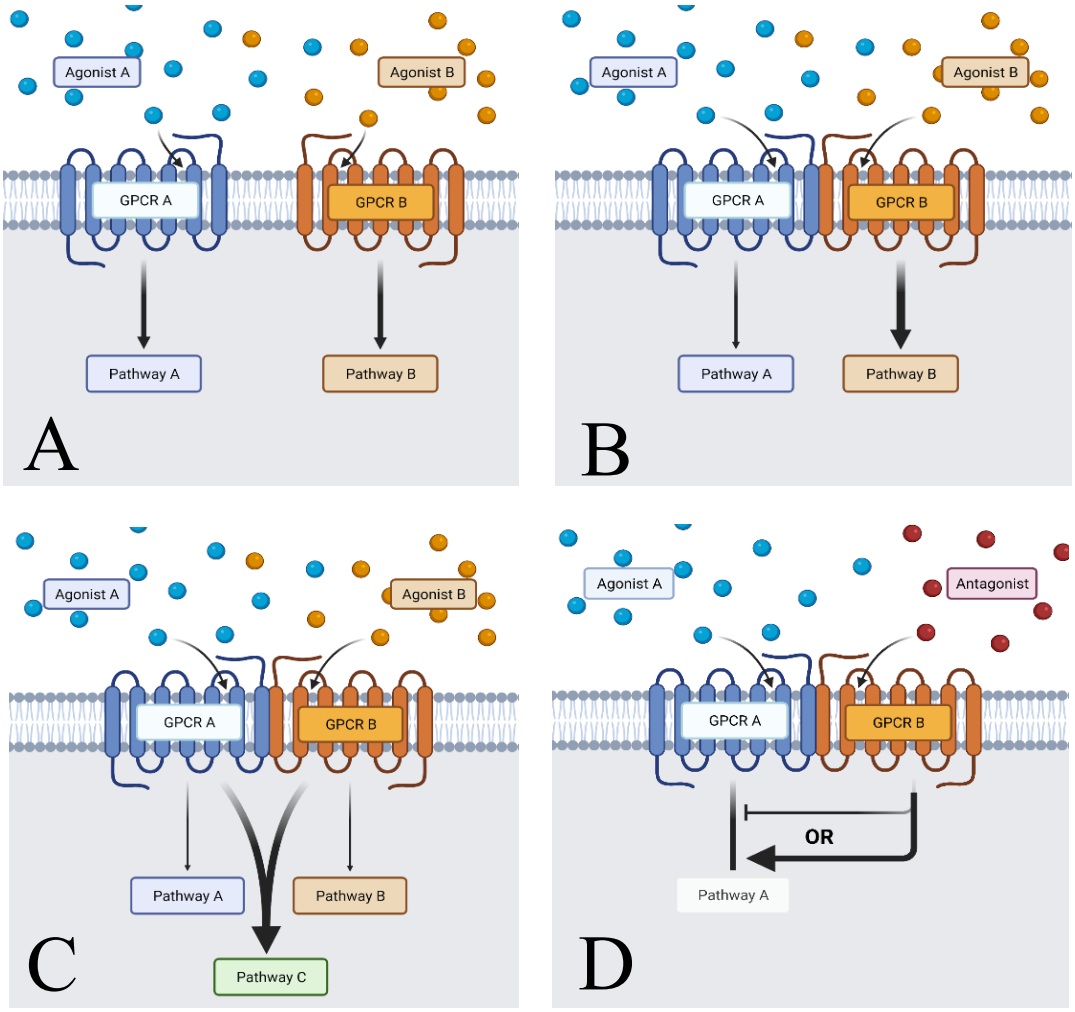

Figure 1.2. Heteromer-Dependant Signaling Changes in Class A GPCR
When no physical association is present, GPCRS signal independently – unable to directly effect the activity of the other GPCR **(A)**. Upon formation of a GPCR heteromer, protein-protein allosteric interactions may lead to preferential signaling through one receptor partner **(B)**, or the generation of a novel signaling pathway **(C)**. Selective antagonism of one receptor partner may result in inhibition or potentiation of signaling through receptor partner **(D)**.

Figure 1.3. Heteromer-Dependant Changes in β-arrestin Recruitment
The formation of a heteromer may affect the behaviour of arrestin recruitment, receptor internalization, and GPCR-independent signaling. When receptors are acting independently, arrestin may be recruited to either receptor following agonist-mediated receptor activation **(A)**. Heteromer formation may lead to allosteric protein-protein interactions which can increase or decrease arrestin recruitment to the heteromer **(B)** or preferentially mobilize arrestin to one receptor partner **(C)**. Antagonist application may result in the reduction of arrestin recruitment to the non-antagonist bound receptor partner and sustained presence on the receptor surface **(D)**. Increases or decreases in arrestin mobilization to the GPCR heteromer may lead to altered receptor internalization and can positively, or negatively affect signaling through G-protein and arrestin-mediated signaling cascades **(E)**.

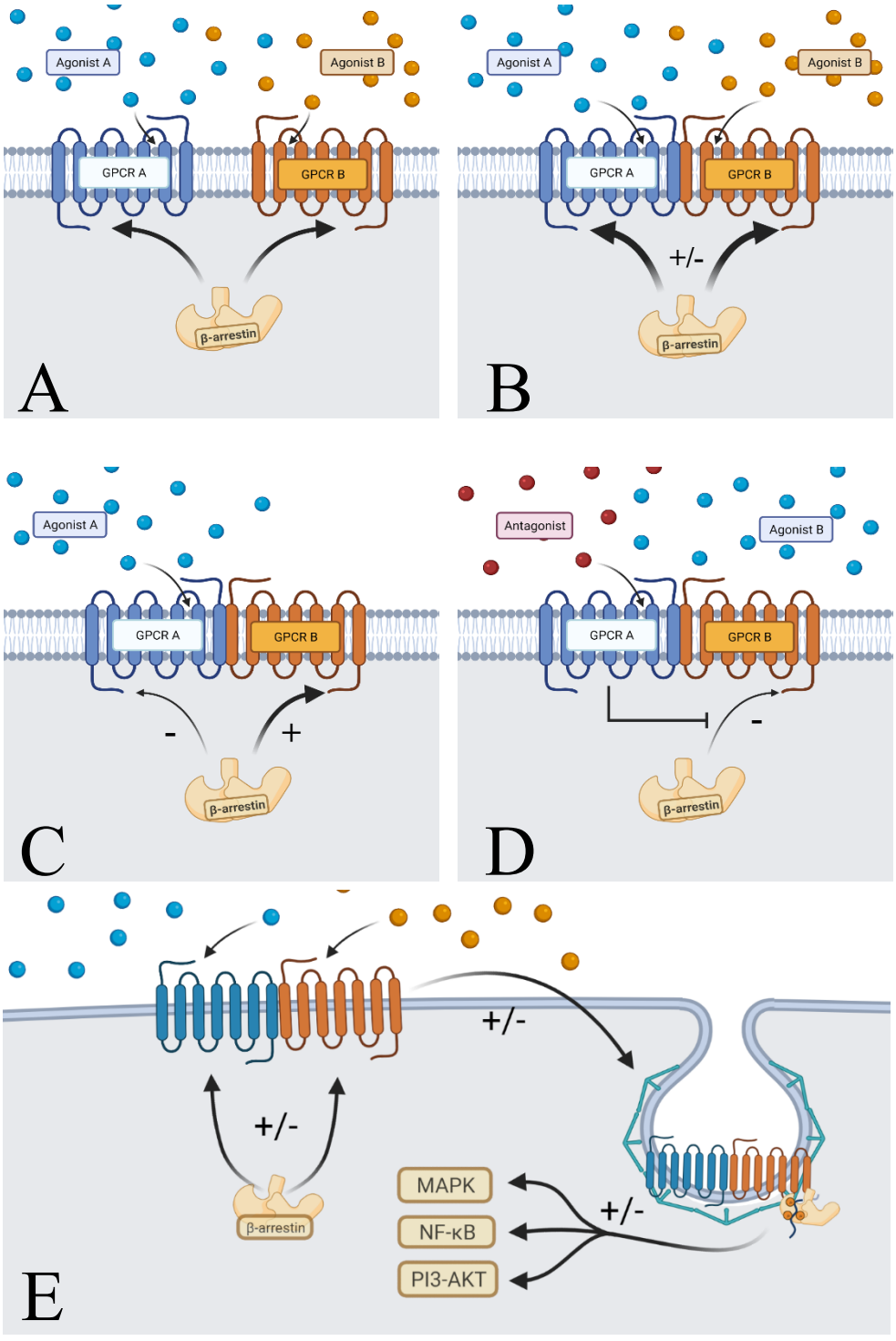
Agonist A
Agonist B
GPCR A
GPCR B
β-arrestin
A
+/-
B
-
+
C
Antagonist
D
MAPK
NF-κB
PI3-AKT
E

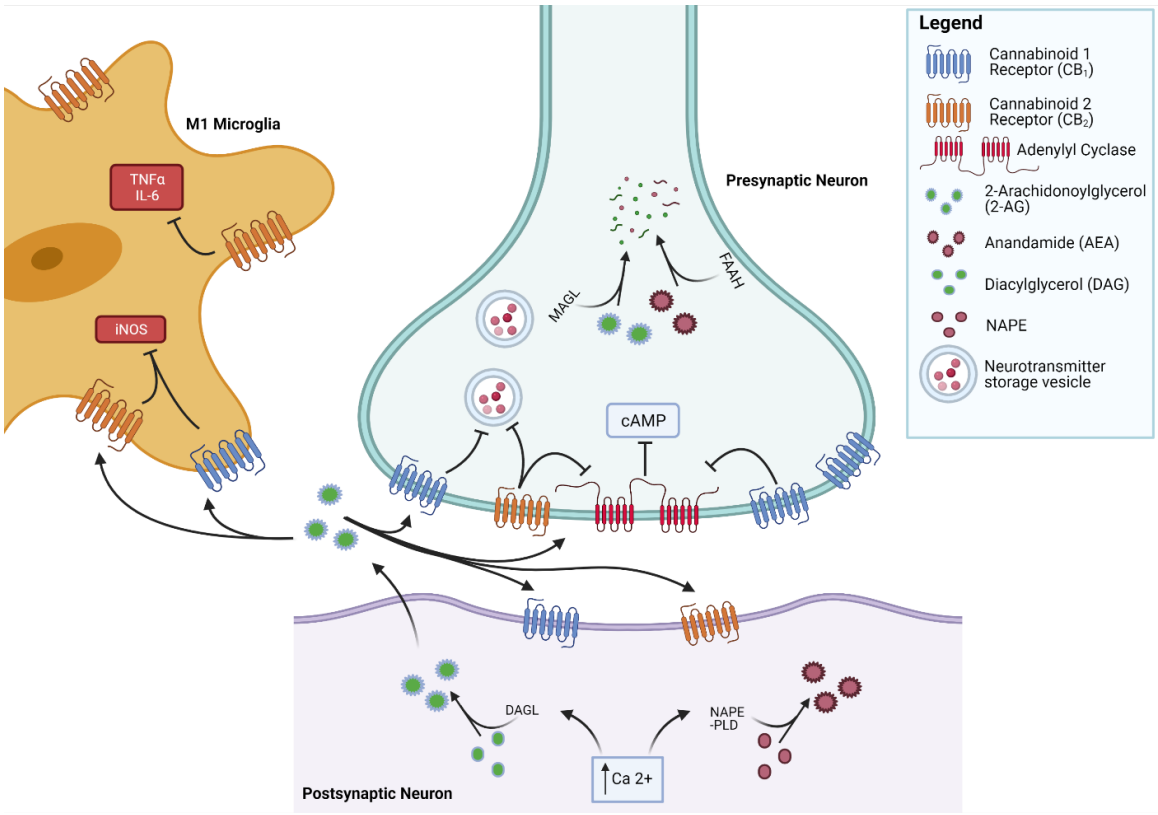

Figure 1.4. The Endocannabinoid System in the Central Nervous System
Endocannabinoids 2-AG and/or AEA are synthesized on-demand from DAGL and NAPE-PLD respectively in response to increases in intracellular calcium in the post-synaptic neuron. Once released, eCBs diffuse to activate CB_1 and/or CB_2 receptors located on presynaptic neurons in retrograde fashion; self-stimulate post-synaptically located receptors; or activate cannabinoid receptors on microglia. CB_1 and CB_2 activation in neurons generally activates Gi proteins to inhibit adenylyl cyclase activity and prevent cAMP accumulation leading to inhibition of neurotransmitter release. In microglia, endocannabinoid activity leads to inhibition of iNOS production, reduction of proinflammatory cytokines, and modulation of microglial phenotype. CB_1 is more densely expressed in neurons, whereas CB_2 is more densely expressed in activated (M1) microglia. These expression patterns have been known to change in certain neurodegenerative disease states.

CHAPTER 2: METHODS

2.1 Reagents

ACEA, HU308, AM251, and AM630 were purchased from Tocris Biosciences (Bristol, UK). CP 55,940 was purchased from Cayman Chemical (Michigan, USA). HU308, AM251, and AM630 were all dissolved in dimethyl sulfoxide (DMSO), while ACEA was dissolved in ethanol (EtOH) and CP 55,940 in methanol (MeOH). All reagents were diluted in Opti-MEM® Reduced-Serum Medium containing 0.1% of the respective solvent for the indicated ligand.

2.2 Plasmid Propagation and Sequencing

Plasmid stocks were generated using bacterial transformation in DH5-α competent E. coli cells (Invitrogen). Our CNR1-Tango (CB_1-Tango) plasmid was graciously donated by Dr. Chris Sinal (Dalhousie University, Halifax, Canada) and CNR2-Tango (CB_2-Tango) plasmid was a gift from Dr. Brian Roth (Addgene plasmid # 66255; http:/net.addgene:66255; RRID: Addgene_66255). The CB_1_pcDNA3.1 (+) plasmid was cloned by Dr. Amina Bagher (Bagher *et al.* 2016 Jan 1) and the 3xHA-CB_2 plasmid was a generous gift from Dr. Robert Laprairie (University of Saskatchewan, Saskatchewan, Canada). See Table 2.1 for full list of plasmids.

2.3 Cell Culture and Transfection

HEK293T cells were used for dual-immunofluorescence experiments. Cells were cultured in 10 cm cell-culture treated dishes and maintained in high glucose Dulbecco's Modified Eagle Medium (DMEM) with 10% Fetal Bovine Serum (FBS), 100 U/ml penicillin, and 100 μg/ml streptomycin. Cells were plated in 24-well cell culture dishes containing poly-d-lysine (PDL)-coated 12 mm round glass coverslips at a density of

30,000 cells/well and allowed to grow for 24 hours at 37ºC and 5% CO_2 before transfection. At least one hour before transfection, cell culture media was replaced with Opti-MEM® Reduced-Serum Medium (no phenol red). To transfect HEK239T cells, master mixes of PEI and cDNA were mixed such that each well of a 24-well plate received 500 ng of the required plasmids diluted in 30 µl Opti-MEM® Reduced-Serum Medium mixed with of 0.75 µl of PEI per well - the total amount of DNA/well was kept constant by using pcDNA3.1 Zeo (+) empty vector as required. Master mixes were briefly vortexed and incubated at room temperature for 20 minutes before being added dropwise to cells in 24-well plate. Four hours after transfection, transfection media was replaced with DMEM containing 1% FBS. HEK293T cells were then left to incubate for ~72 hours at 37ºC and 5% CO_2 until ~70% confluent. All experiments were carried out using cells between passages 3-30.

HTLA cells are a variant of HEK293T stably expressing a tTA-dependant luciferase reporter and a β-arrestin2-TEV fusion gene (Kroeze *et al.* 2015), and were generously donated to our lab from Dr. Chris Sinal (Dalhousie University, Halifax, NS). HTLA cells were cultured in 10 cm cell-culture treated dishes and maintained in high glucose Dulbecco's Modified Eagle Medium (DMEM; without phenol red) containing 10% fetal bovine serum (FBS); 1X NEAA; 1mM sodium pyruvate;100 U/ml penicillin; 100 µg/ml streptomycin; 500 ug/ml Geneticin; 5 ug/ml puromycin; and 200 ug/ml hygromycin (Tango selection media). Cells were maintained at 37ºC and 5% CO_2 until 70-90% confluence and sub-cultured at a 1:5 ratio. For Tango experiments, HTLA cells were plated at 20,000 cell/well in PDL-coated (25 mg/mL) cell-culture treated 96-well plates (clear, flat bottom). Cells were plated in high glucose Dulbecco's Modified Eagle

Medium (DMEM without phenol red) with 10% fetal bovine serum (FBS), 1X NEAA, 1mM sodium pyruvate, 100 U/ml penicillin, 100 µg/ml streptomycin (Tango non-selection media) and incubated at 37ºC and 5% CO_2 for 24 hours before transfection until cells reached 70-90% confluence. HTLA cells were transfected using Lipofectamine 3000 or 2 mg/ml branched Polyethyleneimine (PEI) as indicated. Lipofectamine ® 3000 (Invitrogen) transfection was carried out as per the protocol supplied by the manufacturers. To transfect HTLA cells with PEI, master mixes of plasmid cDNA and PEI were mixed such that each well of a 96-well plate received 100 ng of the required plasmids diluted in 10 µl Opti-MEM® Reduced-Serum Medium mixed with of 0.1 µl of PEI per well - the total amount of DNA/well was kept constant by using pcDNA3.1 Zeo (+) empty vector as required. Plasmid-PEI solutions were vortexed and incubated at room temperature before adding 40 µl HTLA media (no selection) per well and vortexing briefly. Complete transfection solutions were then incubated at room temperature for 20 minutes before being mixed by gentle pipetting and added to the HTLA cell containing 96-well plate at 50 µl per well. Cells were then incubated with transfection solution for 24 hours before continuing with Tango assay (Kroeze *et al.* 2015; Laroche and Giguère 2019).

To determine the effect of serum on the cannabinoid receptor Tango assay, our cell culture protocol was adapted to compare two different methods of serum starvation. The first starvation protocol (referred to as Protocol B) was identical to our standard cell culture protocol above (referred to as Protocol A), with the exception that no HTLA media was used during transfection. Instead, 50 µl Opti-MEM® Reduced-Serum Medium only, per well, was used. Protocol C was likewise identical to our standard

protocol, however after an overnight incubation with the HTLA media-transfection mixture, the culture media was replaced with 50 µl Opti-MEM® Reduced-Serum Medium per well and left to incubate for a further 24 hours before completing the Tango assay. All experiments were carried out using cells between passages 3-30.

2.4 Dual Immunofluorescence

The co-localization of transfected CB_1 and CB_2 in HEK293T cells was observed using dual immunofluorescence staining and confocal microscopy. By first treating transiently transfected cells with primary antibodies against CB_1 and the extracellular HA-tag attached to CB_2, fluorophore-linked secondary antibodies -sensitive against our primary antibodies- are then used label cells that are expressing both receptors of interest. Co-expression is visualized by an overlap in fluorescence emissions unique to the fluorophore-conjugated secondary antibodies in the same cells, as observed on a confocal microscope.

Transiently transfected HEK293T cells were grown on PLD-coated glass coverslips until they reached 60-70% confluence and then fixed with 4% (w/v) paraformaldehyde (PFA) in 1x PBS for 15-20 min. After washing the cells three times using 1X PBS with 20 mM glycine, cells were permeabilized and non-specific antibody binding was blocked by treating cells with 1% (w/v) bovine serum albumin (BSA) with 0.05% Triton X-100 for 60 min at room temperature. Cells were incubated with primary monoclonal rabbit N-terminal CB_1 antibody (1:500; Cell Signaling Technologies) and primary monoclonal mouse N-terminal-HA antibody (1:500; Cell Signaling Technologies) overnight at 4°C. The following day, cells were washed three times with 1X TBS and incubated with AlexaFluor (R) 555 Anti Rabbit IgG Fab2 (1:500; #44135,

Cell Signal Technologies, Massachusetts, USA) and AlexaFluor (R) 488 Anti Mouse IgG Fab2 (1:500; #44085, Cell Signal Technologies, Massachusetts, USA) for 1 hr at room temperature before washing again 3 times with 1X TBS and once with H_2O. Finally, coverslips were mounted on microscopic slides (Fisher Scientific) using Duolink® *in situ* mounting media with DAPI (Sigma-Aldrich, Ontario, Canada). Images of cells were acquired using the Zeiss LSM 710 (upright) laser-scanning microscope**.** Overlap in immunofluorescence from red/orange (555 nM) and green (488 nM) channels in the same cells was interpreted as evidence of co-localization.

2.5 Tango Arrestin Recruitment Reporter Assay

To measure arrestin recruitment to activated CB_1 and CB_2 receptors, the Tango β-arrestin2 recruitment reporter assay was used (Laroche and Giguère 2019). The Tango assay quantifies the interaction between a transiently transfected modified GPCR (GPCR-Tango) and a stably expressed mutant β-arrestin2 in HTLA cells. HTLA cells are derived from HEK293T cells and stably express human β-arrestin2 fused with tobacco etch virus (TEV) protease and a tetracycline-controlled transactivator (tTA) promoter-driven reporter gene (*luc*) to express the luciferase enzyme. GPCR-Tango plasmid cDNA expression is initiated at a CMV promoter site and encodes for a GPCR of interest (in the present case, the CB_1 or CB_2 receptors) tagged to a FLAG epitope on the N-terminal and vasopressin 2 receptor C-terminal tail (V_2 tail) linked to a TEV protease cleavage site (TCS) and terminating with the tTA transcription factor (Fig. 2.2). Following arrestin recruitment to the active GPCR, β-arrestin–TEV fusion proteins cleave the tTA transcription factor at the TCS. Once freed, the tTA is translocated into the nucleus of where it may bind to the promoter region of the stably transfected luciferase reporter,

leading to the expression of luciferase. This interaction turns the transient interactions between β-arrestin2 and the target GPCR into a sustained, cumulative, and quantifiable luciferase emission which is read on a plate reader with detection ranges between 380-600 nm.

Traditionally, the Tango assay has been used in medium to high throughput assays to aid in the identification of orphan receptors and in drug discovery (Kroeze *et al.* 2015). More recently, the Tango arrestin-recruitment reporter assay has been used to measure changes in arrestin recruitment due to the co-expression of two different Class A GPCR, however, data are limited, and this method has not been validated in cells co-expressing cannabinoid receptors (Gao *et al.* 2018). Theoretically, if the Tango assay can quantify ligand-dependant differences in β-arrestin2 recruitment to active receptors, then it should be able to detect changes in β-arrestin2 recruitment due to receptor-receptor interactions. Therefor treating cells co-transfected with Tango-tagged receptor, and non-Tango receptor cDNA should permit the study of heteromer-dependant modulation in β-arrestin2 recruitment. For our assay, CB_1-Tango or CB_2-Tango plasmids were transfected alone, or in combination with non-Tango CB_1_pcDNA3.1 (CB_1) or 3xHA-CB_2 (CB_2) plasmids. Furthermore, transfection of both Tango plasmids (CB_1-Tango and CB_2-Tango) together will allow quantification of the cumulative arrestin recruitment to each receptor in co-transfected cells (Fig. 2.3).

HTLA cells were plated at 2.0 x 10^5 cells/well in flat bottom; clear; cell-culture treated; PDL coated (25 μg/mL) 96-well plates and incubated at 37° C (5% CO_2) for 24 hours before transient transfection (to allow cells to reach 70-90% confluence). All transfections included 25 ng pCMV-βgal per well, and data normalized to *LacZ* gene

expression (abs_{420}). Complete transfection solutions were added at 50 µl/well to HTLA cells and incubated at 37° C (5% CO_2) for 24 hours before treating with drug.

Drug treatments were diluted in Opti-MEM® Reduced-Serum Medium lacking phenol red at the concentrations indicated in the figure legends and added at a volume of 50 µl/well following removal of transfection solutions. HTLA cells were incubated with drug at 37° C (5% CO_2) for 8 hours before removing treatments and washing cells once with 1x PBS (100 µl/well). Cells were lysed by adding 5x Reporter Lysis Buffer (Promega, Wisconsin, USA) diluted to 1x in dH_2O (100 µl/well) and frozen at -80°C for at least 1 hour. After thawing cell lysate, β-galactosidase buffer, and luciferase assay solution (Promega) in 25° C incubator for 2 hours, 30 µl of cell lysate was transferred to a new clear 96-well plate for the β-galactosidase normalization assay, and 10 µl of cell lysate was transferred to a white, opaque 96-well plate for the luminescence assay. Thawed 2x β-gal buffer was added to the β-galactosidase assay plate (30 µl/well) until light yellow color became apparent (~1 minute following the addition of 2x β-gal buffer to the entire plate using an 8-channel multichannel pipette), at which time the reaction was stopped by quickly adding 100µl of 1M Na_2CO_3.

All plates were measured using the FluorostarOMEGA plate reader. β-galactosidase reporter activity was read with absorbance at 420 nm. Luciferase from Tango assay was read using the lens setting with gain set to 3600 following automatic injections of 80 µl/well luciferase assay substrate (Promega). Luciferase assay reagent was warmed in 25° C incubator, submerged in water for 2 hours before assay to standardize reagent temperature to cell lysate temperature. Relative luminescence units (RLU) were calculated by dividing raw luminescence values by β-galactosidase

absorbance from lysate aliquoted from the same wells. Fold-change luminescence was determined by dividing RLU from agonist treated wells by RLU from vehicle treated wells from the same plate. % Luminescence was calculated by dividing RLU from wells treated with vehicle or agonist by wells treated with the maximal value of agonist before being multiplied by 100. In this manner, wells treated with the maximal dose of agonist were set to 100% luminescence, and luminescence from all previous concentrations of agonist were scaled accordingly.

2.6 Z'-Factor Analysis

The Z'-factor is a simple statistical analysis often used to provide quality assurance in high throughput assays (Zhang and Oldenburg 2009). Z'-factor was created as a more robust substitute for more conventional approaches of assessing assay quality such as signal-to-noise ratio (S/N) or signal-to-background ratio (S/B). Unlike S/N or S/B ratios, the Z'-factor calculation (figure 2.4) considers the standard deviation of the lowest (floor) and highest (ceiling) points of an assay output, as well as the absolute value of the difference between these two points (Zhang *et al.* 1999). This allows the measurement of the quality of an assay by defining the usable dynamic range, and results in a score from $0<1$. Ultimately, the closer the Z'-factor is to 1, the better the quality of the assay, and the lower the probability of there being overlap between the variation of the highest and lowest points of the assay. A Z'-factor below zero indicates that overlap between the highest and lowest points of the assay, due to variation, is likely, and that the data should not be used. For our purposes, vehicle treated wells were used as the low reference control (floor) and wells treated with the maximal concentration of agonist were used as the high reference control (ceiling).

2.7 Statistical Analysis

All data was scaled to luminescence in cells transfected with CB_1-Tango or CB_2-Tango only (unless otherwise indicated) and treated with the highest dose of agonist (indicated as 100% luminescence) within the same plate. Replicate data was combined from experiments on independent days unless otherwise indicated in figure legend. Data are presented as the Mean ± standard deviation (SD) or 95% confidence interval (CI), as indicated in figure legend. Statistical analysis and curve fitting were performed using GraphPad version 6.0. Concentration-response curves were fit to non-linear regression model with variable slope (four parameters). Statistical analyses between treatment and/or transfection groups were conducted by two-tailed Student's t-test, one-way or two-way analysis of variance (ANOVA), as indicated. ANOVA *Post-hoc* analyses were performed using Tukey's honest significance test. The level of significance was set to $P < 0.05$.

Table 2.1 DNA Constructs Used in This Thesis

A list of all plasmids used to for experiments. GenBank accession numbers correlate to corresponding inserted genes of interest for each plasmid.

DNA Construct	Description	GenBank Accession Number	Source
CNR1-Tango	N-terminal FLAG-tagged CB1 receptor cloned into empty tango vector with pcDNA3.1(+) backbone	NM_016083	Plasmid was a gift from Dr. Chris Sinal (Dalhousie University, Halifax, Canada)
CNR2-Tango	N-terminal FLAG-tagged CB2 receptor cloned into empty tango vector with pcDNA3.1(+) backbone	NP_001832	Plasmid was a gift from Dr. Bryan Roth (Addgene #66255)
CB_1_pcDNA3.1	Untagged CB1 receptor cloned into pcDNA3.1 Zeo (+)	NM_016083	Construct cloned by Amina Bagher (Bagher *et al.*, 2017)
HA-CB_2	N-terminal 3xHA-tagged CB2 receptor cloned into pcDNA3.1 Zeo (+)	NP_001832	Plasmid was a gift from Dr. Robert Laprarie (University of Saskatchewan, Saskatchewan, Canada)
pCMV-β-gal	Mammalian reporter vector designed to express β-galactosidase in mammalian cells	NC_000913.3	Plasmid was a gift from Dr. Chris Sinal (Dalhousie University, Halifax, NS)

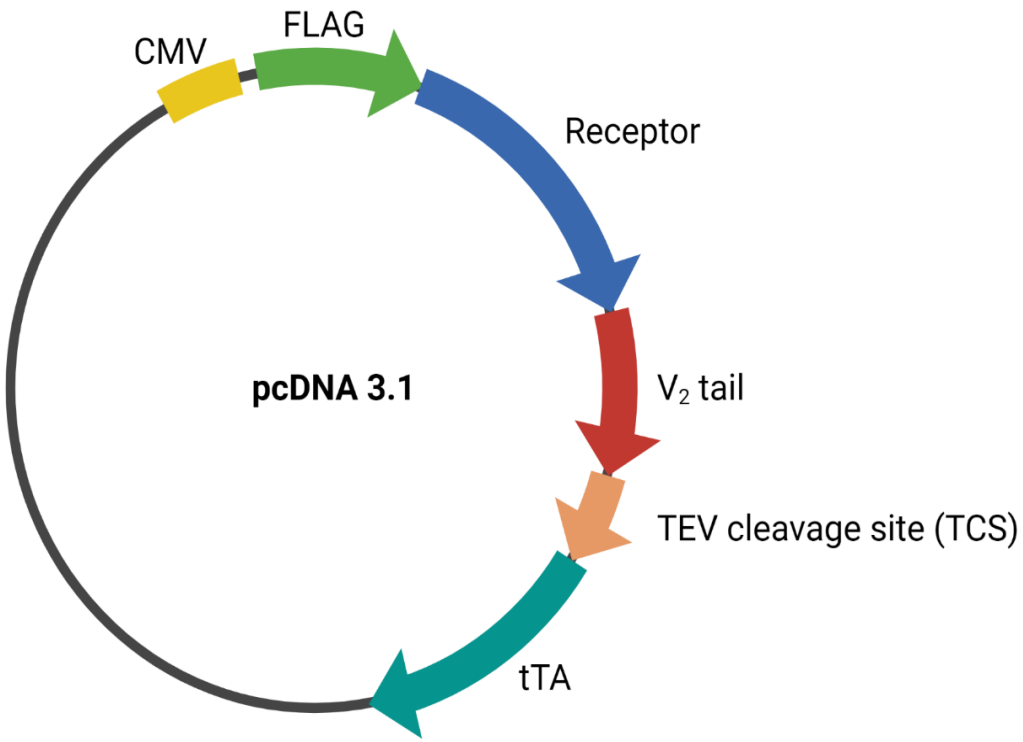

Figure 2.1. GPCR-Tango Plasmid
Tango GPCR cDNA was subcloned into a pcDNA3.1(+) mammalian vector backbone. Plasmid expression is driven by the human cytomegalovirus (CMV) promoter and constructs are expressed in order of a FLAG epitope tag, receptor sequence, vasopressin 2 receptor C-tail (V_2 tail), tobacco etch virus (TEV) protease cleavage site (TCS), and tetracycline controlled transactivator (tTA) transcription element.

Figure 2.2. Tango Assay to Measure Changes in β-Arrestin2 Recruitment Following Co-Transfection of Class A GPCR

Tango-tagged receptors recruit TEV-*β*-arrestin2 fusion protein following agonist-induced receptor activation leading to translocation of tTA transcription factor into nucleus and sustained luciferase expression **(A)**. This relationship is the standard for comparison to observe any changes in cells co-transfected with either receptor. In the event of heteromer formation, selective or non-selective agonism may alter arrestin recruitment to either receptor. Co-transfection of Tango receptors will show cumulative change in arrestin recruitment to both receptors **(B)**. Co-transfection of Tango GPCR with non-Tango GPCR will allow selective quantification of arrestin recruitment to Tango receptor partner in the presence of the non-Tango partner **(C)**. By utilizing each transfection method, the Tango assay can be used to compare baseline β-arrestin2 activity following transfection of either receptor alone with cumulative β-arrestin2 activity and recruitment to each receptor in co-transfected cells. These assays can be carried out using selective, or non-selective agonism, and to test the relative effect of antagonists.

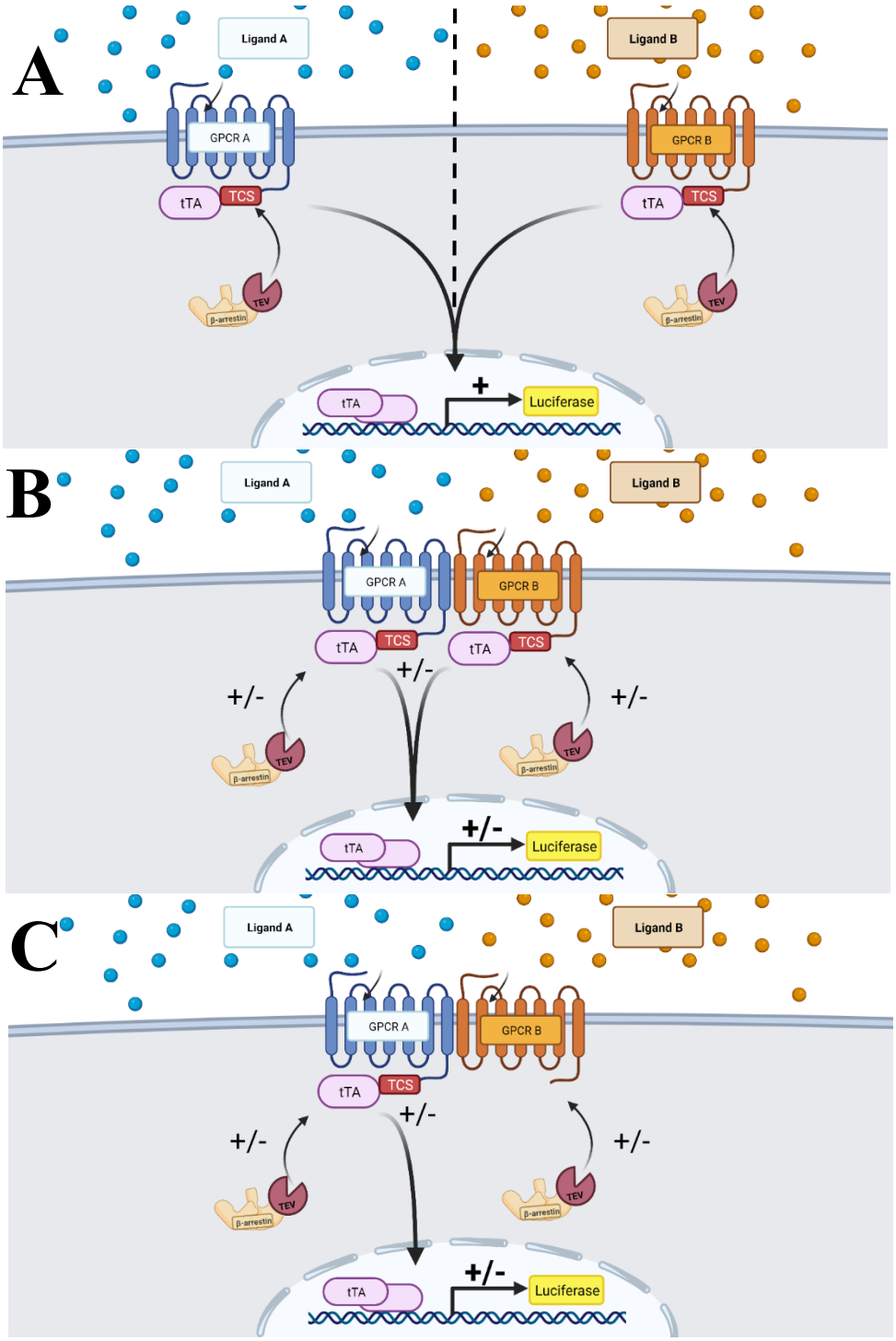
A
Ligand A
Ligand B
GPCR A
GPCR B
tTA
TCS
TEV
β-arrestin
+
Luciferase
B
+/-
C

$$Z' = 1 - (3\sigma_{c+} + 3\sigma_{c-})/(|\mu_{c+} - \mu_{c-}|)$$

Figure 2.3 Z-Factor Equation to Assess Assay Quality
Z'-factor, as defined by Zhang and Oldenburg (Zhang *et al.* 1999) is a statistical method to quantify assay quality where (σc+) and (σc−) represent the standard deviation for the high and low reference controls, respectively, and |μc+–μc−| is the absolute value between the high and low reference control points. Z'-Factor values between 0.5 to 1 are considered moderate to excellent assay quality (a value of 1.0 is not possible), while 0 – 0.5 is considered poor. A Z'-factor score of < 0 means that the variation between the highest and lowest points of the assay may overlap.

CHAPTER 3: RESULTS

3.1 Validation of the Tango Arrestin-Recruitment Reporter Assay to Study Interactions Between CB_1 and CB_2 Receptors

The Tango β-Arrestin reporter assay detects transient β-arrestin2-GPCR interactions following agonist activation and reports the interaction as sustained and cumulative luminescence emission via reporter-driven luciferase expression in HTLA cells, which are modified HEK293T cell line (Kroeze *et al.* 2015). Increases in luminescence are interpreted as receptor activation and physical interaction between β-arrestin2 and Tango receptor. Unless otherwise indicated, luminescence and β-arrestin2 recruitment are considered synonymous when referring to experimental results.

3.1.1 The Effect of CP 55,940 Incubation Time on Luminescence in the Cannabinoid Receptor Tango Assay

Agonist incubation times for Tango assays are reported to be highly dependant on both the GPCR of interest and the selected agonist (Wang *et al.* 2004; Kroeze *et al.* 2015). An appropriate agonist incubation time produces saturable luminescence that increase in proportion to the agonist concentration. Therefore, it was necessary to standardise the Tango assay incubation period for both CB_1-Tango or CB_2-Tango using the selected agonist, CP 55,940. Transfected HTLA cells were incubated with 0, 0.01, 0.1, 0.25, 0.5, 0.75, 1, and 5 μM of the non-selective CBr agonist CP 55,940 for 6, 8, or 18 hr. An incubation of 6 hr did not generate a saturable luminescence curve in cells expressing CB_1-Tango (Table 3.1). An incubation time of 18 hr did not generate a concentration-dependent luminescence curve in cells expressing CB_2-Tango (Fig. 3.2). An incubation time of 8 hr with CP 55,940 generated saturable concentration-response curves in cells expressing either CB_1-Tango or CB_2-Tango receptors. The EC_{50} for CP

55,940-induced β-arrestin2 recruitment to CB_1-Tango was 240 nM (CI: 134 to 428 nM), and 123 nM (CI: 62.2 to 244 nM) at CB_2-Tango. An 8 hr CP 55,940 incubation period was selected and used in all proceeding experiments involving CP 55,940 agonism.

3.1.2 Assessing the Sensitivity and Reliability of the CB_1 and CB_2-Tango Assay

A primary outcome of this thesis depended on measuring the relative change in β-arrestin2 recruitment to CB_1-Tango or CB_2-Tango-tagged receptors in the presence or absence of CB_1 or CB_2 receptors. Our goal was to determine if these receptors were interacting in heteromeric complexes to modulate agonist-induced β-arrestin2 recruitment. A low fold-change in luminescence in CP 55,940-treated cells over vehicle-treated cells could reduce assay sensitivity and mask potential differences between groups. CB_1- and CB_2-Tango data was plotted as a fold-change of CP 55,940-treated cells relative to cells treated with only vehicle (OptiMEM I SFM containing 0.1% MeOH) and I assessed the accuracy and variability in the assay using the Z' factor calculation (Zhang and Oldenburg 2009). Peak fold changes were found to be 1.49 (CI:1.34 - 1.56) and 2.64 (CI: 2.38 - 2.88) for CB_1-Tango and CB_2-Tango, respectively (Fig.3.3). Using fold-change luminescence from cells treated with 10 μM CP 55,940 (maximal dose used) relative to vehicle-treated cells, CB_1-Tango cells had a Z' factor of 0.47, while CB_2-Tango cells had a Z' factor < 0.00. The Z' factors indicate low and poor assay accuracy for CB_1- and CB_2-Tango, respectively, using the specific assay conditions. A calculated Z' factor lower than zero indicates that variation in luminescence between vehicle and treatment conditions may overlap (Zhang and Oldenburg 2009). This low assay accuracy was identified as an essential factor to resolve

before the Tango assay could be used to quantify relative to β-arrestin2 recruitment to CB_1 and CB_2.

3.1.3 The Effect of Serum Starvation on CB_1-Tango and CB_2-Tango Assay Sensitivity

Serum starvation is a common practice in cell-based assays to minimize the effects of protein found in serum that might increase background or basal assay activity (Pirkmajer and Chibalin 2011). Furthermore, testing the sensitivity of cells to serum is a recommended step in GPCR-based arrestin-recruitment assay validation (Wang *et al.* 2004). To determine if the low assay sensitivity was a result of serum-dependant activity, two alternate serum starvation protocols (Protocol B and Protocol C) were tested, and resultant fold-change luminescence was compared to the luminescence from cells cultured following the serum-containing standard Tango protocol (Protocol A). Neither serum starvation method had a significant effect on peak fold-change assay luminescence relative to that observed in cells subjected to protocol A when comparing maximal fold-change in CB_1-Tango expressing cells (protocol B, $p = 0.400$; protocol C, $p = 0.893$) or in CB_2-Tango expressing cells (protocol B, $p = 0.973$; protocol C, $p = 0.999$). In addition, Z' factor calculations for both alternate protocols in cells expressing either the CB_1-Tango or CB_2-Tango receptor showed poor assay performance ($Z' < 0.00$; Fig. 3.4).

3.1.4 The Effect of Lipofectamine® 3000 Compared to PEI Transfection on CB1- and CB2-Tango Assay Sensitivity

Cannabinoid ligands are highly lipophilic, and Lipofectamine® 3000 is a lipid-based cationic transfection medium. To determine if Tango assay sensitivity was affected by the lipid-based transfection medium, fold-change luminescence in cells transfected with Lipofectamine® 3000 were compared to cells transfected using the non-lipid

polycation polyethyleneimine (PEI),which has been used by previous groups to study cannabinoid receptor function in cell-based assays (Callén *et al.*, 2012; Kim *et al.*, 2017; Navarro *et al.*, 2018),. Cells transfected with PEI (2 mg/ml; 0.10 µl per well) had increased concentration-response plateaus in both CB_1- **(**p=0.001**)** and CB_2-Tango (p=0.003) receptor expressing cells treated with CP 55,940 compared to cells transfected using Lipofectamine® 3000. Specifically, cells transfected with CB_1-Tango using PEI had an increased peak fold-change luminescence of ~ 49% (CI 48.63 to 53.55%) relative to cells transfected with Lipofectamine® 3000 (Fig. 3.6). Likewise, cells transfected with CB_2-Tango using PEI had an increase of ~24% (CI 20.19 to 27.44%) over Lipofectamine® 3000 transfected cells (Fig. 3.7). In addition, switching to PEI-based transfection increased the calculated Z' factor to 0.88 and 0.77 for CB_1-Tango and CB_2-Tango, respectively (Zhang and Oldenburg 2009). PEI transfection was selected as the primary transfection reagent for all further Tango experiments.

3.1.5 Activity of Selective and Non-Selective Agonism on Cells Transfected with CB_1-Tango or CB_2-Tango

Cells transfected with Tango receptor cDNAs were treated with increasing concentrations of the CB_1-selective agonist ACEA, the CB_2-selective agonistHU308 and the non-selective agonist CP 55,940 and incubated for 8-hr. ACEA did not produce a concentration-response curve in cells expressing CB_1-Tango after 8 hr of incubation (Fig. 3.8A). Similarly, HU308 did not produce a concentration-response curve in cell expressing CB_2-Tango (Fig. 3.9B). HU308 was unable to produce any detectable response at CB_1-Tango (Figure 3.8B) and ACEA was unable to produce any detectable luminescence at CB_2-Tango (Figure 3.9A). In short, in our hands, CP 55,940 produced

higher arrestin-dependant luminescence in both CB_1-Tango and CB_2-Tango assays relative to CB_1- and CB_2- selective agonists.

3.1.6 The Effect of Normalization on CB_1- and CB_2-Tango Assay Variability

Luciferase assays are well known for a high degree of plate-to-plate variation in emissions (Repele and Manu 2019). Variation can arise from technical errors (pipetting, reagent mixing, reagent temperature, relative number of cells in cells *etc*.) or biological differences such as the passage number of cells (age) and physiologic state of the cells on a given day. This variation is observed as large standard deviation (SD) in the CP 55,940 concentration-response curves for CB_1- (Fig. 3.10) and CB_2-Tango (Fig. 3.11) assays when expressing data as RLU or fold change luminescence over cells treated with vehicle only. To account for high variation in day-to-day relative luminescence, we normalized the data within each replicate plate/day to the maximal response per plate. This was done by expressing RLU from cells treated with the maximal dose of CP 55,940 (2.50 μM) as 100% luminescence, and scaling RLU at all other concentrations of CP 55,940 accordingly. While this eliminates the use of absolute luminesce values, this form of normalization is well supported by our experimental objectives. Specifically, we aimed to determine if co-expression of CB_1 and CB_2 receptors changes arrestin recruitment to either receptor. Therefore, by transfecting the plasmid combinations to be compared within the same plate and scaling data to maximal luminescence in cells transfected with only one receptor, we were able to quantify changes in arrestin recruitment as a percentage of luminescence from cells transfected with CB_1-Tango or CB_2-Tango only and treated with 2.50 μM of CP 55,940. This method decreased plate-to-plate variability in both CB_1- (Fig. 3.10C) and CB_2-Tango (Fig 3.11C) assays, relative to expressing the data as RLU or fold-change. All further data are expressed as % Luminescence.

Figure 3.1. The Effect of CP 55,940 Incubation Time on β-Arrestin2-Dependant Luminescence in the CB_1-Tango Assay

Tango saturation curves obtained from HTLA cells transiently transfected with 25 ng of CB_1-Tango cDNA using Lipofectamine® 3000. Concentration response curves of CP 55,940 induced β-arrestin2 mobilization to activated CB_1-Tango following 6 hr, 8 hr, or 18 hr of incubation with agonist as indicated. Luminescence (RLU) was obtained by dividing raw luminescence values by β-galactosidase absorbance (ABS_{420}) from the same cells. Curves were generated using non-linear regression analysis with variable slope (four parameters). Data are presented as mean +/- standard deviation (SD); n=3 from a single experiment.

A

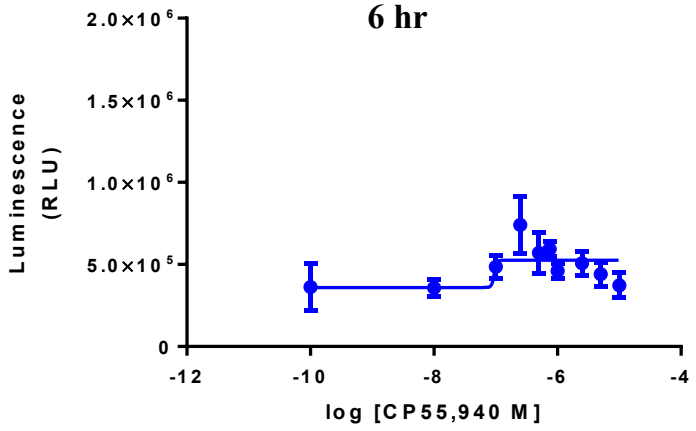
6 hr
Luminescence (RLU)
2.0×10^6
1.5×10^6
1.0×10^6
5.0×10^5
0
-12
-10
-8
-6
-4
log [CP55,940 M]

B

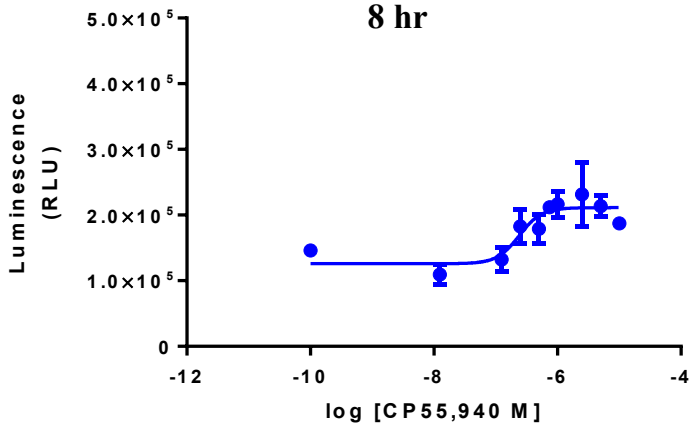
8 hr
Luminescence (RLU)
5.0×10^5
4.0×10^5
3.0×10^5
2.0×10^5
1.0×10^5
0
-12
-10
-8
-6
-4
log [CP55,940 M]

C

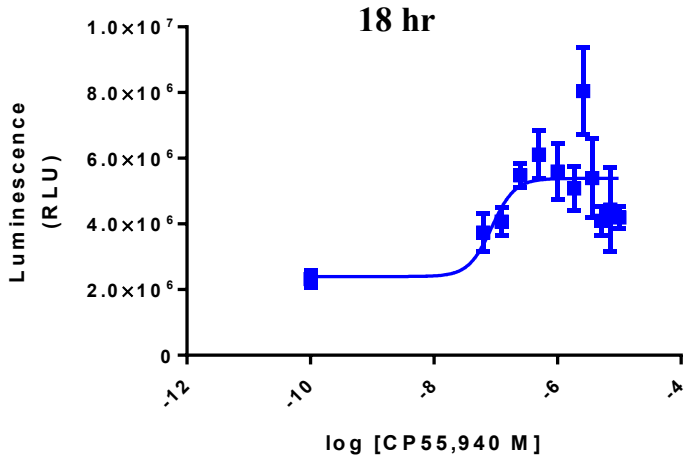
18 hr
Luminescence (RLU)
1.0×10^7
8.0×10^6
6.0×10^6
4.0×10^6
2.0×10^6
0
-12
-10
-8
-6
-4
log [CP55,940 M]

Figure 3.2. The Effect of CP 55,940 Incubation Time on β-Arrestin2-Dependant Luminescence in the CB_2-Tango Assay

Tango saturation curves obtained from HTLA cells transiently transfected with 25 ng of CB_2-Tango cDNA using Lipofectamine® 3000. Concentration response curves represent CP 55,940 induced β-arrestin2 mobilization to activated CB_2-Tango following 6 hr, 8 hr, or 18 hr of incubation with agonist as indicated. Luminescence (RLU) was obtained by dividing raw luminescence values by β-galactosidase absorbance (ABS_{420}) from the same cells. Curves were generated using non-linear regression analysis with variable slope (four parameters). Data are presented as mean +/- standard deviation (SD); n=3 from a single experiment.

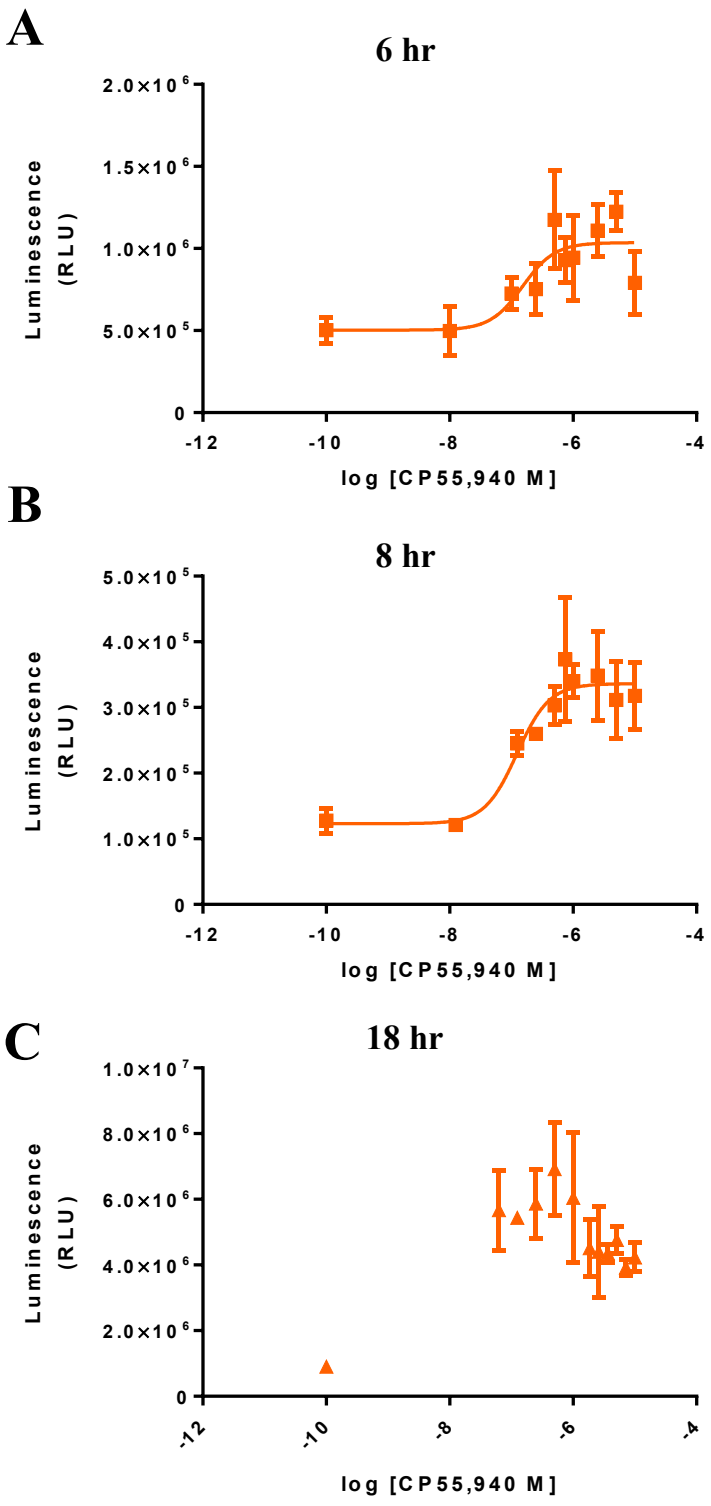
A
6 hr
Luminescence (RLU)
2.0×10 6
1.5×10 6
1.0×10 6
5.0×10 5
0
-12
-10
-8
-6
-4
log [CP55,940 M]
B
8 hr
Luminescence (RLU)
5.0×10 5
4.0×10 5
3.0×10 5
2.0×10 5
1.0×10 5
0
-12
-10
-8
-6
-4
log [CP55,940 M]
C
18 hr
Luminescence (RLU)
1.0×10 7
8.0×10 6
6.0×10 6
4.0×10 6
2.0×10 6
0
-12
-10
-8
-6
-4
log [CP55,940 M]

Table 3.1. The Effect of CP 55,940 Incubation Time on β-Arrestin2-Dependant Luminescence in CB_1-Tango and CB_2-Tango Assays

Data were generated by treating HTLA cells transfected with 25 ng CB_1-Tango or CB_2-Tango cDNA with Lipofectamine® 3000. Curves were fit using non-linear regression analysis with variable slope (four parameters). Data are expressed as mean and 95% confidence intervals (CI); n=3 from a single experiment; ~ indicates the curve generated was an ambiguous fit; n/a indicates that the software was not able to fit a curve to the data.

Receptor	Incubation Time (hr)	E_{min}	E_{max}	Log EC_{50} (M)	EC_{50} (M)
CB_1-Tango	**6**	~	~	~	~
	8	1.22e+005 [9.81e+004 to 1.46e+005]	2.12e+005 [1.98 e+005 to 2.41 e+005]	-6.63 [-7.14 to -6.12]	2.34e-007 [7.21e-008 to 7.59e-007]
	18	2.26e+006 [8.84e+005 to 3.79e+006]	5.42e+006 [4.88e+006 to 6.02e+006]	-7.36 [-8.21 to -6.51]	4.35e-008 [6.11e-009 to 3.110e-007]
CB_2-Tango	**6**	4.75e+005 [2.82e+005 to 6.68e+005]	1.06e+006 [9.18e+005 to 1.20e+006]	-6.91 [-7.62 to -6.21]	1.22e-007 [2.43e-008 to 6.18e-007]
	8	1.12e+005 [6.57e+004 to 1.59e+005]	3.45e+005 [3.14e+005 to 3.76e+005]	-7.02 [-7.44 to -6.59]	9.58e-008 [3.58e-008 to 2.56e-007]
	18	n/a	n/a	n/a	n/a

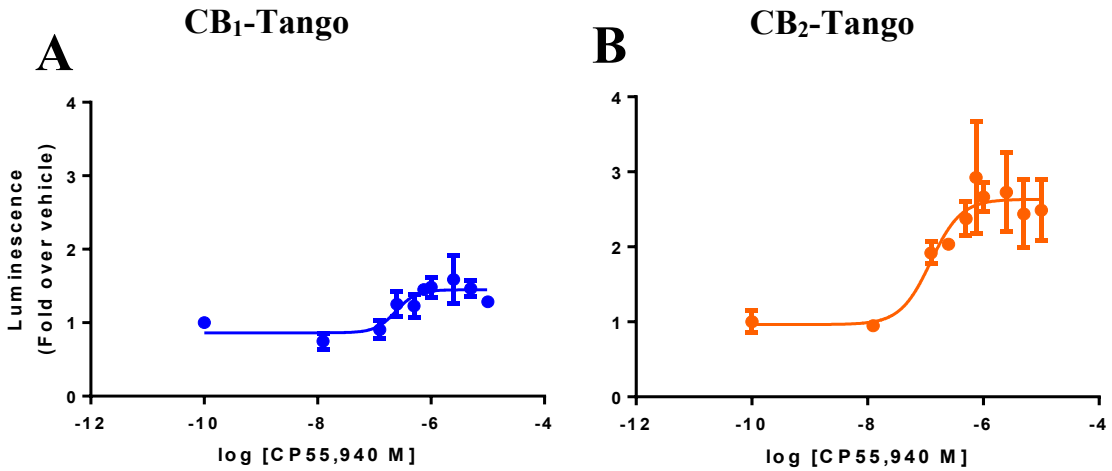

C

Receptor	E_{min}	E_{max}	Log EC_{50} (M)	EC_{50}	Z' Factor
CB_1-Tango	0.86 [0.72 to 1.01]	1.49 [1.34 to 1.56]	-6.62 [-6.87 to -6.37]	2.40e-007 [1.34e-007 to 4.28e-007]	0.47
CB_2-Tango	0.96 [0.63 to 1.30]	2.6 [2.38 to 2.88]	-6.91 [-7.03 to -6.61]	1.23e-007 [6.22e-008 to 2.44e-007]	< 0.00

Figure 3.3. Assessment of Assay Sensitivity in Cells Transfected with CB_1-Tango or CB_2-Tango cDNA

Concentration response data from HTLA cells transiently transfected with either 25 ng of CB_1-Tango or CB_2-Tango cDNA using Lipofectamine® 3000 using the standard Tango Assay. **(A, B)** Concentration response curves represent CP 55,940 induced β-arrestin2 mobilization to activated CB_1-Tango or CB_2-Tango after 8 hr of incubation with agonist. Luminescence (Fold over vehicle) was obtained by dividing RLU from cells treated with increasing concentrations of CP 55,940 with cells treated with vehicle only (0.1% MeOH). Data are presented as mean +/- SD; n=3 from a single experiment. **(C)** E_{min}, E_{max}, Log EC_{50} and EC_{50} values of CP 55,940 at CB_1-Tango or CB_2-Tango. Z' factors were calculated from cells treated with vehicle and cells treated with 10 µM CP 55,940. Data are presented as mean +/- 95% CI; n=3 from a single experiment.

Figure 3.4. The Effect of Serum Starvation on CB_1-Tango Assay Sensitivity
Concentration response data from HTLA cells transiently transfected with 25 ng of CB_1-Tango cDNA using Lipofectamine® 3000 using three different cell culture conditions. **(A)** Concentration response curves represent CP 55,940 induced β-arrestin2 mobilization to activated CB_1-Tango after 8 hr of incubation with agonist using cell culture protocol A, B and C as indicated. Luminescence (Fold over vehicle) was obtained by dividing RLU from cells treated with increasing concentrations of CP 55,940 by cells treated with vehicle (0.1% MeOH). Data are presented as mean +/- SD; n=3 from a single experiment **(B)** E_{max} values of CP 55,940 activity at CB_1-Tango. Z' factors were calculated from ccells treated with vehicle and ccells treated with 10 μM CP 55,940. Data are presented as mean +/- 95% CI; n=3 from a single experiment.

A

Protocol A

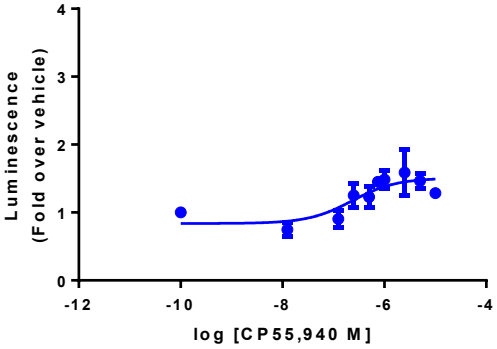

Protocol B

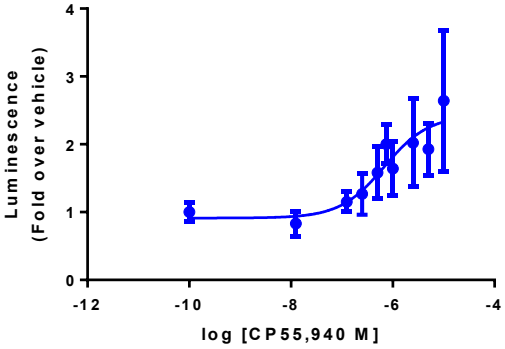

Protocol C

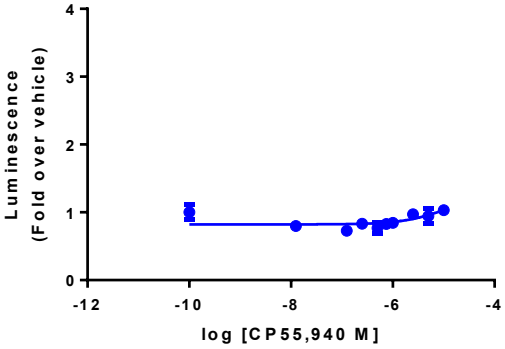

B

Protocol	E_{max}	Z' Factor	Assay Accuracy
A	1.45 [1.34 to 1.56]	0.47	Moderate
B	2.90 [0.01 to 5.78]	< 0.0	Poor
C	0.99 [0.91 to 1.07]	< 0.0	Poor

Figure 3.5. The Effect of Serum Starvation on CB_2-Tango Assay Sensitivity
Concentration response data from HTLA cells transiently transfected with 25 ng of CB_2-Tango cDNA using Lipofectamine® 3000 using three different culture conditions. **(A)** Concentration response curves represent CP 55,940 induced β-arrestin2 mobilization to activated CB_2-Tango after 8 hr of incubation with agonist using cell culture protocol A, B and C as indicated. Luminescence (Fold over vehicle) was obtained by dividing RLU from ccells treated with increasing concentrations of CP 55,940 by ccells treated with vehicle (0.1% MeOH). Data are presented as mean +/- SD; n=3 from a single experiment **(B)** E_{max} values of CP 55,940 activity at CB_2-Tango. Z' factors were calculated from cells treated with vehicle and cells treated with 10 μM CP 55,940. Data are presented as mean +/- 95% CI; n=3 from a single experiment.

A

Protocol A

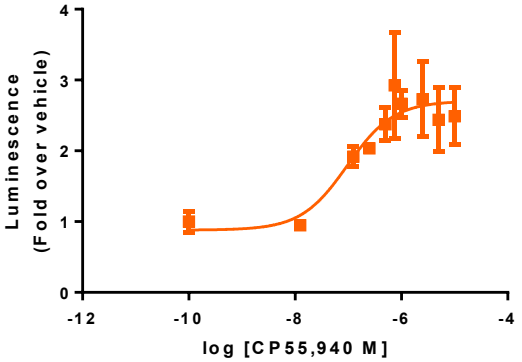

Protocol B

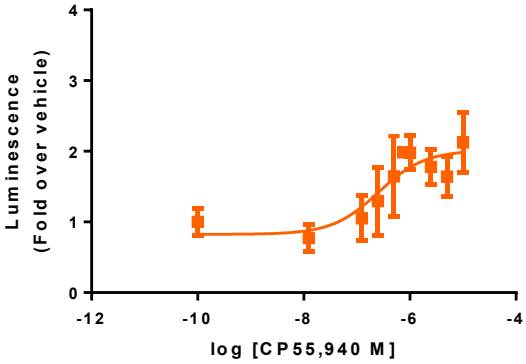

Protocol C

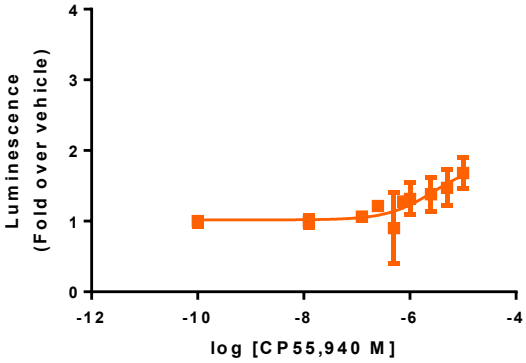

B

Protocol	E_{max}	Z' Factor	Assay Accuracy
A	2.64 [2.38 to 2.88]	< 0.0	Poor
B	1.90 [1.70 to 2.11]	< 0.0	Poor
C	2.56 [-7.01 to 12.13]	< 0.0	Poor

Figure 3.6. Comparison of PEI and Lipofectamine® 3000 Transfection on CP 55,940-dependant concentration-response in CB_1-Tango Assay

Tango data from HTLA cells transiently transfected with 25 ng of CB_1-Tango cDNA using Lipofectamine® 3000 or PEI. **(A)** Concentration-response curves represent CP 55,940 induced β-arrestin2 mobilization to activated CB_1-Tango after 8 hr of incubation with agonist. Luminescence (Fold over vehicle) was obtained by dividing RLU from cells treated with increasing concentrations of CP 55,940 with cells treated with vehicle (0.1% MeOH). Data presented as mean +/- SD **(B)** E_{max} values for CB_1-Tango assay in cells transfected with Lipofectamine® 3000 or PEI. Data are presented as mean +/- SD; n=3 from a single experiment. **(C)** E_{min}, E_{max}, Log EC_{50} and EC_{50} values of CP 55,940 activity at CB_1-Tango. Z' factors were generated based on RLU data of vehicle treated cells and cells treated with 10 μM CP 55,940. Data are presented as mean +/- 95% CI; n=3 from a single experiment; * indicates $p > 0.05$ between transfection methods.

A

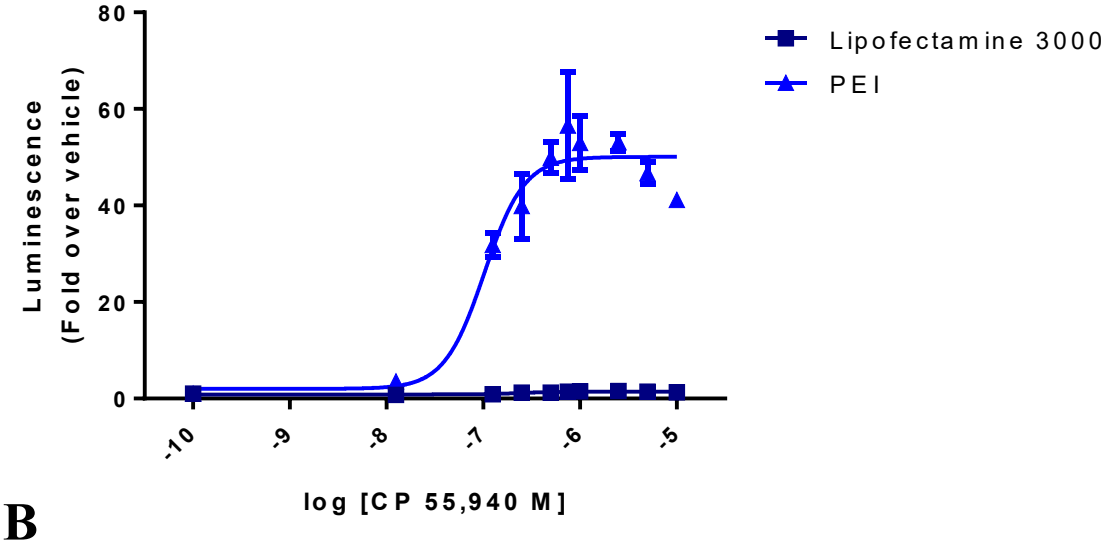

B

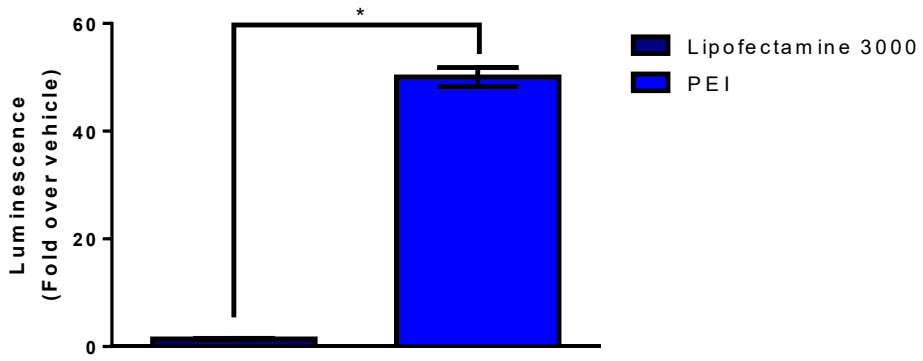

C

Receptor	Transfection Reagent	E_{max}	Log EC_{50} (M)	EC_{50} (M)	Z' Factor
CB_1-Tango	Lipofectamine® 3000	1.45 [1.34 to 1.56]	-6.62 [-6.87 to -6.37]	2.34e-007 [1.34e-007 to 4.28e-007]	0.47
	PEI	50.10* [46.42 to 53.69]	-6.99 [-7.17 to -6.80]	1.03e-007 [6.79e-008 to 1.58e-007]	0.88

Figure 3.7. Comparison of PEI and Lipofectamine 3000® Transfection on CP 55,940-Dependant concentration response in CB_2-Tango Assay

Tango data from HTLA cells transiently transfected with 25 ng of CB_2-Tango cDNA using Lipofectamine® 3000 or PEI. **(A)** Concentration response curves represent CP 55,940 induced β-arrestin2 mobilization to activated CB_2-Tango after 8 hr of incubation with agonist. Luminescence (Fold over vehicle) was obtained by dividing RLU from cells treated with increasing concentrations of CP 55,940 with cells treated with vehicle (0.1% MeOH). Data presented as mean +/- SD. **(B)** E_{max} values for CB_2-Tango assay in cells transfected with Lipofectamine® 3000 or PEI. Data are presented as mean +/- SD **(C)** E_{min}, E_{max}, Log EC_{50} and EC_{50} values of CP 55,940 activity at CB_1-Tango. Z' factors were generated based on RLU data of vehicle treated cells and cells treated with 10 μM CP 55,940. Data are presented as mean +/- CI; n=3 from a single experiment; * indicates $p > 0.05$ between transfection methods.

A

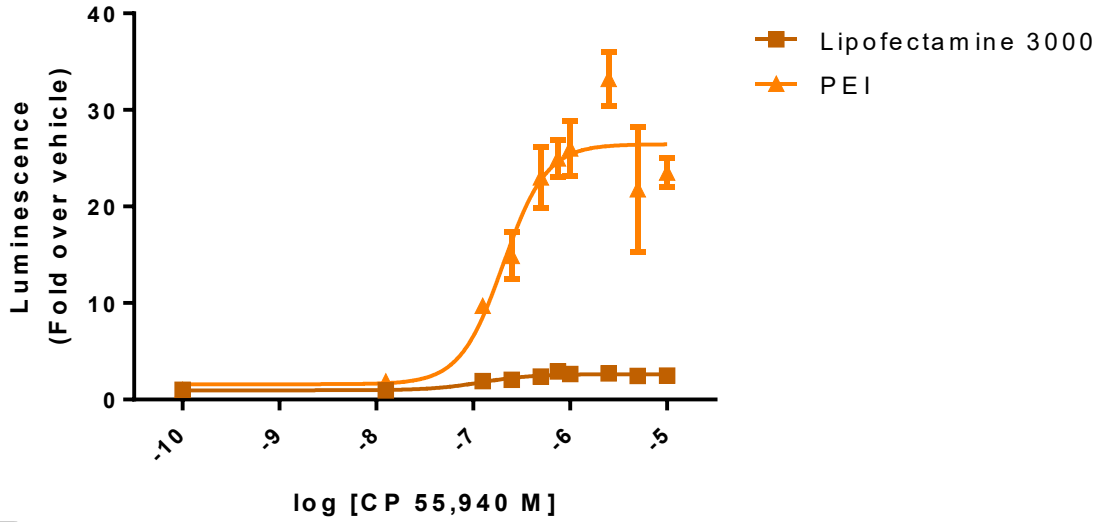

B

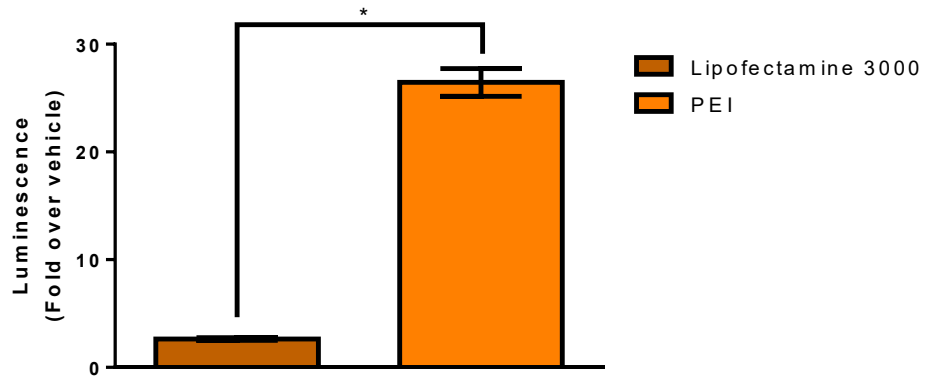

C

Receptor	Transfection Reagent	E_{max}	Log EC_{50} (M)	EC_{50} (M)	Z' Factor
CB_2-Tango	Lipofectamine® 3000	2.64 [2.38 to 2.88]	-6.91 [-7.21 to -6.61]	1.23e-007 [6.22e-008 to 2.44e-007]	< 0.00
	PEI	26.42 * [23.80 to 29.1]	-6.69 [-6.85 to -6.53]	2.04e-007 [1.42e-007 to 2.94e-007]	0.77

Figure 3.8. The Effect of ACEA Relative to CP,55940 on β-Arrestin Recruitment to CB_1-Tango

Tango data from HTLA cells transiently transfected with 25 ng of CB_1-Tango cDNA using PEI. **(A, B)** Concentration response curves represent CP 55,940, ACEA, or HU308 induced β-arrestin2 mobilization to activated CB_1-Tango after 8 hr of incubation with agonist, as indicated. Luminescence (Fold over vehicle) was obtained by dividing RLU from cells treated with increasing concentrations of CP 55,940 with cells treated with vehicle (0.1% MeOH or EtOH or DMSO) from the same treatment. Data presented as mean +/- SD; n=3 from a single experiment.

A

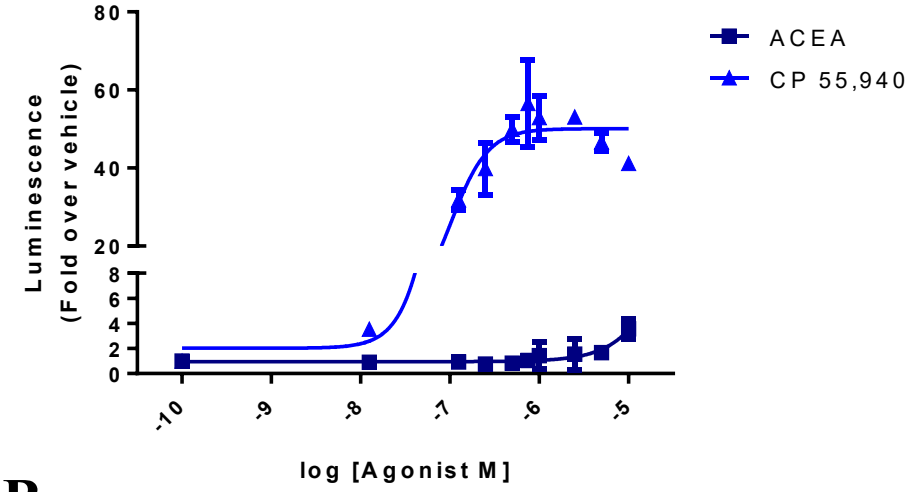
Luminescence
(Fold over vehicle)
80
60
40
20
8
6
4
2
0
-10
-9
-8
-7
-6
-5
log [Agonist M]
ACEA
CP 55,940

B

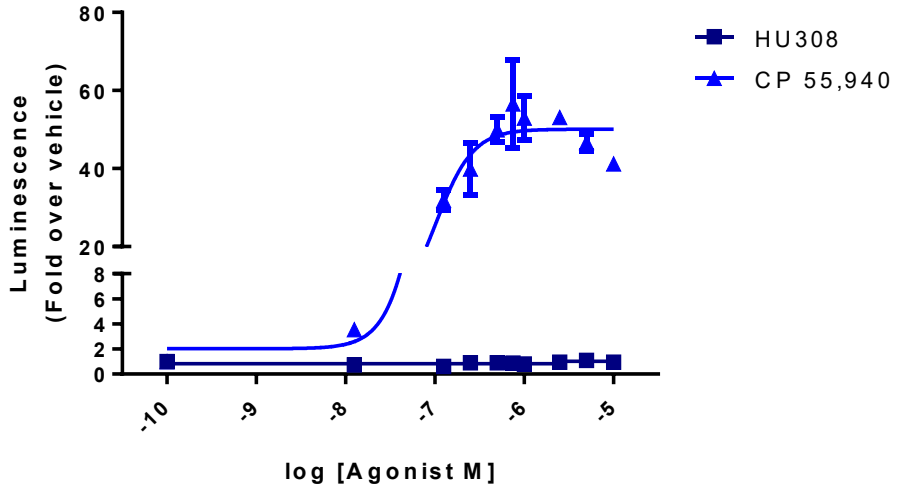
Luminescence
(Fold over vehicle)
80
60
40
20
8
6
4
2
0
-10
-9
-8
-7
-6
-5
log [Agonist M]
HU308
CP 55,940

Figure 3.9. The Effect of HU308 Relative to CP,55940 on β-Arrestin Recruitment to CB_2-Tango

Tango data from HTLA cells transiently transfected with 25 ng of CB_2-Tango cDNA using PEI. **(A, B)** Concentration response curves represent CP 55,940, ACEA, or HU308 induced β-arrestin2 mobilization to activated CB_2-Tango after 8 hr of incubation with agonist, as indicated. Luminescence (Fold over vehicle) was obtained by dividing RLU from cells treated with increasing concentrations of CP 55,940 with cells treated with vehicle (0.1% MeOH or EtOH or DMSO) from the same treatment. Data presented as mean +/- SD; n=3 from a single experiment.

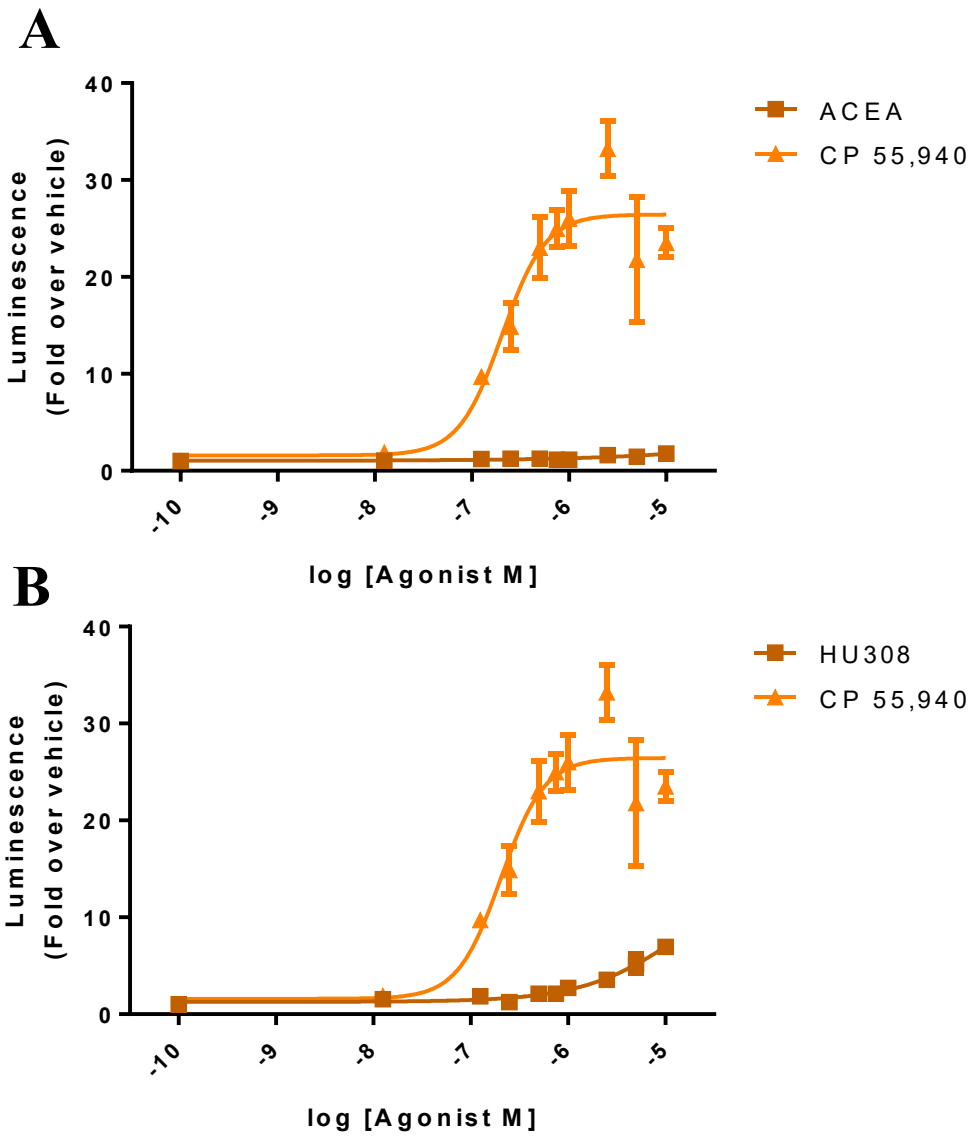
A
Luminescence
(Fold over vehicle)
40
30
20
10
0
-10
-9
-8
-7
-6
-5
log [Agonist M]
ACEA
CP 55,940
B
Luminescence
(Fold over vehicle)
40
30
20
10
0
-10
-9
-8
-7
-6
-5
log [Agonist M]
HU308
CP 55,940

Figure 3.10. The Effect of Normalization on CB_1-Tango Assay Variability
Tango data from HTLA cells transiently transfected with 25 ng of CB_1-Tango cDNA using PEI. Concentration response curves represent CP 55,940 induced β-arrestin2 mobilization to activated CB_1-Tango after 8 hr of incubation with agonist. **(A)** Luminescence (RLU) was obtained by dividing raw luminescence from cells treated with increasing concentrations of CP 55,940 with β-galactosidase emissions (420 nm) from cell lysate taken from the same cells. **(B)** Luminescence (Fold over vehicle) was obtained by dividing RLU from cells treated with increasing concentrations of CP 55,940 by cells treated with vehicle only (0.1% MeOH) from the same plate. **(C)** % Luminescence was generated by scaling all RLU to cells treated with 2.5 μM CP 55,940, which was set to 100% luminescence. All scaling was done within the same plate before combining replicate values. Data are presented as a mean +/- SD; n=6, experiments carried out on 6 different days.

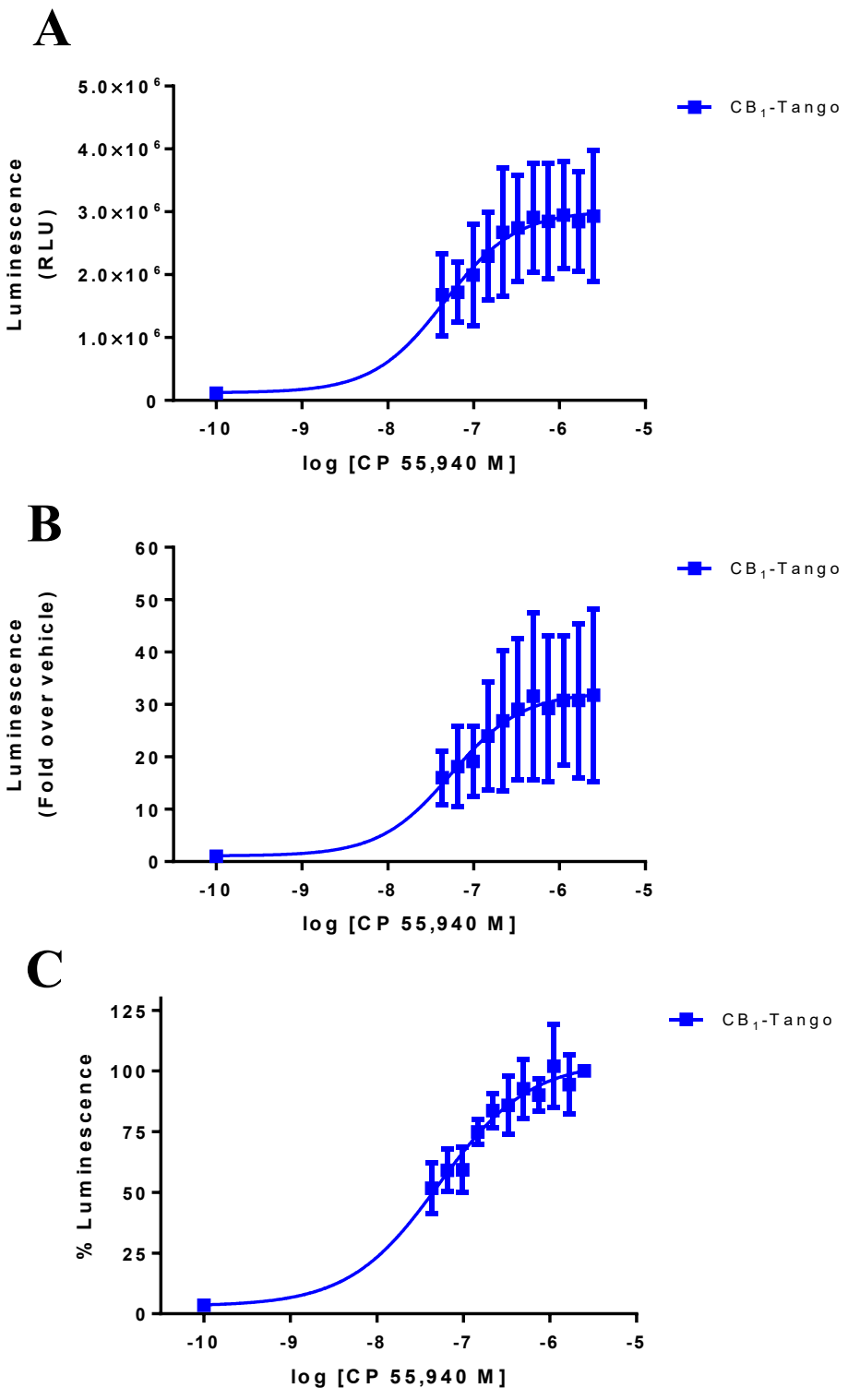
A
Luminescence (RLU)
5.0×10^6
4.0×10^6
3.0×10^6
2.0×10^6
1.0×10^6
0
-10
-9
-8
-7
-6
-5
log [CP 55,940 M]
CB1-Tango
B
Luminescence (Fold over vehicle)
60
50
40
30
20
10
0
-10
-9
-8
-7
-6
-5
log [CP 55,940 M]
CB1-Tango
C
% Luminescence
125
100
75
50
25
0
-10
-9
-8
-7
-6
-5
log [CP 55,940 M]
CB1-Tango

Figure 3.11. The Effect of Normalization on CB_2-Tango Assay Variability
Tango data from HTLA cells transiently transfected with 25 ng of CB_2-Tango cDNA using PEI. Concentration response curves represent CP 55,940 induced β-arrestin2 mobilization to activated CB_2-Tango after 8 hr of incubation with agonist. **(A)** Luminescence (RLU) was obtained by dividing raw luminescence from cells treated with increasing concentrations of CP 55,940 with β-galactosidase emissions (420 nm) from cell lysate taken from the same cells. **(B)** Luminescence (Fold over vehicle) was obtained by dividing RLU from cells treated with increasing concentrations of CP 55,940 by cells treated with vehicle only (0.1% MeOH) from the same plate. **(C)** % Luminescence was generated by scaling all RLU to cells treated with 2.5 μM CP 55,940, which was set to 100% luminescence. All scaling was done within the same plate before combining replicate values. Data are presented as a mean +/- SD; n=3 independent experiments carried out on 3 different days.

A

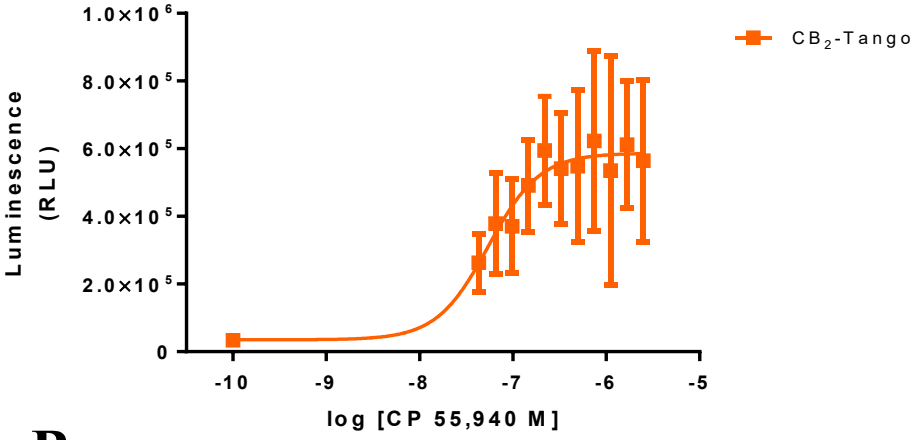
1.0×10 6
8.0×10 5
6.0×10 5
4.0×10 5
2.0×10 5
0
Luminescence (RLU)
-10
-9
-8
-7
-6
-5
log [CP 55,940 M]
CB2-Tango

B

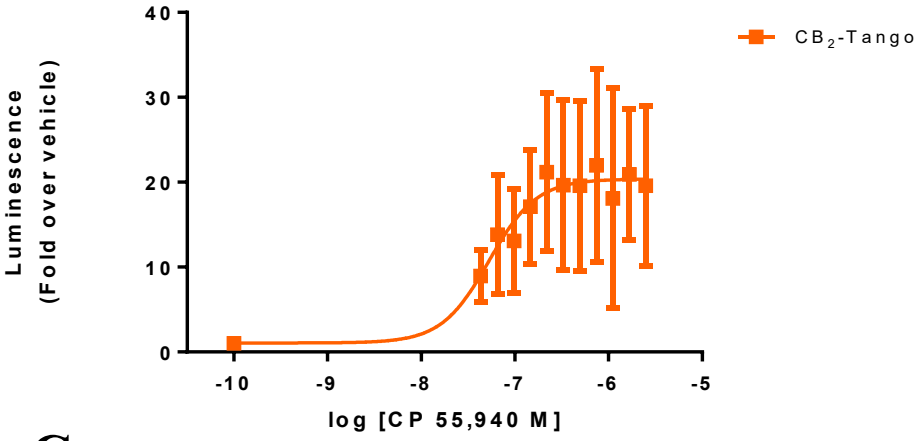
40
30
20
10
0
Luminescence (Fold over vehicle)
-10
-9
-8
-7
-6
-5
log [CP 55,940 M]
CB2-Tango

C

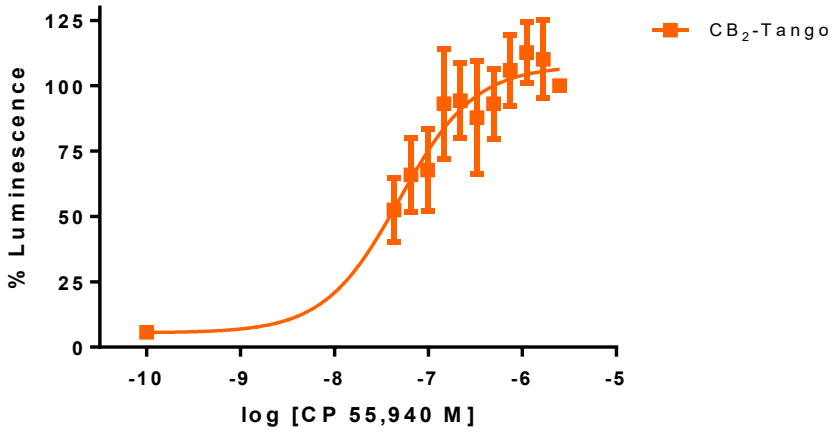
125
100
75
50
25
0
% Luminescence
-10
-9
-8
-7
-6
-5
log [CP 55,940 M]
CB2-Tango

3.2 Allosteric Interactions Between the CB_1 and CB_2 Receptor Modulate β-Arrestin2 Recruitment

3.2.1 CB_1 and CB_2 are Co-Expressed and Co-Localize in Transiently Transfected HEK293T Cells

HEK293T cells were transfected in 12-well plates lined with PDL-coated 12mm coverslips with empty pcDNA3.1 vector backbone, CB_1_pcDNA, 3xHA-CB_2, or a combination of CB_1_pcDNA and 3xHA-CB_2 72 hours before treatment with primary antibodies against CB_1 and HA-tagged CB_2. Cells transfected with only pcDNA backbone did not display anti-CB_1 or HA-CB_2 dependant staining (Fig. 3.12). HEK293T cells transfected with 125ng CB_1_pcDNA were positive for CB_1-dependant immunofluorescence but lacked ant-HA-dependant staining (Fig. 3.13). Likewise, 3xHA-CB_2 transfection resulted in positive staining for the anti-HA antibody and lacked fluorescence staining for CB_1 (Fig. 3.14). Finally, co-transfected cells were positive for both anti-CB_1 and HA-tagged CB_2. In addition to dual staining in the same cells, certain cells were positive for yellow staining, indicating that receptors were close enough in proximity to cause overlap between the red (CB_1) and green (HA-CB_2) channels, indicative of receptor co-localization. Notably, despite pre-mixing plasmids encoding both receptors before transfection, not all cells co-expressed CB_1 and HA-CB_2 (Fig. 3.15).

3.2.2 Co-Expression of CB_1 and CB_2 Reduced CP 55,940-Induced β-arrestin2 Recruitment to CB_1 in Transiently Transfected HTLA Cells

To determine if β-arrestin2 translocation was altered in cells co-expressing CB_1 and CB_2, we measured β-arrestin2 recruitment via the Tango reporter assay in cells transfected with CB_1-Tango or CB_2-Tango and non-Tango CB_1 or CB_2 cDNA. Tango receptors will be called CB_1-Tango or CB_2-Tango, while receptors without the Tango reporter will be

referred to as either CB_1 or CB_2 throughout this thesis. Several combinations of Tango and non-Tango receptor combinations were treated with CP 55,940 to selectively measure β-arrestin2 recruitment to each receptor partner and to measure cumulative changes in β-arrestin2 recruitment to both Tango receptors. In either case, Tango-dependant luminescence was compared to luminescence of cells transfected with either CB_1-Tango or CB_2-Tango alone, in the same plate. Replicate data from experiments carried out on independent days was combined to determine the effect of treatment and receptor composition.

The CP 55,940-induced E_{max} of cells transfected with CB_1-Tango and CB_2 was73.34% relative to cells expressing CB_1-Tango alone (E_{max}=106.00; Fig. 3.16). This is interpreted as a ~33% reduction (CI 0.22 to 65.88; p=0.048) in β-arrestin2 recruitment to the CB_1 receptor in the presence of CB_2 following non-selective activation of both receptors. While there appears to be a modest shift to the right in the dose-response curve (Fig. 3.16), there was no significant difference in the EC_{50} of CP 55,940 between transfection groups (Fig. 3.16B). To ensure that the transfection of CB_2 cDNA did not result in any luminescence, cells transfected with 25 ng of CB_2 were treated with increasing concentrations of CP 55,940. Following stimulation with CP 55,940 non-Tango-tagged CB_2 did not produce any luminescence (Fig. 3.16). To control for the effect of doubling the relative concentration of receptor-encoding plasmid cDNA on detectable luminescence, an additional group was transfected with CB_1-Tango and non-Tango CB_1. There was no difference in luminescence between cells transfected with CB_1-Tango compared to CB_1-Tango and CB_1 (Fig. 3.17). The CP 55,940-induced E_{max} in cells co-transfected with both CB_1-Tango and CB_2-Tango receptor cDNA was not

different than that observed in cells transfected with CB_1-Tango alone (Fig. 3.18A). To ensure that this was not due to a limited amount of TEV-B-arrestin2 fusion protein in the HTLA cells or luciferase, and to determine the upper limits for detection of luminescence, we also transfected cells with double the mass of CB_1-Tango cDNA. Following treatment with CP 55,940, cells transfected with 50 ng cDNA for CB_1-Tango showed a significant increase in peak luminescence of ~64% ($p=0.002$; CI 32.46 to 95.54%) relative to cells transfected with 25 ng cDNA for CB_1-Tango and a ~74% ($p=0.008$; CI 43.10 to 106.2%) increase relative to those transfected with CB_1-Tango and CB_2-Tango (Fig. 3.18B/Table 3.2). Neither TEV-linked β-arrestin2, luciferase or the luciferase detection levels were limiting factors in the assay. As such, we assumed that an allosteric interaction between CB_1 and CB_2 lead to a net decrease in total β-arrestin2 translocation in cells expressing both CB_1-Tango and CB_2.

To directly compare CP 55,940-induced β-arrestin2 recruitment between all transfection groups, experiments were repeated using an alternative experimental design. Plates were transfected with CB_1-Tango or CB_2-Tango, CB_1-Tango and CB_2, and CB_1-Tango and CB_2-Tango in different rows and treated with 125 nM CP 55,940. This dose was selected as it represents the ~EC_{70} for CP 55,940 to recruit β-arrestin2 to both CB_1 and CB_2. EC_{70} was selected to detect changes in the upper and lower ends of detectable changes in luminescence. This method was used to express β-arrestin2-dependant luminescence in each transfection condition, relative to cells transfected with CB_1-Tango alone. CP 55,940 induced ~48% less ($p<0.001$; CI 28.78 to 67.23%) β-arrestin2-dependant luminescence in CB_2-Tango than CB_1-Tango, whereas the response in cells transfected with CB_1-Tango and CB_2 were ~30% lower ($p=0.002$; CI 10.33 to 48.78%)

than that observed for cells expressing CB_1-Tango (Fig. 3.19). Both CB_2-Tango and CB_1-Tango and CB_2 groups were significantly lower than cells transfected with CB_1-Tango and CB_2-Tango ($p<0.001$, respectively). While the lower relative efficacy of CP 55,940 to recruit β-arrestin2 to CB_2-Tango, relative to CB_1-Tango, is of note, it does not explain the lack of increased luminescence when both Tango plasmids were co-transfected and co-activated.

3.2.3 Co-Expression of CB_1 and CB_2 Reduces CP 55,940-Induced B-arrestin2 Recruitment to CB_2 in Transiently Transfected HTLA Cells

In addition to testing changes in β-arrestin2-recruitment CB_1-Tango following CP 55,940 stimulation (section 3.2.2), we also assessed the same changes relative to CB_2. HTLA cells were transfected with CB_2-Tango in the presence and absence of Tango and non-Tango labelled CB_1 and CB_2-encoding plasmids. Agonist-dependant luminescence was expressed relative to that observed in cells expressing CB_2-Tango only in, assays performed within the same plate. Replicate data was generated following independent experiments carried out on different days.

CP 55,940 stimulation of cells transfected with CB_2-Tango and CB_1 resulted in an E_{max} of 73.44% relative to cells transfected with CB_2-Tango only. This indicated that the presence of CB_1 reduced β-arrestin2 recruitment to CB_2 by ~37% ($p=0.013$; CI 8.98 to 67.74%) when both receptors were co-agonised (Fig. 3.20). The decreased efficacy of CP 55,940 to induce β-arrestin2 recruitment to CB_2-Tango in the presence of CB_1 was not accompanied by a change in potency, as no change in EC_{50} was observed (Fig. 3.21). CP 55,940 treatment in cells transfected with CB_1 alone did not induce any luminescence. In contrast with the levels of β-arrestin2 recruitment observation in cells co-transfected with

CB_2-Tango and CB_1, the E_{max} in cells transfected with 25 ng each CB_2-Tango and CB_2 cDNA were not different to cells transfected with CB_2-Tango alone ($p=0.677$) following treatment with CP 55,940.

CP 55,940-induced β-arrestin2 recruitment in cells transfected with both CB_1-Tango and CB_2-Tango cDNA yielded a ~64% ($p=0.011$; CI 14.40 to 113.40%) increase in luminescence relative to CB_2-Tango (Fig. 3.22A). Furthermore, the relative increase in β-arrestin2-dependant luminescence in CB_1-Tango and CB_2-Tango co-transfected cells was not different compared to that observed in cells transfected with two times the mass of CB_2-Tango (50 ng; Fig. 3.22B). To directly compare luminescence from cells of our different transfection groups to CB_2-Tango only, we transfected HTLA cells with CB_2-Tango, CB_1-Tango, CB_2-Tango and CB_1, and CB_1-Tango and CB_2-Tango before treating with 125 nM CP 55,940. CP 55,940 was roughly 2-fold more efficacious at recruiting β-arrestin2 to CB_1-Tango, relative to CB2-Tango ($p<0.001$; CI 56.87 to 130.91%; Fig. 3.23). As expected from dose-response experiments (Fig. 3.20), the presence of CB_1 reduced β-arrestin2 recruitment to CB_2 by ~39% ($p=0.034$; CI 2.46 to 76.44%). Inversely, combining CB_1-Tango and CB_2-Tango resulted in an approximately two-fold increase in total β-arrestin2 recruitment relative to CB_2-Tango ($p<0.001$; CI 76.03 to 150.01%). The relative level of β-arrestin2 recruitment in cells transfected with CB_1-Tango and CB_2-Tango was not different than cells transfected with CB_1-Tango only ($p=0.485$).

3.2.4 The Effect of Receptor Stoichiometry on Arrestin Recruitment to CB_1- and CB_2-Tango Receptors

Cannabinoid receptor expression is dynamic and has been shown to change during various CNS disease states (Zou and Kumar 2018). As such, we chose to model various expression levels of CB_1 and CB_2 receptors and determine if arrestin recruitment was altered in response to agonist stimulation. HTLA cells were transfected with a constant mass of 25 ng of either CB_1-Tango or CB_2-Tango cDNA alone or in combination with 5 ng, 25 ng, or 50 ng of CB_1 or CB_2 cDNA. Transfected cells were then treated with increasing concentrations of CP 55,940. To determine if any changes in β-arrestin2-dependant luminescence were due to specific interactions between CB_1 and CB_2, Tango and Non-Tango plasmids of the same cognate receptor were also co-transfected for comparison. To understand cumulative effects of both receptors, relative to either CB_1- or CB_2-Tango receptor alone, 25 ng of CB_1- or CB_2-Tango plasmids were also co-transfected with 5 ng, 25 ng, or 50 ng of the heteromer partner Tango plasmid.

Relative to cells transfected with CB_1-Tango only, cells transfected with an additional 25 ng of CB_2 produced ~33 % less arrestin-dependant luminescence ($p=0.048$; CI 0.22 to 65.90%), while cells transfected with an additional 50 ng CB_2 produced ~40% less luminescence ($p=0.020$; CI 6.92 to 72.61%) (Fig. 3.24A). β-arrestin recruitment in cells transfected with CB_1-Tango and 10 ng of CB_2 were not different than that observed in cells transfected with CB_1-Tango alone. There was no difference in luminescence between co-transfected cells with CB_1-Tango and 5 ng, 25 ng, or 50 ng CB_2 (Fig. 3.24A). Co-Transfection of 25 ng CB_1-Tango and 5 ng, 25 ng, or 50 ng of CB_1 did not produce any difference in luminescence compared to cells transfected with CB_1-Tango only (Fig

3.24B). Likewise, β-arrestin recruitment in cells transfected with 25 ng CB_1-Tango and 5 ng, 25 ng, or 50 ng of CB_2-Tango were not different to that observed in cells transfected with CB_1-Tango only (Fig. 3.24C). There was no significant change in the E_{max} between cells transfected with CB_1-Tango only, or in combination with CB_2, or CB_2-Tango plasmids at any ratio. So, a 1:1 and 1:2 ratio of CB_1:CB_2 were both able to illicit significant decreases in β-arrestin2 to CB_1-Tango but were not significantly different to one another. Furthermore, despite doubling, and tripling the transfected mass of Tango-receptor encoding plasmid, the addition of CB_2-Tango, at any level, was not different than luminescence relative to CB_1-Tango alone.

Relative to cells transfected with CB_2-Tango only, the addition of CB_1 at a mass of 25 ng, and 50 ng, resulted in a ~38% reduction in luminescence (p=0.0131; CI 8.98 to 67.71%) and ~45% reduction in luminescence (p=0.005; CI 16.4 to 75.2%), respectively (Fig. 3.25A). There was a ~31% reduction in arrestin dependant luminescence at CB_2-Tango when co-transfected with 50 ng of Non-Tango CB_2 (p=0.0315; CI 2.91 to 59.31%). Between CB_2 plasmid co-transfected groups, cells transfected with CB_2-Tango and 50 ng CB_2 emitted ~30% less luminescence than cells transfected with CB_2-Tango and 10 ng CB_2 (p=0.0357; 2.11 to 38.52%) (Fig. 3.25B). Following the addition of CB_1-Tango cDNA with CB_2-Tango, no significant difference was noted in cells transfected with 10 ng CB_1-Tango. However, the addition of 25 ng and 50 ng of CB_1-Tango resulted in a ~64% (p=0.012; CI 14.41 to 133%) and ~123% (p<0.0001; CI 73.50 to 172%), respectively, over cells transfected with CB_2-Tango alone. Furthermore, groups transfected with CB_2-Tango and 50 ng CB_1-Tango produced ~93% more luminescence than cells transfected with CB_2-Tango and 10 ng CB_1-Tango (p=0.001; CI 43.81 to

143%) and ~59% more luminescence than cells transfected with CB_2-Tango and 25 ng CB_1-Tango (p=0.0196; CI 9.60 to 109%) (Fig. 3.25C).

3.2.5 Selective Antagonism Potentiates CP 55,940-Dependant β-arrestin2 Recruitment in Cells Co-Transfected with CB_1 and CB_2

Next, we aimed to determine if selective antagonism of CB_1 or CB_2 could influence β-arrestin2 recruitment to the opposite receptor following treatment with CP 55,940. We used the selective antagonists/inverse agonists AM251 (306-fold selective for CB_1 over CB_2; Tocris, UK) and AM630 (165-fold selective for CB_2 over CB_1; Tocris, UK.

The first step in assessing the potential for cross-antagonism in cells transfected with CB_1 and CB_2 receptors was to determine the relative selectivity of the antagonists AM251 and AM630 following treatment with 125 nM CP 55,940 with respect to β-arrestin recruitment. As expected, AM251 was more efficacious at antagonising CP 55,940-dependant arrestin mobilization to CB_1 with an IC_{50} of 12.51 nM (Fig. 3.26) relative to CB_2. AM251 was able to block CP 55,940-induced β-arrestin2 recruitment to CB_2 but at much higher concentrations than CB_1, with an IC_{50} at CB_2 of 760.60 nM (Fig. 3.27). On the other hand, AM630 was able to block CP 55,940 activity at CB_2 and CB_1, albeit with a ~4-fold higher potency at CB_2. Specifically, AM630 exhibited an IC_{50} of 1210.00 nM at the CB_1 receptor (CI 758.21 nM to 1865.02 nM; Fig. 3.28) and an IC_{50} of 291.50 nM at CB_2 (CI 216.22 nM to 402.81 nM; Fig. 3.29). Of note, the reported CB_2-selective ligand AM630 was able to inhibit β-arrestin2 recruitment to CB_1 following CP 55,940 agonism by ~99% at micromolar concentrations and achieved sub-maximal inhibition at nanomolar concentrations (Fig. 3.28). The CB_1-selective AM251 was not

able to maximally inhibit CP 55,940-induced arrestin recruitment to CB_2 at any of the concentrations tested (Fig. 3.27).

Next, we quantified the differences in CP 55,940 receptor activation in cells expressing CB_1-Tango and CB_2, or CB_2-Tango and CB_1, relative to cells transfected with either Tango plasmid alone in the presence of selective antagonists. There was no difference in AM251 IC_{50} in cells expressing CB_1-Tango and CB_2, relative to those expressing CB_1-Tango alone (Fig. 3.30). We could not fit data from AM251 treatment in cells co-expressing CB_2-Tango and CB_1 which precluded a comparison of IC_{50} values between cells transfected with CB_2-Tango and CB_2-Tango and CB1 to a curve (Fig. 3.31). There was no difference in AM630 IC_{50} in cells transfected with CB_1-Tango and CB_2, relative to CB_1-Tango only (Fig. 3.32). Similarly, the AM630 IC_{50} value of cells transfected with CB_2-Tango did not differ compared to the AM630 IC_{50} value observed in cells transfected in CB_2-Tango and CB_1 (Fig. 3.33). In each experiment where Tango receptors were treated with their receptor-selective antagonist, co-expression of a CB receptor with Tango reporter and a non-Tango CB receptor resulted in a lower Emax compared to cells transfected with only the CB-Tango plasmid (Fig. 3.30/Fig.3.33). This pattern persisted in cells expressing CB_1-Tango and CB_2 following AM630 treatment (Fig. 3.32), while AM251 in cells co-expressing CB_2-Tango and CB_1 appeared to block this difference (Fig. 3.31).

To directly compare the effect of antagonist treatment on CP 55,940-induced β-arrestin2 recruitment between transfection groups, and to resolve the poor curve generation from cells expressing CB_2-Tango and CB_1 following AM251 treatment, we also transfected separate rows of a 96-well plate with CB_1-Tango, CB_1-Tango and CB_2,

CB_2-Tango, CB_2-Tango and CB_1, and CB_1-Tango and CB_2-Tango. Each group was treated with either vehicle (SFM with 0.1% MeOH and 0.1%DMSO), 125 nM CP 55,940, or 125 nM CP 55,940 with 500 nM AM251 or AM630, or 500 nM AM251 or AM630 alone. In this instance, 100% β-arrestin2 recruitment was assigned to cells treated with CP 55,940 from the same transfection group. In cells co-expressing CB_1-Tango and CB_2-Tango, AM251 was able to induce a ~53% reduction in β-arrestin2 recruitment relative to cells treated with 125 nM CP 55,940 only ($p<0.001$; CI 39.42 to 67.02%), which was ~41% less efficacious than in cells transfected with CB_1-Tango only ($p<0.001$; CI 26.99 to 54.60%; Fig. 3.34A) and ~45% more efficacious relative to cells transfected with CB_2-Tango only ($p<0.001$; CI 22.96 to 67.67%; Fig. 3.34B). AM630 antagonism in CB_1-Tango/CB_2-Tango co-transfected cells was able to induce a ~27% reduction in β-arrestin2 recruitment ($p<0.001$; CI 13.72 to 41.32%) compared to CP 55,940 treatment in the same cell group. This level of inhibition was no different than the efficacy of AM630 in cells transfected with CB_1-Tango only (Fig. 3.34A), and ~23% less efficacious than in cells transfected with CB_2-Tango only ($p<0.042$; CI 0.36 to 45.06%; Fig. 3.34B). In summary, AM251 and AM630 had a lower relative efficacy in cells co-transfected with CB_1-Tango and CB_2-Tango, compared to their efficacy in CB_1-Tango and CB_2-Tango expressing cells, respectively. As these differences could be explained by the addition of the second CP 55,940 activated cannabinoid receptor, we also mirrored this experiment in cells co-expressing CB_1-Tango and CB_2, and CB_2-Tango and CB_1. AM251 was able to maximally inhibit CP 55,940-induced β-arrestin2 recruitment in cells transfected with CB_1-Tango alone, and in cells transfected with CB_1-Tango and CB_2. Treatment with AM630 was able to reduce β-arrestin2 recruitment in CB_1-Tango cells by ~29% (P<

0.001; CI 19.40-39.19%), while AM630 inhibited β-arrestin2 by ~15% in cells transfected with CB_1-Tango and CB_2 ($p<0.001$; CI 4.86 to 24.65%) (Fig. 3.35A). In CB_1-Tango/CB_2 cells, AM630 was able to inhibit CP 55,940 β-arrestin2 recruitment with ~14% less efficacy than in CB_1-Tango only cells. In cells transfected with CB_2-Tango, AM251 was not able to inhibit β-arrestin2 recruitment. In cells co-transfected with CB_2-Tango and CB_1, AM251 increased β-arrestin2 recruitment to CB_2-Tango by ~46% over CB_2-Tango cells treated with AM251 ($p<0.001$; CI 18.55 to 73.08%). The same increase in β-arrestin2 recruitment to CB_2-Tango in co-transfected cells corresponded to a ~38% increase in β-arrestin2 recruitment over treated with CP 55,940 activation in either CB_2-Tango only or co-transfected cells ($p<0.001$; CI 18.55 to 73.08%; Fig. 3.35B). There was no difference in the ability of AM630 to inhibit CP 55,940-induced β-arrestin2 recruitment in cells transfected with CB_2-Tango alone or in the presence of CB_1 (Fig. 3.35B). In short, it appears that antagonising CB_1 or CB_2 in cells co-expressing CB_1 and CB_2 exerted agonist-like effects on the partner receptor.

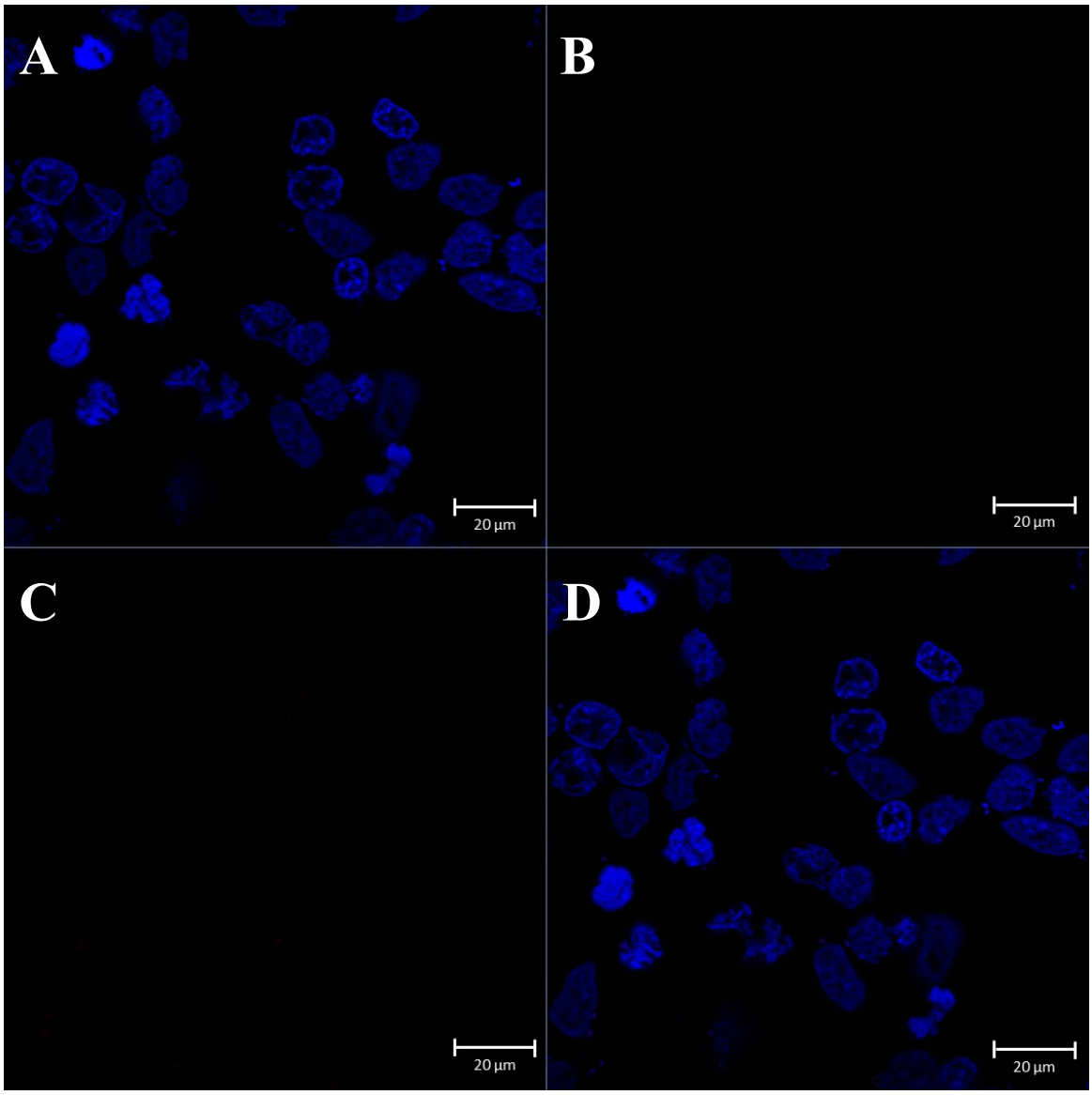

Figure 3.12. The Effect of pcDNA3.1 Transfection on Anti-CB_1 and Anti-HA Primary Antibody Dependant Immunofluorescence

Confocal microscopy images of HEK293A cells transiently transfected with empty pcDNA3.1 backbone (0.5 µg). Panels represent DAPI stained nuclei **(A)**, anti-HA primary antibody **(B)**, anti-CB_1 primary antibody **(C)**, and merged channels **(D)**. All panel images are split from the same confocal image. Protein colocalization is shown in yellow in merged panels. Scale bars, 20 µm.

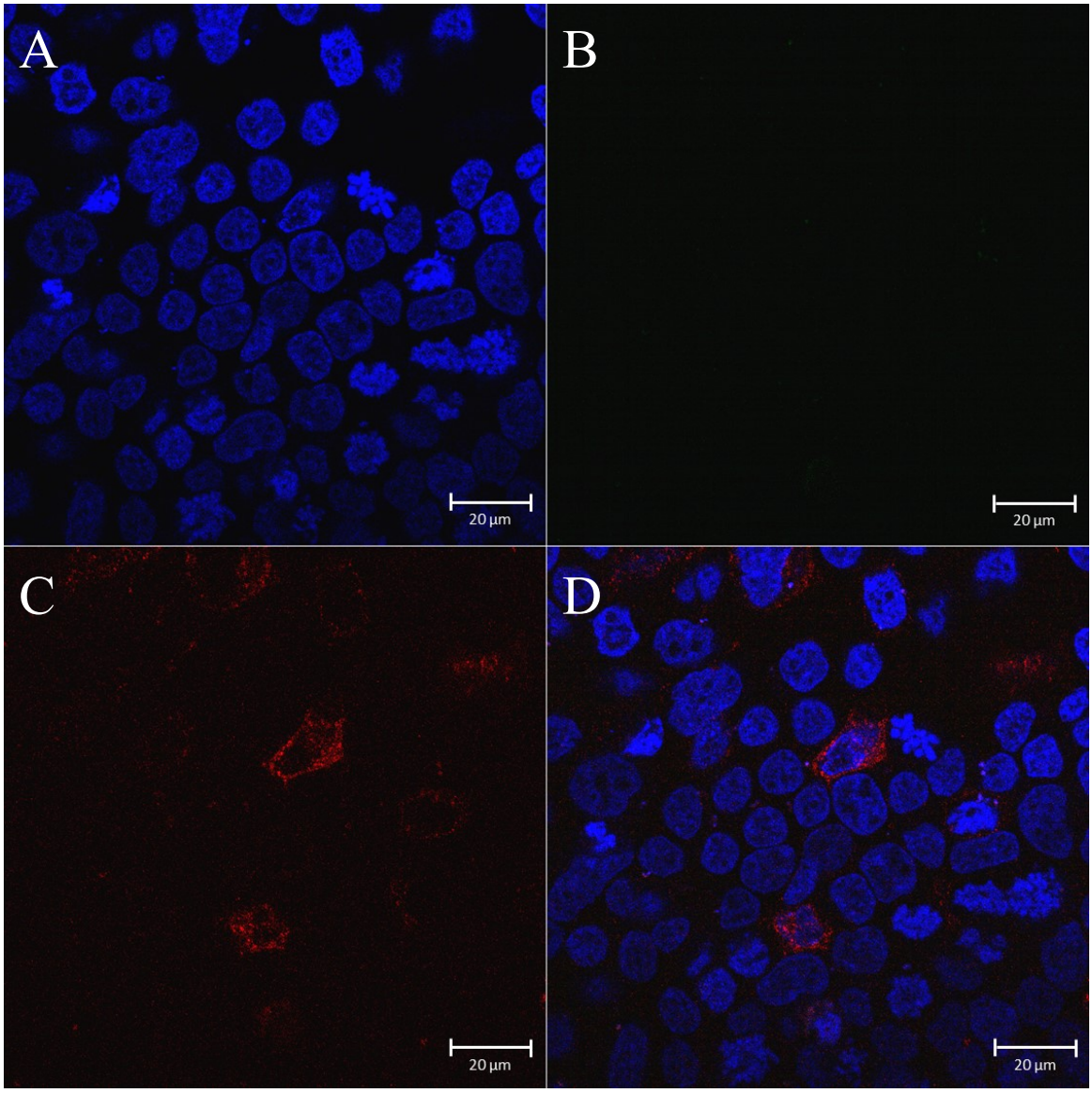

Figure 3.13. The Effect of CB_1_pcDNA Transfection on Anti-CB_1 and Anti-HA Primary Antibody Dependant Immunofluorescence

Confocal microscopy images of HEK293A cells transiently transfected with 3xHA-CB_2 cDNA (0.125 µg). Panels represent DAPI stained nuclei **(A)**, anti-HA primary antibody **(B)**, anti-CB_1 primary antibody **(C)**, and merged channels **(D)**. All panel images are split from the same confocal image. Protein colocalization is shown in yellow in merged panels. Scale bars, 20 µm.

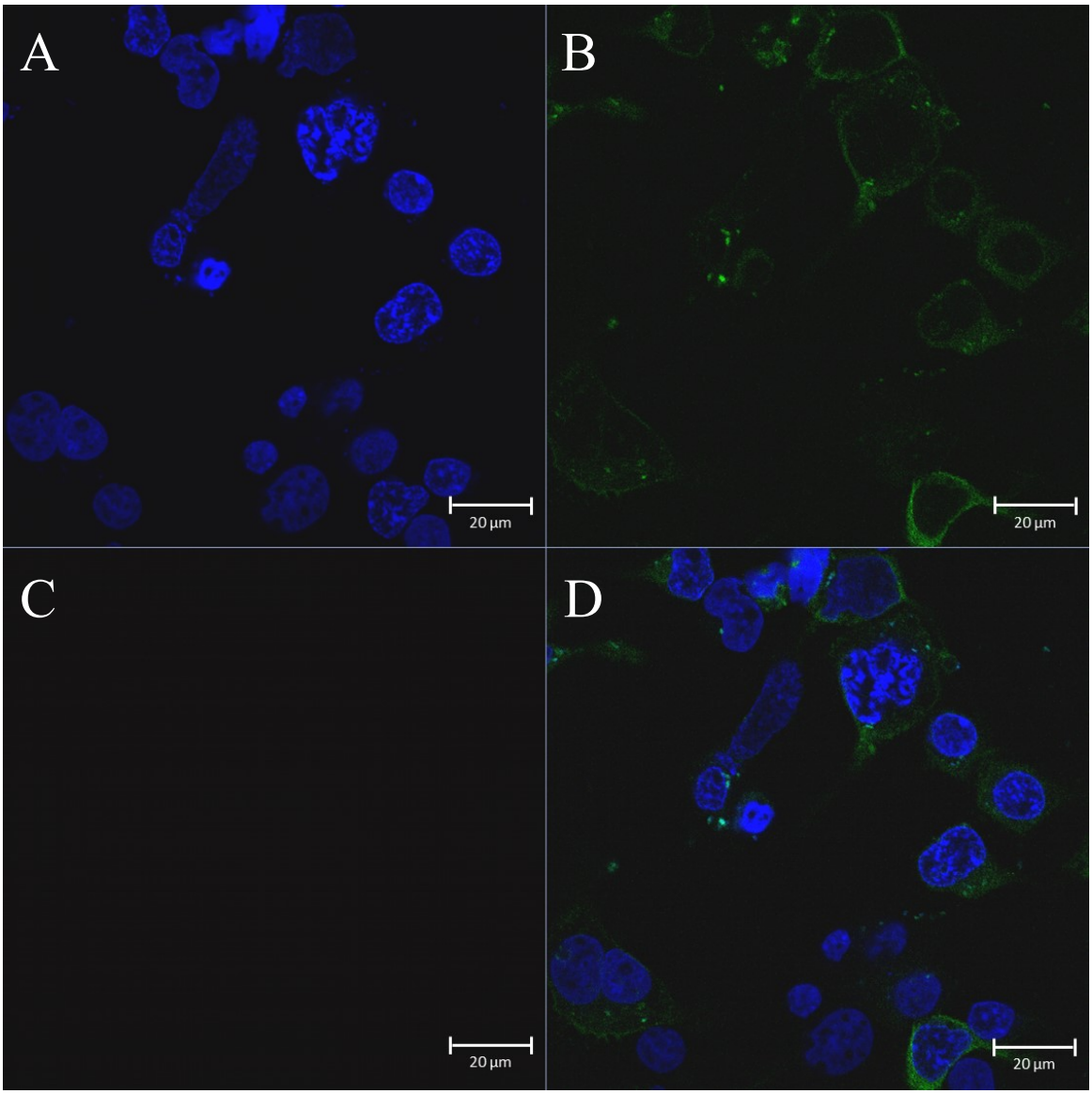

Figure 3.14. The Effect of 3xHA-CB_2 Transfection on Anti-CB_1 and Anti-HA Primary Antibody Dependant Immunofluorescence

Confocal microscopy images of HEK293A cells transiently transfected with CB_1_pcDNA cDNA (0.125 µg). Panels represent DAPI stained nuclei (A), anti-HA primary antibody (B), anti-CB_1 primary antibody (C), and merged channels (D). All panel images are split from the same confocal image. Protein colocalization is shown in yellow in merged panels. Scale bars, 20 µm.

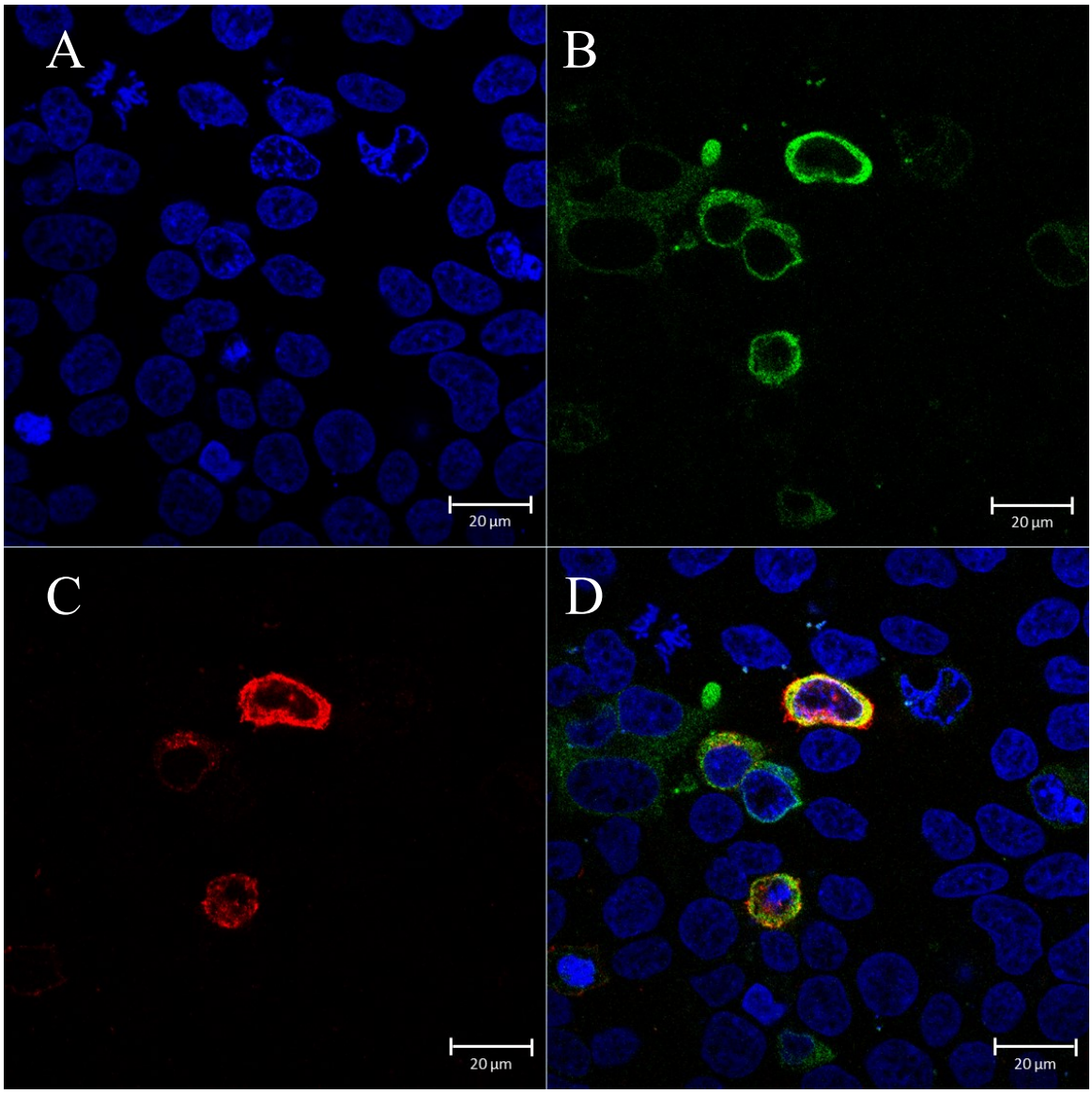

Figure 3.15. The Effect of CB_1_pcDNA and 3xHA_CB_2 Co-Transfection on Anti-CB_1 and Anti-HA Primary Antibody Dependant Immunofluorescence

Confocal microscopy images of HEK293A cells transiently transfected with 3xHA_CB_2 cDNA (0.125 µg) and CB_1_pcDNA (0.125 µg). Panels represent DAPI stained nuclei (A), anti-HA primary antibody (B), anti-CB_1 primary antibody (C), and merged channels (D). All panel images are split from the same confocal image. Protein colocalization is shown in yellow in merged panels. Scale bars, 20 µm.

Figure 3.16. The Effect of CB_2 on CP 55,940-Induced β-Arrestin Recruitment to CB_1-Tango

Tango concentration response curves of agonist-induced β-arrestin2 mobilization in HTLA cells treated with increasing concentrations of CP 55,940. HTLA cells were transiently transfected with either 25 ng CB_1-Tango or 25 ng each of CB_1-Tango and 3xHA-CB_2 cDNA followed by 8 hr of agonist incubation. % Luminescence data were generated by normalizing RLU to cells treated with the maximal dose of CP 55,940 (2.50 μM) in cells transfected with CB_1-Tango only. Normalization was carried out within plates before combining replicate data. **(A)** Curves are fit using non-linear regression analysis with variable slope (four parameters). Data are presented as mean +/- SD (**B)** E_{min}, E_{max}, Log EC_{50}, and EC_{50} values were derived using non-linear regression analysis with variable slope (four parameters). Data are presented as mean and 95% CI. n=3, experiments carried out on 3 different days. * indicates $p < 0.05$.

A

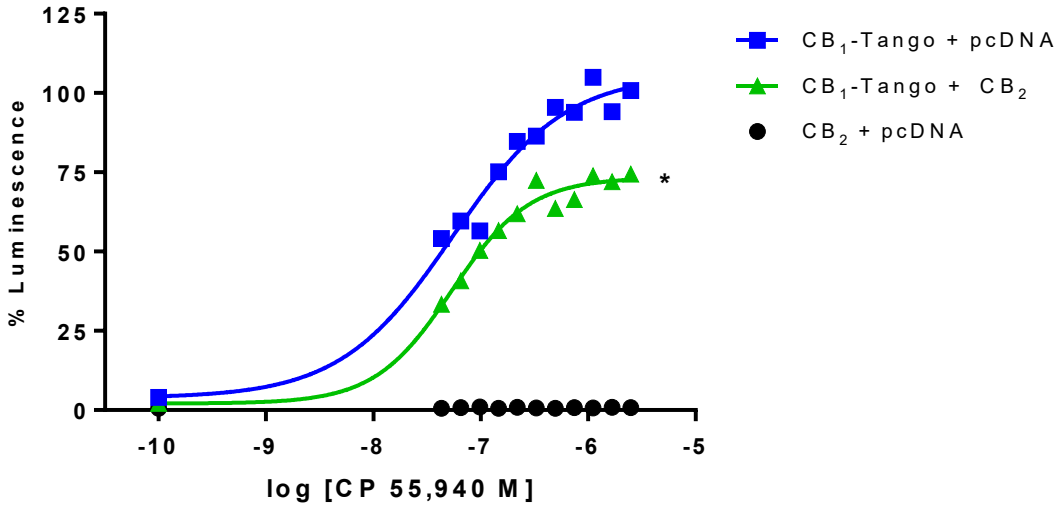

B

	CB_1-Tango + pcDNA	**CB_1-Tango + CB_2**
E_{min}	3.81 [-8.05 to 15.67]	2.06 [-10.21 to 14.32]
E_{max}	106.0 [91.49 to 120.40]	73.34 * [64.81 to 81.87
Log EC_{50} (M)	-7.26 [-7.46 to -7.06]	-7.27 [-7.48 to -7.06]
EC_{50} (M)	5.49e-008 [3.44e-008 to 8.77e-008]	5.37e-008 [3.33e-008 to 8.66e-008]

Figure 3.17. The Effect of CB_1 on CP 55,940-Induced β-Arrestin Recruitment to CB_1-Tango

Tango concentration response curves of agonist-induced β-arrestin2 mobilization in HTLA cells treated with increasing concentrations of CP 55,940. HTLA cells were transiently transfected with either 25 ng CB_1-Tango or 25 ng each of CB_1-Tango and CB_1_pcDNA cDNA followed by 8 hr of agonist incubation. % Luminescence data were generated by normalizing RLU to cells treated with the maximal dose of CP 55,940 (2.50 μM) in cells transfected with CB_1-Tango only. Normalization was carried out within plates before combining with replicate data. **(A)** Curves are fit using non-linear regression analysis with variable slope (four parameters). Data are presented as mean +/- SD **(B)** E_{min}, E_{max}, Log EC_{50}, and EC_{50} values were derived using non-linear regression analysis with variable slope (four parameters). Data are presented as mean and 95% CI. n=3, experiments carried out on 3 different days. n.s. indicates no significant difference.

A

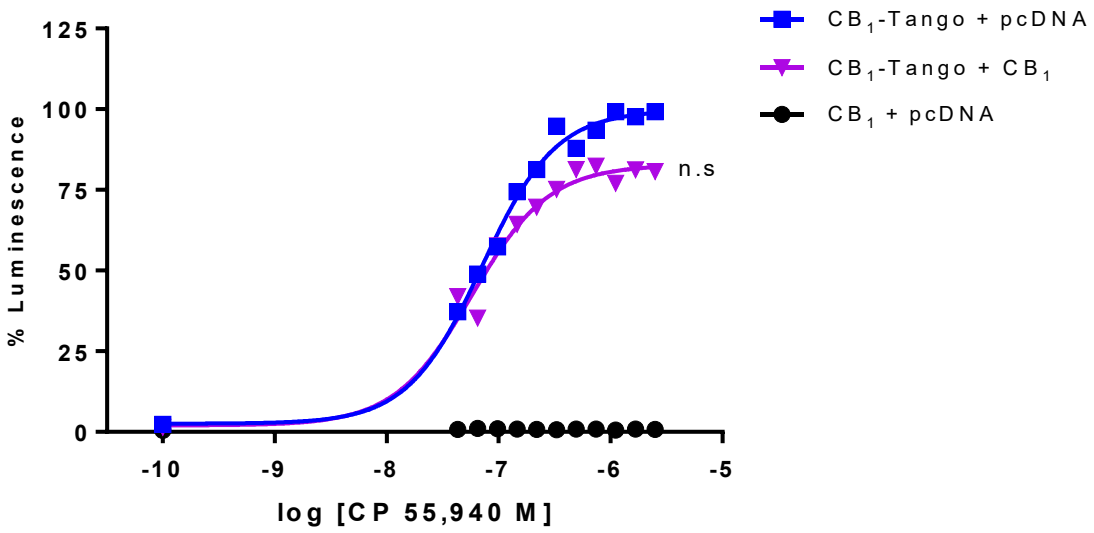

B

	CB1-Tango	**CB1-Tango + CB1**
Emin	2.55 [-11.80 to 16.89]	1.99 [-13.73 to 17.71]
Emax	99.73 [90.03 to 109.43]	82.75 [72.13 to 93.38]
Log EC50 (M)	-7.15 [-7.31 to -6.99]	-7.24 [-7.46 to -7.02]
EC50 (M)	7.06e-008 [4.87e-008 to 1.02e-007]	5.77e-008 [3.45e-008 to 9.65e-008]

Figure 3.18. The Effect of CB_1- and CB2-Tango Co-Transfection on CP 55,940-Induced β-Arrestin Recruitment Relative to CB_1-Tango Alone

Tango concentration response curves of agonist-induced β-arrestin2 mobilization in HTLA cells treated with increasing concentrations of CP 55,940. HTLA cells are transiently transfected with either 25 ng CB_2-Tango or 25 ng each of CB_2-Tango and CB_1-Tango cDNA followed by 8 hr of agonist incubation. % Luminescence data were generated by normalizing RLU to cells treated with the maximal dose of CP 55,940 (2.50 μM) in cells transfected with CB_2-Tango only. Normalization was carried out within plates before combining replicate data. **(A)** Curves are fit using non-linear regression analysis with variable slope (four parameters). Data are presented as mean +/- SD (**B)** Histograms represent E_{max} values derived using non-linear regression analysis with variable slope (four parameters) for cells transfected with 25 ng CB_2-Tango only, 25 ng each CB_2-Tango and CB_1-Tango, or 50 ng of CB_2-Tango cDNA. Data are presented as mean and 95% CI. n=3, experiments carried out on 3 different days. * indicates $p < 0.05$; n.s. indicates $p > 0.05$.

A

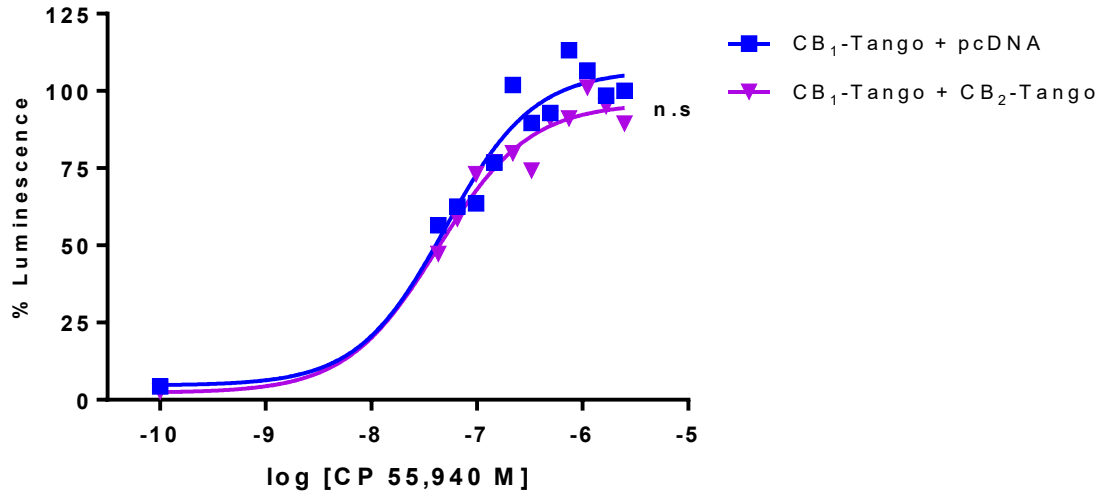
125
100
75
50
25
0
% Luminescence
-10
-9
-8
-7
-6
-5
log [CP 55,940 M]
n.s
CB1-Tango + pcDNA
CB1-Tango + CB2-Tango

B

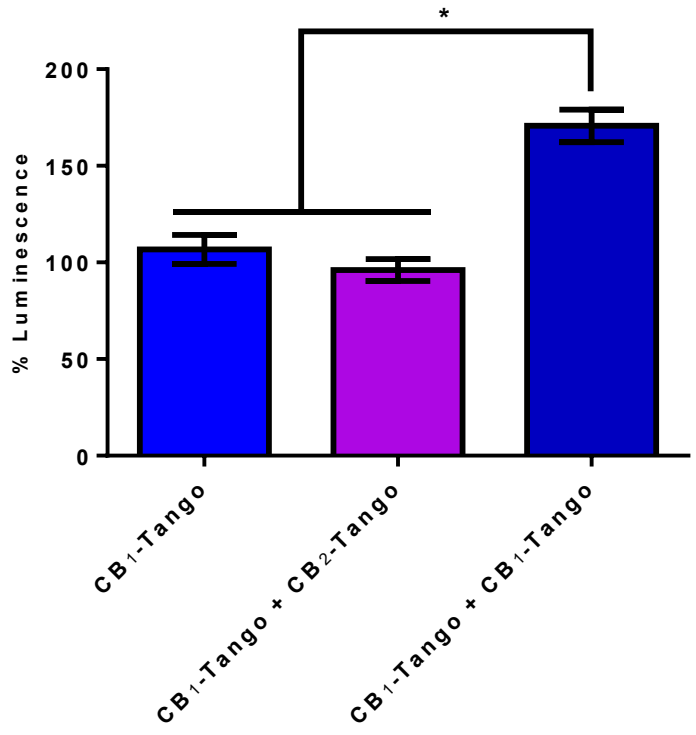
*
200
150
100
50
0
% Luminescence
CB1-Tango
CB1-Tango + CB2-Tango
CB1-Tango + CB1-Tango

Table 3.2. The Effect of CB_1- and CB_2-Tango Co-Transfection on CP 55,940-Induced Luminescence in the Tango β-arrestin2 Recruitment Assay

HTLA cells were transiently transfected with 25 ng CB_1-Tango, 25 ng each of CB_1-Tango and CB_2-Tango, or 50 ng CB_1-Tango cDNA followed by 8 hr of agonist incubation. Data are expressed as % Luminescence, which were generated by normalizing RLU to cells treated with the maximal dose of CP 55,940 (2.5 μM in cells transfected with CB_1-Tango only. Normalization was carried out within plates before combining replicate data. E_{min}, E_{max}, Log EC_{50}, and EC_{50} values were derived using non-linear regression analysis with variable slope (four parameters). Data are presented as mean and 95% CI. n=3, experiments carried out on 3 different days. * indicates $p < 0.05$.

	CB_1-Tango	**CB_1-Tango + CB_2-Tango**	**CB_1-Tango + CB_1-Tango**
E_{min}	4.64 [-13.72 to 22.99]	2.26 [-17.86 to 22.38]	13.34 [-15.32 to 42.01]
E_{max}	106.73 [91.35 to 122.02]	96.06 [78.96 to 113.11]	170.70 * [159.3 to 182.10]
Log EC_{50} (M)	-7.30 [-7.55 to -7.05]	-7.37 [-7.70 to -7.04]	-7.73 [-9.00 to -6.45]
EC_{50} (M)	5.02e-008 [2.80e-008 to 8.95e-008]	4.25e-008 [1.98e-008 to 9.12e-008]	1.88e-008 [9.97e-010 to 3.45e-007]

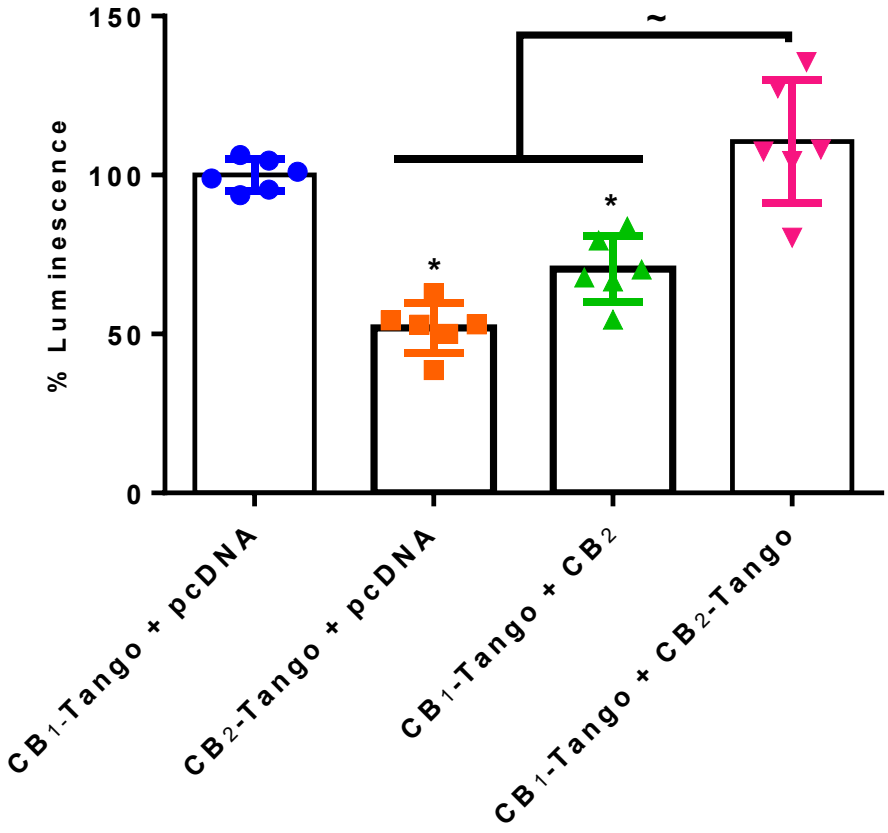

Figure 3.19. The Effect of CP 55,940 Agonism on β-Arrestin Recruitment Between Transfection Conditions Relative to CB_1-Tango

Data represents CP 55,940 (125 nM)-induced β-arrestin2 mobilization in cells transiently transfected with 25 ng CB_1-Tango; 25 ng CB_2-Tango; each 25 ng CB_1-Tango and 3xHA_CB_2; or each 25 ng CB_1- and CB_2-Tango cDNA following 8 hr of agonist incubation. Data are expressed as % Luminescence and generated by normalizing RLU to cells transfected with CB_1-Tango only and treated with CP 55,940 (125 nM; expressed as 100% Luminescence). Normalization was carried out within plates before combining with replicate data. Data was analyzed using One-way ANOVA with Tukey's *post hoc* test of significance and presented as mean +/- SD; n=6, experiments carried out on 3 different days. * indicates $p < 0.05$ compared to cells transfected with CB_1-Tango only; ~ indicates $p < 0.05$ between groups.

Figure 3.20. The Effect of CB_1 on CP 55,940-Induced β-Arrestin Recruitment to CB_2-Tango

Tango concentration response curves of agonist-induced β-arrestin2 mobilization in HTLA cells treated with increasing concentrations of CP 55,940. HTLA cells were transiently transfected with either 25 ng CB_2-Tango or 25 ng each of CB_2-Tango and CB_1_pcDNA3.1 cDNA followed by8 hr of agonist incubation. % Luminescence data were generated by normalizing RLU to cells treated with the maximal dose of CP 55,940 (2.50 μM) in cells transfected with CB_2-Tango only. Normalization was carried out within plates before combining with replicate data. **(A)** Curves are fit using non-linear regression analysis with variable slope (four parameters). Data are presented as mean +/- SD (**B)** E_{min}, E_{max}, Log EC_{50}, and EC_{50} values were derived using non-linear regression analysis with variable slope (four parameters). Data are presented as mean and 95% CI. n=3, experiments carried out on 3 different days. * indicates $p < 0.05$

A

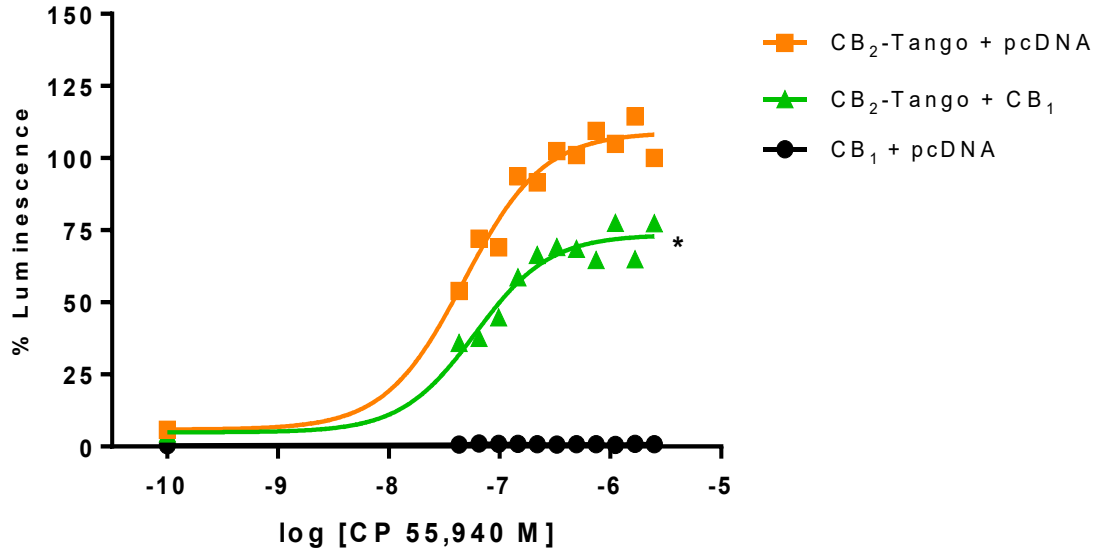

B

	CB_2-Tango	**CB_2-Tango + CB_1**
E_{min}	5.90 [-12.36 to 24.46]	4.92 [-12.96 to 22.80]
E_{max}	109.00 [96.08 to 121.91]	73.44 * [61.62 to 85.26]
Log EC_{50} (M)	-7.32 [-7.55 to -7.10]	-7.22 [-7.51 to -6.93]
EC_{50} (M)	4.77e-008 [2.84e-008 to 8.01e-008]	6.03e-008 [3.09e-008 to 1.17e-007]

Figure 3.21. The Effect of CB_2 on CP 55,940-Induced β-Arrestin Recruitment to CB_2-Tango

Tango concentration response curves of agonist-induced β-arrestin2 mobilization in HTLA cells treated with increasing concentrations of CP 55,940. HTLA cells were transiently transfected with either 25 ng CB_2-Tango or 25 ng each of CB_2-Tango and 3xHA-CB_2 cDNA followed by 8 hr of agonist incubation. % Luminescence data were generated by normalizing RLU to cells treated with the maximal dose of CP 55,940 (2.50 μM) in cells transfected with CB_2-Tango only. Normalization was carried out within plates before combining with replicate data. **(A)** Curves are fit using non-linear regression analysis with variable slope (four parameters). Data are presented as mean +/- SD (**B)** E_{min}, E_{max}, Log EC_{50}, and EC_{50} values were derived using non-linear regression analysis with variable slope (four parameters). Data are presented as mean and 95% CI. n=3, experiments carried out on 3 different days. n.s. indicates $p > 0.05$

A

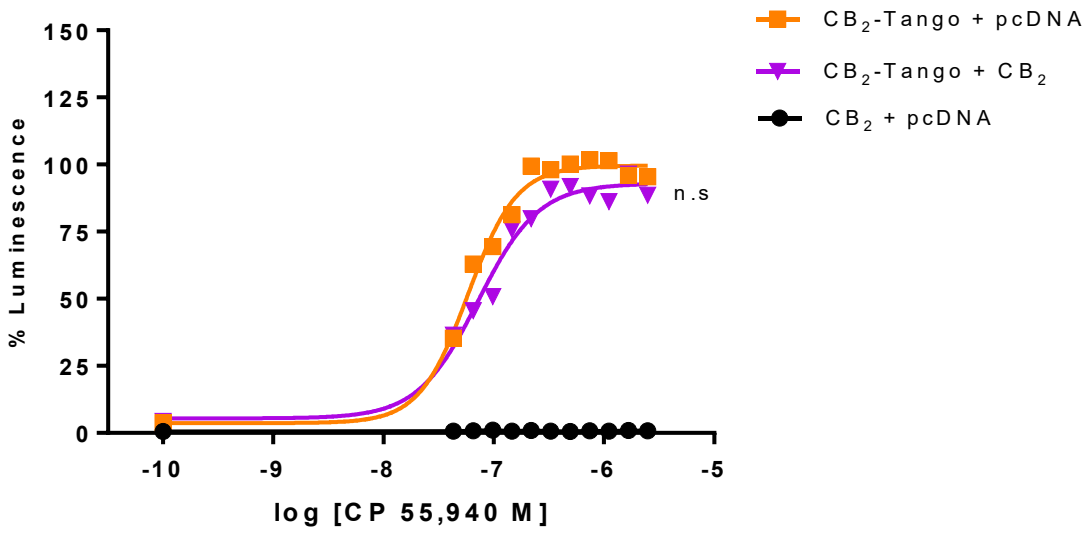

B

	CB_2-Tango	**CB_2-Tango + CB_2**
E_{min}	3.68 [-16.96 to 24.31]	5.43 [-16.88 to 27.75]
E_{max}	99.61 [89.45 to 109.8]	92.96 [79.96 to 106.0]
Log EC_{50} (M)	-7.23 [-7.40 to -7.07]	-7.14 [-7.74 to -6.91]
EC_{50} (M)	5.84e-008 [3.98e-008 to 8.58e-008]	7.21e-008 [4.19e-008 to 1.24e-007]

Figure 3.22. The Effect of CB_1- and CB2-Tango Co-Transfection on CP 55,940-Induced β-Arrestin Recruitment Relative to CB_2-Tango Alone

Tango concentration response curves of agonist-induced β-arrestin2 mobilization in HTLA cells treated with increasing concentrations of CP 55,940. HTLA cells are transiently transfected with either 25 ng CB_2-Tango or 25 ng each of CB_2-Tango and CB_1-Tango cDNA followed by 8 hr of agonist incubation. % Luminescence data were generated by normalizing RLU to cells treated with the maximal dose of CP 55,940 (2.50 μM) in cells transfected with CB_2-Tango only. Normalization was carried out within plates before combining with replicate data. **(A)** Curves are fit using non-linear regression analysis with variable slope (four parameters). Data are presented as mean +/- SD (**B)** Histograms represent E_{max} values derived using non-linear regression analysis with variable slope (four parameters) for cells transfected with 25 ng CB_2-Tango only, 25 ng each CB_2-Tango and CB_1-Tango, or 50 ng of CB_2-Tango cDNA. E_{max} values were compared using one-way Data are presented as mean and 95% CI. n=3, experiments carried out on 3 different days. * indicates $p < 0.05$

A

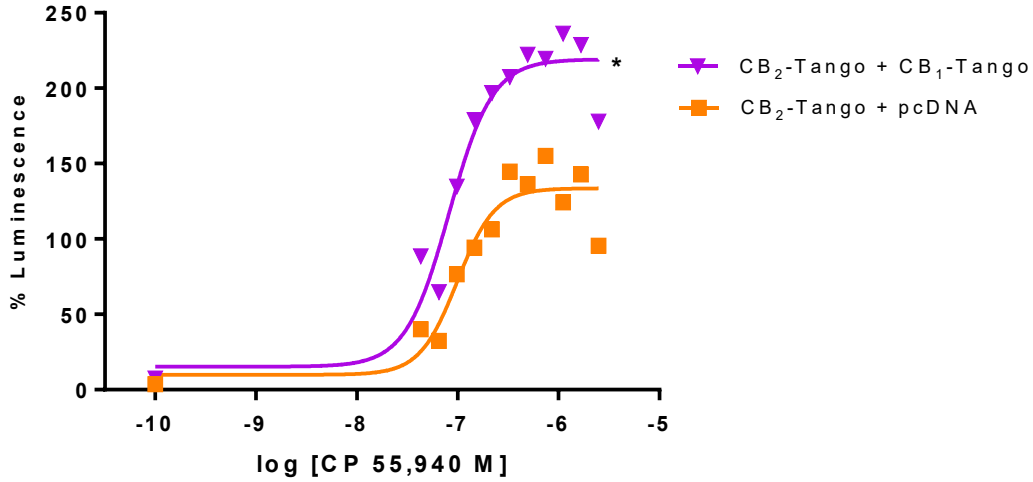
250
200
150
100
50
0
% Luminescence
-10
-9
-8
-7
-6
-5
log [CP 55,940 M]
*
CB2-Tango + CB1-Tango
CB2-Tango + pcDNA

B

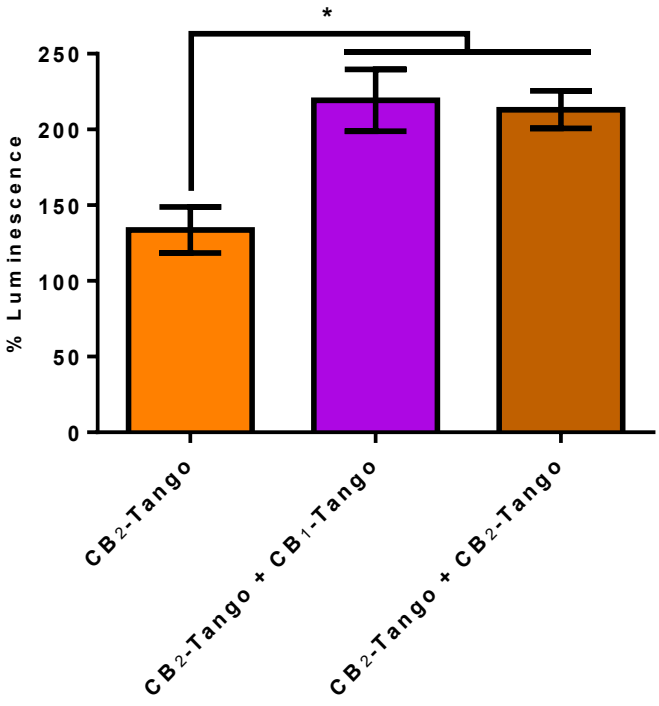
*
250
200
150
100
50
0
% Luminescence
CB2-Tango
CB2-Tango + CB1-Tango
CB2-Tango + CB2-Tango

Table 3.3. The Effect of CB_1- and CB2-Tango Co-Transfection on CP 55,940-Induced Luminescence in the Tango β-arrestin2 Recruitment Assay

HTLA cells were transiently transfected with 25 ng CB_2-Tango, 25 ng each of CB_2-Tango and CB_1-Tango, or 50 ng CB_2-Tango cDNA followed by 8 hr of agonist incubation. All data are expressed as % Luminescence, which were generated by normalizing RLU to cells treated with the maximal dose of CP 55,940 (2.5 μM) in cells transfected with CB_2-Tango only. Normalization was carried out within plates before combining with replicate data. E_{min}, E_{max}, Log EC_{50}, and EC_{50} values were derived using non-linear regression analysis with variable slope (four parameters). Data are presented as mean and 95% CI. n=3, experiments carried out on 3 different days. * indicates $p < 0.05$.

	CB_2-Tango	**CB_2-Tango + CB_1-Tango**	**CB_2-Tango + CB_2-Tango**
E_{min}	9.90 [-24.31 to 44.11]	15.28 [-32.99 to 63.55]	14.46 [-11.88 to 40.79]
E_{max}	133.62 [115.71 to 151.50]	219.12 * [195.12 to 243.21]	213.13* [198.53 to 227.72]
Log EC_{50} (M)	-7.00 [-7.20 to -6.81]	-7.09 [-7.27 to -6.90]	-7.33 [-7.47 to -7.18]
EC_{50} (M)	9.88e-008 [6.26e-008 to 1.56e-007]	8.21e-008 [5.41e-008 to 1.25e-007]	4.71e-008 [3.40e-008 to 6.51e-008]

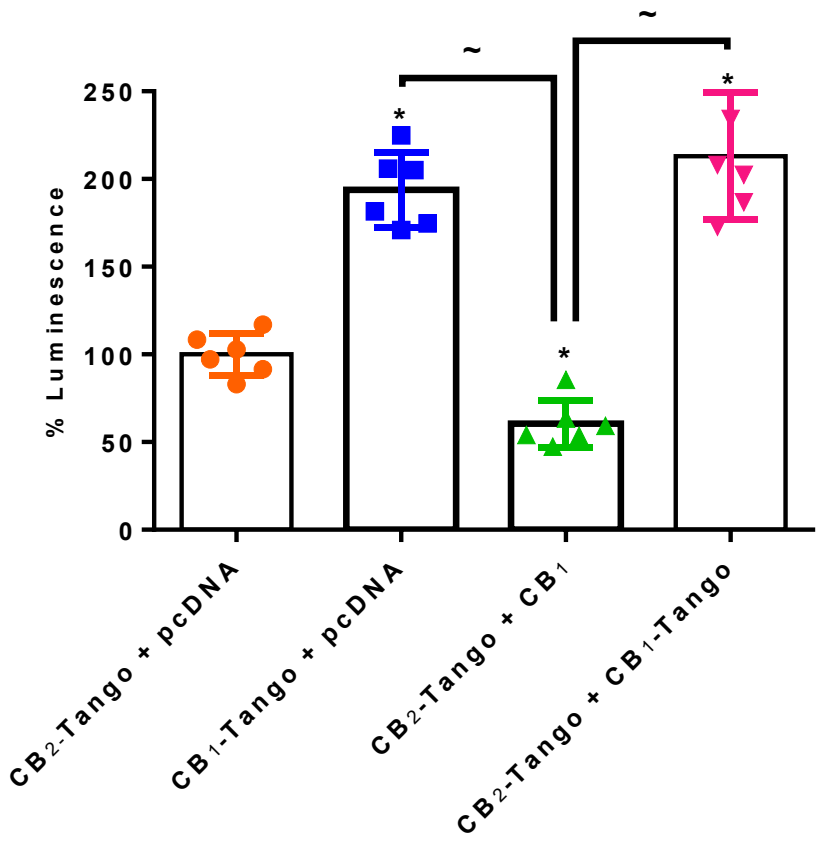

Figure 3.23. The Effect of CP 55,940 Agonism on β-Arrestin Recruitment Between Transfection Conditions Relative to CB_2-Tango

Data represents CP 55,940 (125 nM) induced β-arrestin2 mobilization in cells transiently transfected with either 25 ng CB_2-Tango, 25 ng CB_1-Tango, each 25 ng CB_2-Tango and CB_1_pcDNA, or each 25 ng CB_2- and CB_1-Tango cDNA followed by 8 hr of agonist incubation. Data are expressed as % Luminescence and generated by normalizing RLU to cells transfected with CB_2-Tango only and treated with CP 55,940 (125 nM). Normalization was carried out within plates before combining with replicate data. Data analyzed using One-way ANOVA with Tukey's post hoc test of significance and presented as mean +/- SD; n=6, experiments carried out on 3 different days. * indicates $p < 0.05$ compared to cells transfected with CB_1-Tango only; ~ indicates $p < 0.05$ between groups.

Figure 3.24. The Effect of Receptor Stoichiometry on β-arrestin Recruitment to CB_1-Tango

Tango data from HTLA cells transiently transfected with 25 ng of CB_1-Tango cDNA alone or in combination with 5 ng, 25 ng, or 50 ng of CB_2 (non-Tango) cDNA **(A)**, Non-Tango CB_1 **(B)**, or CB_2-Tango **(C)** cDNA. Concentration response curves represent CP 55,940 induced β-arrestin2 mobilization to CB_1-Tango after 8 hr of incubation with agonist. Data are presented as a mean +/- SD; n=3, experiments carried out on 3 different days. * indicates $p<0.05$ relative to CB_1-Tango only cells; ns indicates no significant differences relative to CB_1-Tango only cells.

A

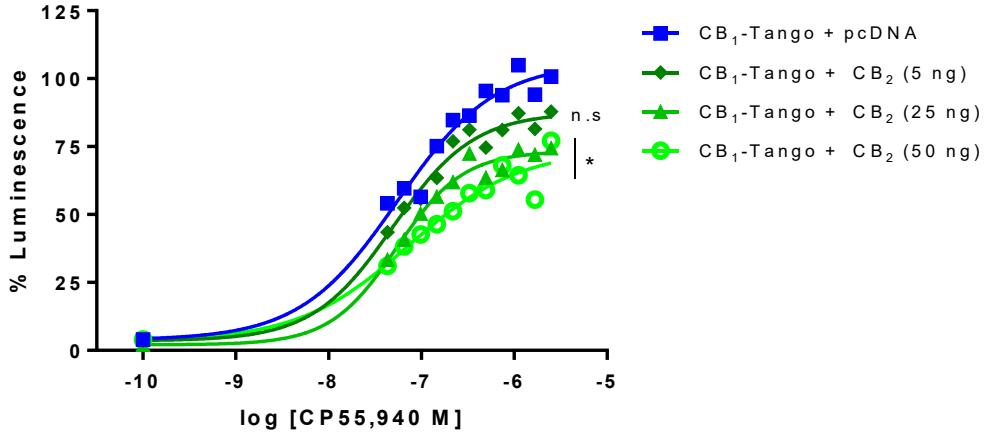
% Luminescence
125
100
75
50
25
0
-10
-9
-8
-7
-6
-5
log [CP55,940 M]
n.s
*
CB1-Tango + pcDNA
CB1-Tango + CB2 (5 ng)
CB1-Tango + CB2 (25 ng)
CB1-Tango + CB2 (50 ng)

B

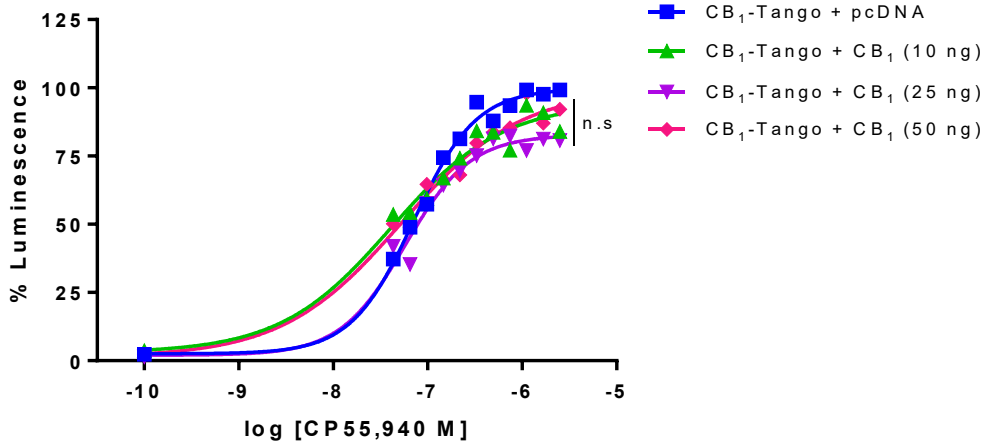
% Luminescence
125
100
75
50
25
0
-10
-9
-8
-7
-6
-5
log [CP55,940 M]
n.s
CB1-Tango + pcDNA
CB1-Tango + CB1 (10 ng)
CB1-Tango + CB1 (25 ng)
CB1-Tango + CB1 (50 ng)

C

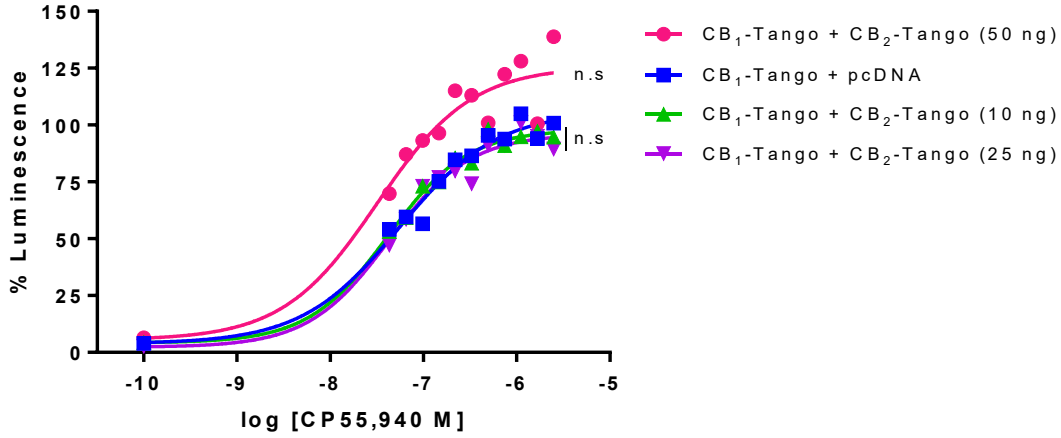
% Luminescence
150
125
100
75
50
25
0
-10
-9
-8
-7
-6
-5
log [CP55,940 M]
n.s
n.s
CB1-Tango + CB2-Tango (50 ng)
CB1-Tango + pcDNA
CB1-Tango + CB2-Tango (10 ng)
CB1-Tango + CB2-Tango (25 ng)

Figure 3.25. The Effect of Receptor Stoichiometry on β-arrestin Recruitment to CB_2-Tango

Tango data from HTLA cells transiently transfected with 25 ng of CB_2-Tango cDNA alone or in combination with 5 ng, 25 ng, or 50 ng of CB_1 cDNA **(A)**, CB_2 **(B)**, or CB_1-Tango **(C)** cDNA. Concentration response curves show CP 55,940 induced β-arrestin2 mobilization to CB_2-Tango after 8 hr of incubation with agonist. Data are presented as a mean +/- SD; n=6, experiments carried out on 6 different days. * indicates $p<0.05$ relative to CB_1-Tango only cells; ns indicates no significant differences relative to CB_1-Tango only cells.

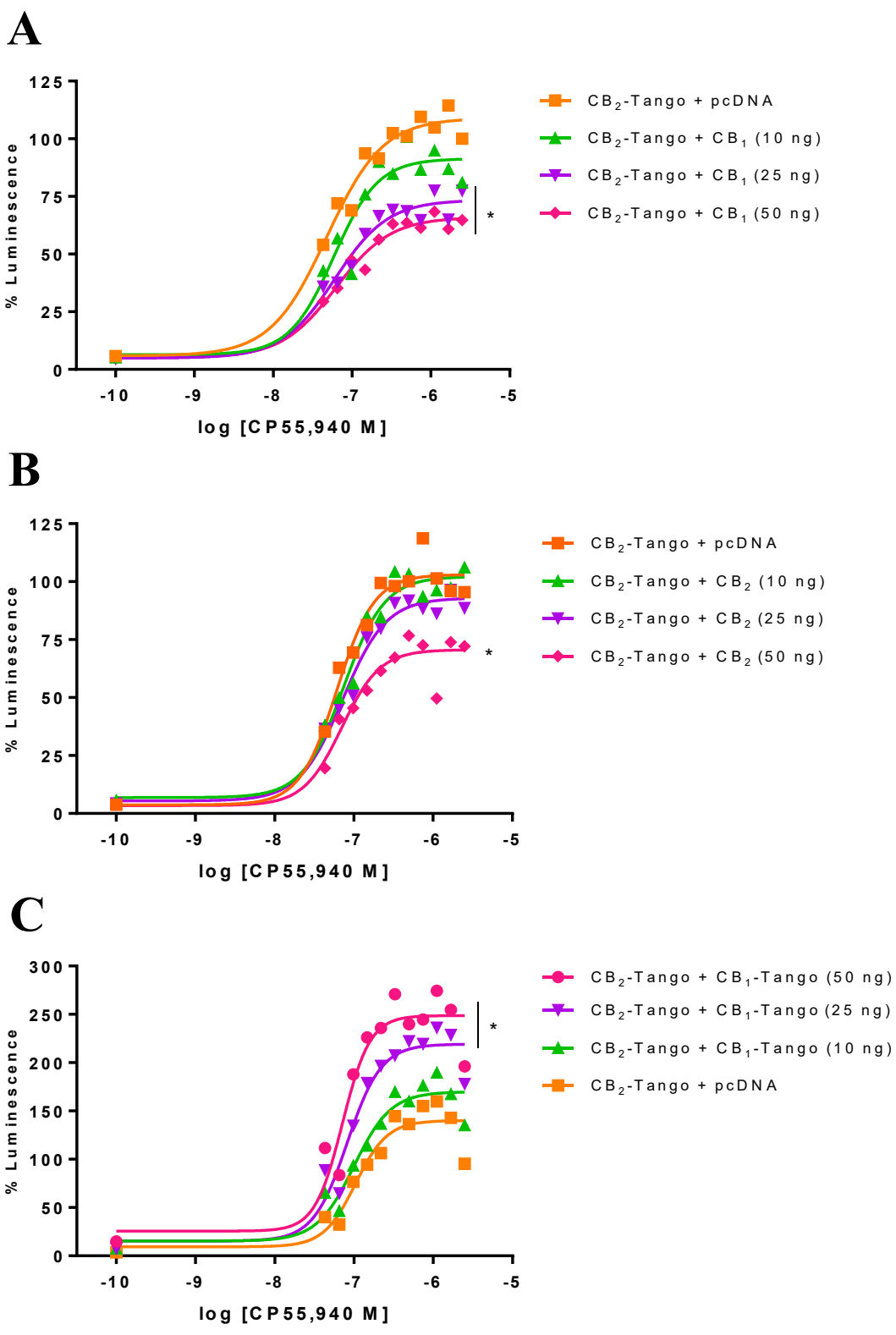
A
% Luminescence
log [CP55,940 M]
CB2-Tango + pcDNA
CB2-Tango + CB1 (10 ng)
CB2-Tango + CB1 (25 ng)
CB2-Tango + CB1 (50 ng)
*
B
% Luminescence
log [CP55,940 M]
CB2-Tango + pcDNA
CB2-Tango + CB2 (10 ng)
CB2-Tango + CB2 (25 ng)
CB2-Tango + CB2 (50 ng)
*
C
% Luminescence
log [CP55,940 M]
CB2-Tango + CB1-Tango (50 ng)
CB2-Tango + CB1-Tango (25 ng)
CB2-Tango + CB1-Tango (10 ng)
CB2-Tango + pcDNA
*

Figure 3.26. The Effect of AM251 Antagonism on CP 55,940-Dependant β-Arrestin Recruitment to CB_1-Tango

CB_1- Tango concentration response curve represents the effect of the CB_1 selective inverse agonist AM251 on CP 55,940-induced β-arrestin2 mobilization in HTLA cells treated with 125 nM CP 55,940 and increasing concentrations of AM251. HTLA cells are transiently transfected with 25 ng CB_1-Tango cDNA and pre-treated with antagonist for 30 min before 8 hr of incubation with a combination of agonist and antagonist. % Luminescence data were generated by normalizing RLU to cells treated with CP 55,940 only (125 nM; expressed as 100% Luminescence) within plates. **(A)** Curve generation was derived using non-linear regression analysis with variable slope (four parameters). Data are presented as mean +/- SD (**B)** E_{min}, E_{max}, Log IC_{50}, and IC_{50} values were derived using non-linear regression analysis with variable slope (four parameters). Data are presented as mean and 95% CI. n=6, experiments carried out on 2 different days

A

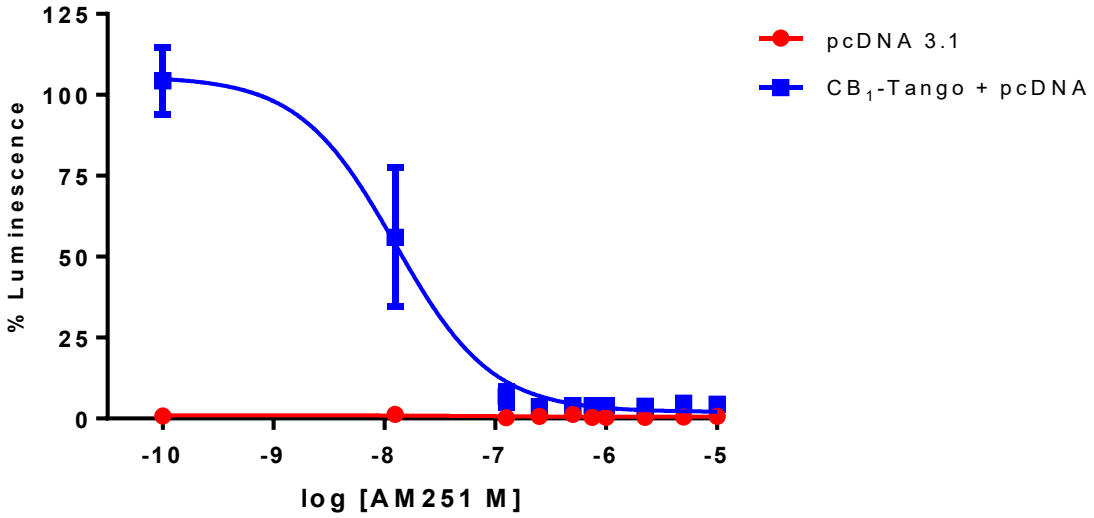

B

CB_1-Tango	
E_{min}	2.01 [-0.38 to 4.40]
E_{max}	105.70 [98.84 to 112.61]
Log IC_{50} (M)	-7.90 [-8.02 to -7.78]
IC_{50} (M)	1.25e-008 [9.49e-009 to 1.68e-008]

Figure 3.27. The Effect of AM251 Antagonism on CP 55,940-Dependant β-Arrestin Recruitment to CB_2-Tango

CB_2- Tango concentration response curve represents the effect of the CB_1 selective inverse agonist AM251 on CP 55,940-induced β-arrestin2 mobilization in HTLA cells treated with 125 nM CP 55,940 and increasing concentrations of AM251. HTLA cells are transiently transfected with 25 ng CB_2-Tango cDNA and pre-treated with antagonist for 30 min before 8 hr of incubation with a combination of agonist and antagonist. % Luminescence data were generated by normalizing RLU to cells treated with CP 55,940 only (125 nM; expressed as 100% Luminescence) within plates. **(A)** Curve generation was derived using non-linear regression analysis with variable slope (four parameters). Data are presented as mean +/- SD (**B)** E_{min}, E_{max}, Log IC_{50}, and IC_{50} values were derived using non-linear regression analysis with variable slope (four parameters). Data are presented as mean and 95% CI. n=6, experiments carried out on 2 different days

A

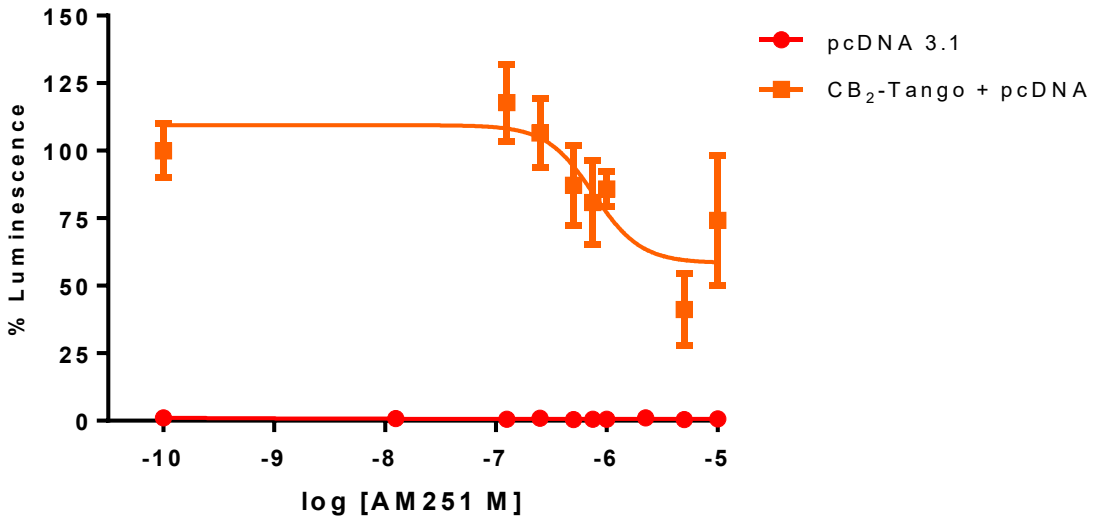

B

CB_2-Tango	
E_{min}	58.42 [45.45 to 71.38]
E_{max}	109.50 [96.98 to 121.91]
Log IC_{50} (M)	-6.12 [-6.36 to -5.88]
IC_{50} (M)	7.61e-007 [4.38e-007 to 1.32e-006]

Figure 3.28. The Effect of AM630 Antagonism on CP 55,940-Dependant β-Arrestin Recruitment to CB_1-Tango

CB_1- Tango concentration response curve represents the effect of the CB_2 selective inverse agonist AM630 on CP 55,940-induced β-arrestin2 mobilization in HTLA cells treated with 125 nM CP 55,940 and increasing concentrations of AM630. HTLA cells are transiently transfected with 25 ng CB_1-Tango cDNA and pre-treated with antagonist for 30 min before 8 hr of incubation with a combination of agonist and antagonist. % Luminescence data were generated by normalizing RLU to cells treated with CP 55,940 only (125 nM; expressed as 100% Luminescence) within plates. **(A)** Curve generation was derived using non-linear regression analysis with variable slope (four parameters). Data are presented as mean +/- SD (**B)** E_{min}, E_{max}, Log IC_{50}, and IC_{50} values were derived using non-linear regression analysis with variable slope (four parameters). Data are presented as mean and 95% CI. n=6, experiments carried out on 2 different days

A

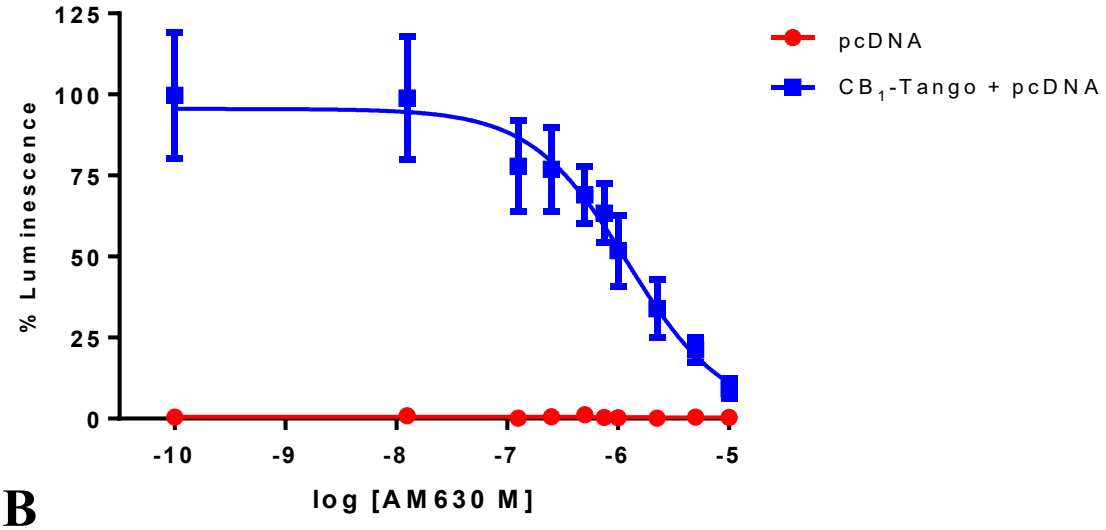

B

CB_1-Tango	
E_{min}	0.91 [-10.48 to 12.30]
E_{max}	95.54 [89.14 to 101.91]
Log IC_{50} (M)	-5.92 [-6.10 to -5.73]
IC_{50} (M)	1.21e-006 [7.58e-007 to 1.86e-006]

Figure 3.29. The Effect of AM630 Antagonism on CP 55,940-Dependant β-Arrestin Recruitment to CB_2-Tango

CB_2- Tango concentration response curve represents the effect of the CB_2 selective inverse agonist AM630 on CP 55,940-induced β-arrestin2 mobilization in HTLA cells treated with 125 nM CP 55,940 and increasing concentrations of AM630. HTLA cells are transiently transfected with 25 ng CB_2-Tango cDNA and pre-treated with antagonist for 30 min before 8 hr of incubation with a combination of agonist and antagonist. % Luminescence data were generated by normalizing RLU to cells treated with CP 55,940 only (125 nM; expressed as 100% Luminescence) within plates. **(A)** Curve generation was derived using non-linear regression analysis with variable slope (four parameters). Data are presented as mean +/- SD (**B)** E_{min}, E_{max}, Log IC_{50}, and IC_{50} values were derived using non-linear regression analysis with variable slope (four parameters). Data are presented as mean and 95% CI. n=6, experiments carried out on 2 different days

A

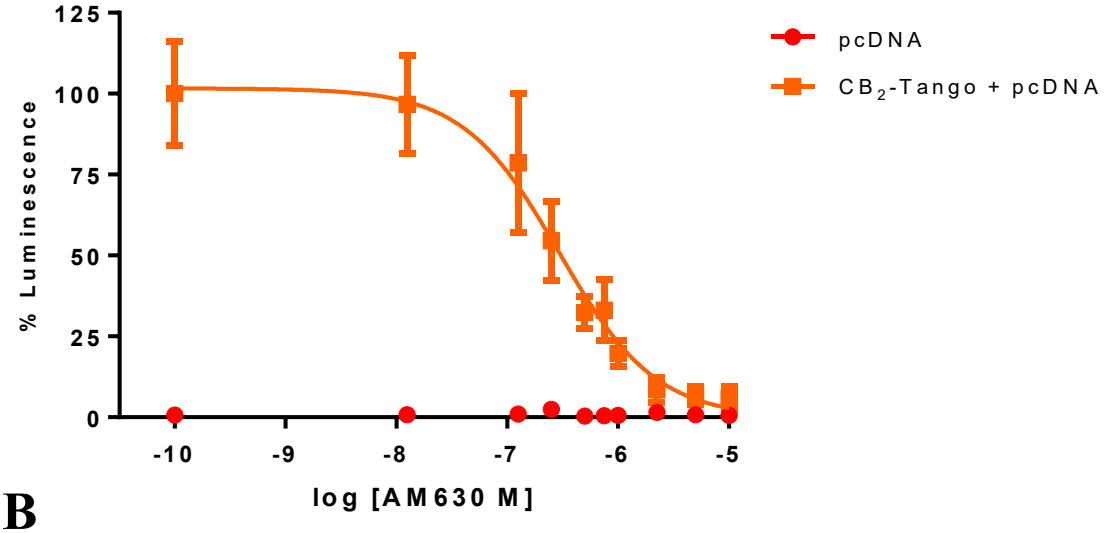

B

CB_2-Tango	
E_{min}	-0.09 [-6.41 to 6.21]
E_{max}	101.60 [94.93 to 108.42]
Log IC_{50} (M)	-6.53 [-6.66 to -6.64]
IC_{50} (M)	2.92e-007 [2.16e-007 to 4.03e-007]

Figure 3.30. The Effect of CB_2 on AM251 Antagonism of CP 55,940-Dependant β-Arrestin Recruitment to CB_1-Tango

Tango concentration response curves the effect of the CB_1 selective inverse agonist AM251 on CP 55,940-induced β-arrestin2 mobilization in HTLA cells treated with 125 nM CP 55,940 and increasing concentrations of AM251. HTLA cells are transiently transfected with either 25 ng CB_1-Tango or 25 ng each of CB_1-Tango and 3xHA-CB_2 cDNA and pre-treated with antagonist for 30 min before 8 hr of incubation with a combination of agonist and antagonist. % Luminescence data were generated by normalizing RLU to cells treated with CP 55,940 only (125 nM; expressed as 100% Luminescence) in cells transfected with CB_1-Tango only. Normalization was carried out within plates before combining with replicate data. **(A)** Curves are fit using non-linear regression analysis with variable slope (four parameters). Data are presented as mean +/- SD (**B)** E_{min}, E_{max}, Log IC_{50}, and IC_{50} values were derived using non-linear regression analysis with variable slope (four parameters). Data are presented as mean and 95% CI. n=6, experiments carried out on 2 different days. * indicates $p < 0.05$

A

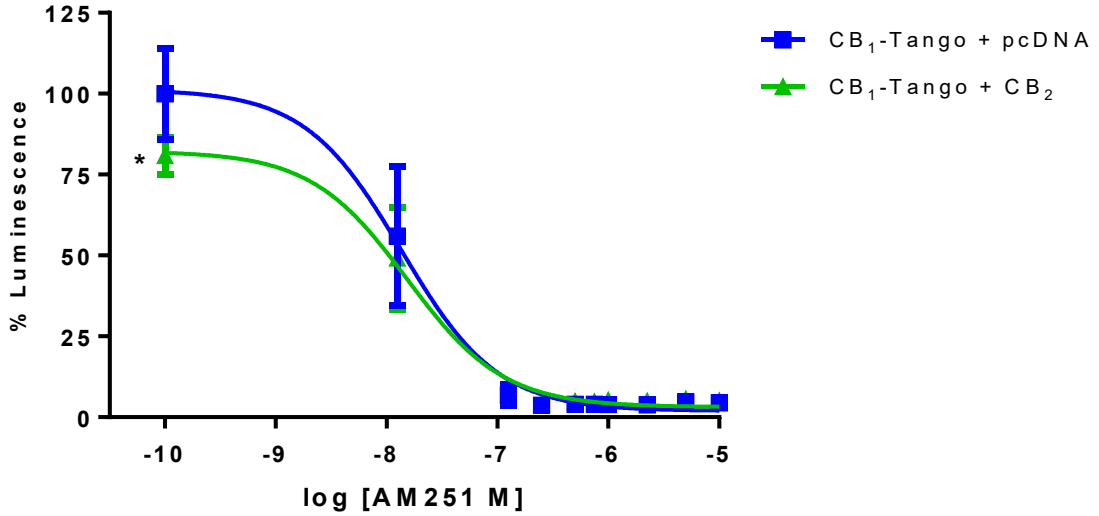

B

	CB_1-Tango	**CB_1-Tango + CB_2**
E_{min}	1.94 [-0.68 to 4.54]	3.13 [1.30 to 4.97]
E_{max}	101.30 [94.57 to 108.11]	82.21* [77.11 to 87.32]
Log IC_{50} (M)	-7.87 [-8.00 to -7.74]	-7.82 [-7.94 to -7.70]
IC_{50} (M)	1.36e-008 [9.98e-009 to 1.84e-008]	1.53e-008 [1.16e-008 to 2.01e-008]

Figure 3.31. The Effect of CB_1 on AM251 Antagonism of CP 55,940-Dependant β-Arrestin Recruitment to CB_2-Tango

Tango concentration response curves the effect of the CB_1 selective inverse agonist AM251 on CP 55,940-induced β-arrestin2 mobilization in HTLA cells treated with 125 nM CP 55,940 and increasing concentrations of AM251. HTLA cells are transiently transfected with either 25 ng CB_2-Tango or 25 ng each of CB_2-Tango and CB_1_pcDNA3.1 cDNA and pre-treated with antagonist for 30 min before 8 hr of incubation with a combination of agonist and antagonist. % Luminescence data were generated by normalizing RLU to cells treated with CP 55,940 only (125 nM; expressed as 100% Luminescence) in cells transfected with CB_2-Tango only. Normalization was carried out within plates before combining with replicate data. **(A)** Curves are fit using non-linear regression analysis with variable slope (four parameters). Data are presented as mean +/- SD (**B)** E_{min}, E_{max}, Log IC_{50}, and IC_{50} values were derived using non-linear regression analysis with variable slope (four parameters). Data are presented as mean and 95% CI. n=6, experiments carried out on 2 different days. * indicates $p < 0.05$; ~ indicates that the curve generated was an ambiguous fit.

A

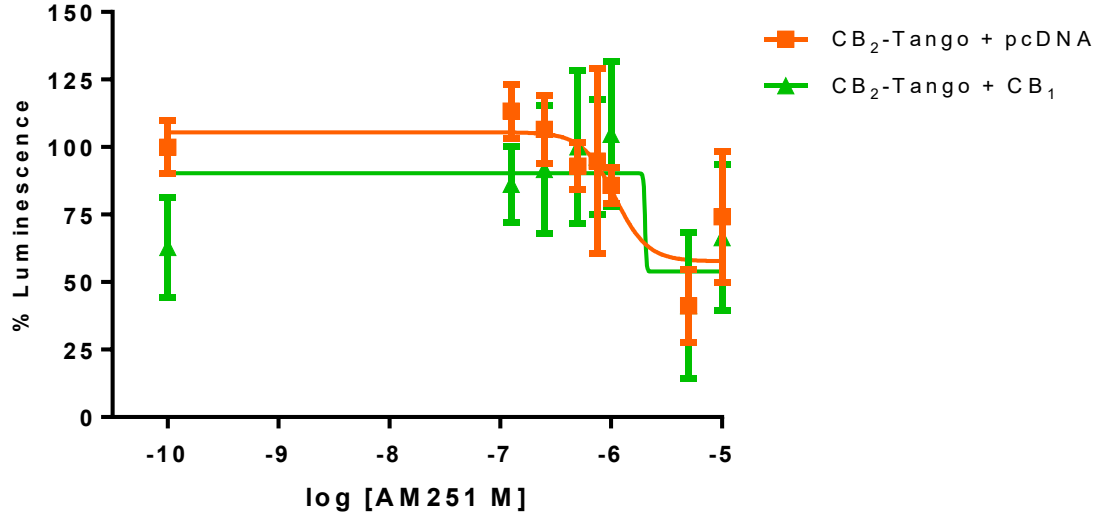

B

	CB_2-Tango	**CB_2-Tango + CB_1**
E_{min}	57.70 [44.46 to 70.94]	53.89 [38.35 to 69.42]
E_{max}	105.50 [94.46 to 116.50]	90.29 [81.33 to 99.26]
Log IC_{50} (M)	-5.97 [-6.24 to -5.68]	~
IC_{50} (M)	1.08e-006 [5.75e-007 to 2.02e-006]	~

Figure 3.32. The Effect of CB_2 on AM630 Antagonism of CP 55,940-Dependant β-Arrestin Recruitment to CB_1-Tango

Tango concentration response curves the effect of the CB_2 selective inverse agonist AM630 on CP 55,940-induced β-arrestin2 mobilization in HTLA cells treated with 125 nM CP 55,940 and increasing concentrations of AM630. HTLA cells are transiently transfected with either 25 ng CB_1-Tango or 25 ng each of CB_1-Tango and 3xHA-CB_2 cDNA and pre-treated with antagonist for 30 min before 8 hr of incubation with a combination of agonist and antagonist. % Luminescence data were generated by normalizing RLU to cells treated with CP 55,940 only (125 nM; expressed as 100% Luminescence) in cells transfected with CB_1-Tango only. Normalization was carried out within plates before combining with replicate data. **(A)** Curves are fit using non-linear regression analysis with variable slope (four parameters). Data are presented as mean +/- SD (**B)** E_{min}, E_{max}, Log IC_{50}, and IC_{50} values were derived using non-linear regression analysis with variable slope (four parameters). Data are presented as mean and 95% CI. n=6, experiments carried out on 2 different days. * indicates $p < 0.05$

A

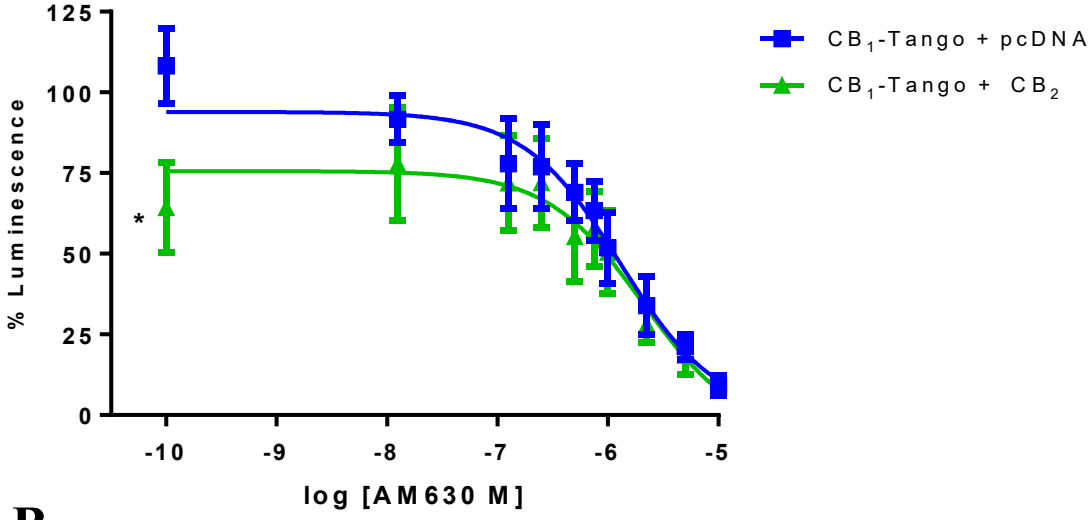

B

	CB_1-Tango	**CB_1-Tango + CB_2**
E_{min}	-0.91 [-11.78 to 9.96]	-4.93 [-19.87 to 10.88]
E_{max}	93.94 [88.03 to 99.85]	75.62 * [69.01 to 82.24]
Log IC_{50} (M)	-5.89 [-6.06 to -5.72]	-5.68 [-5.96 to -5.41]
IC_{50} (M)	1.29e-006 [9.25e-007 to 2.095e-006]	1.84e-006 [9.91e-007 to 3.40e-006]

Figure 3.33. The Effect of CB_2 on AM630 Antagonism on CP 55,940-Dependant β-Arrestin Recruitment to CB_2-Tango

Tango concentration response curves the effect of the CB_2 selective inverse agonist AM630 on CP 55,940-induced β-arrestin2 mobilization in HTLA cells treated with 125 nM CP 55,940 and increasing concentrations of AM630. HTLA cells are transiently transfected with either 25 ng CB_2-Tango or 25 ng each of CB_2-Tango and CB_1_pcDNA3.1 cDNA and pre-treated with antagonist for 30 min before 8 hr of incubation with a combination of agonist and antagonist. % Luminescence data were generated by normalizing RLU to cells treated with CP 55,940 only (125 nM; expressed as 100% Luminescence) in cells transfected with CB_2-Tango only. Normalization was carried out within plates before combining with replicate data. **(A)** Curves are fit using non-linear regression analysis with variable slope (four parameters). Data are presented as mean +/- SD (**B)** E_{min}, E_{max}, Log IC_{50}, and IC_{50} values were derived using non-linear regression analysis with variable slope (four parameters). Data are presented as mean and 95% CI. n=6, experiments carried out on 2 different days. * indicates $p < 0.05$

A

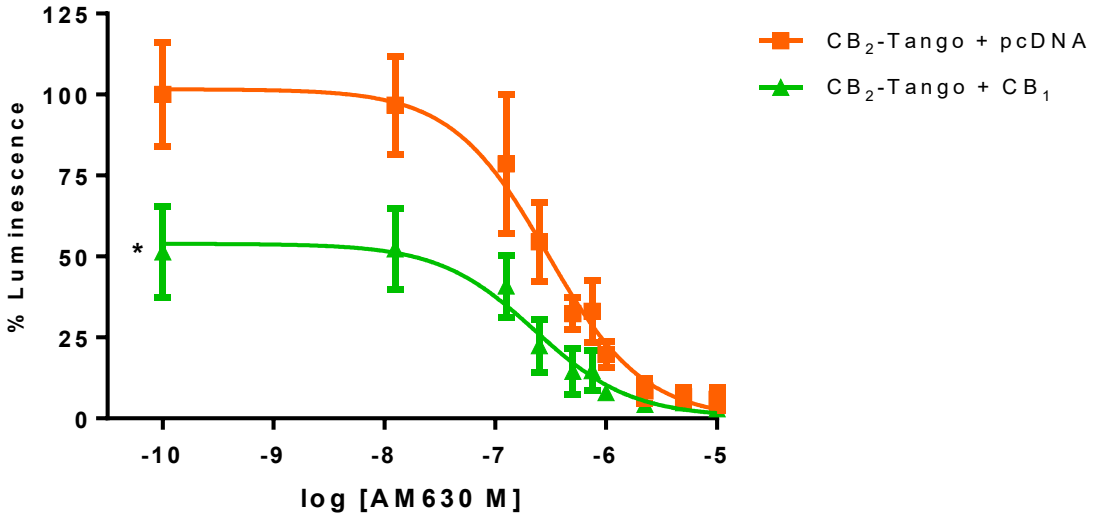

B

	CB_2-Tango	**CB_2-Tango + CB_1**
E_{min}	-0.08 [-6.41 to 6.21]	0.45 [-4.76 to 5.61]
E_{max}	101.60 [94.93 to 108.40]	53.92* [48.78 to 59.07]
Log IC_{50} (M)	-6.53 [-6.66 to -6.40]	-6.64 [-6.85 to -6.44]
IC_{50} (M)	2.91e-007 [2.16e-007 to 4.03e-007]	2.27e-007 [1.41e-007 to 3.66e-007]

Figure 3.34. The Effect Antagonism on CP 55,940-Dependant β-Arrestin Recruitment in Cells Co-Transfected with CB_1-Tango and CB_2-Tango

Histograms represent β-arrestin2 mobilization in HTLA cells treated with 125 nM CP 55,940 alone or in combination with 500 nM AM251 or AM630. Controls included cells treated with vehicle (OptiMEM I SFM with 0.1% MeOH and 0.1% DMSO) or 500 nM AM251 or AM630 alone. Drug treatments in HTLA cells transiently transfected with 25 ng or both CB_1-Tango and CB_2-Tango cDNA were compared to cells transfected with 25 ng CB_1-Tango **(A)** or 25 ng CB_2-Tango cDNA **(B)**. Cells were pre-treated with antagonist for 30 min before incubation with CP 55,940 and indicated antagonist. Differences in % Luminescence values between treatment groups were evaluated using two-way ANOVA with Tukey's post hoc test of significance. Data are presented as mean and SD. n=3 independent experiments carried out on 3 different days. * indicates $p < 0.05$ compared to vehicle treated cells; ^ indicates $p < 0.05$ compared to cells treated with 125 nM CP 55,940 only; # indicates $p < 0.05$ compared to cells treated with 125 nM CP 55,940 and 500 nM AM251; ~ indicates $p < 0.05$ between the indicated groups.

A

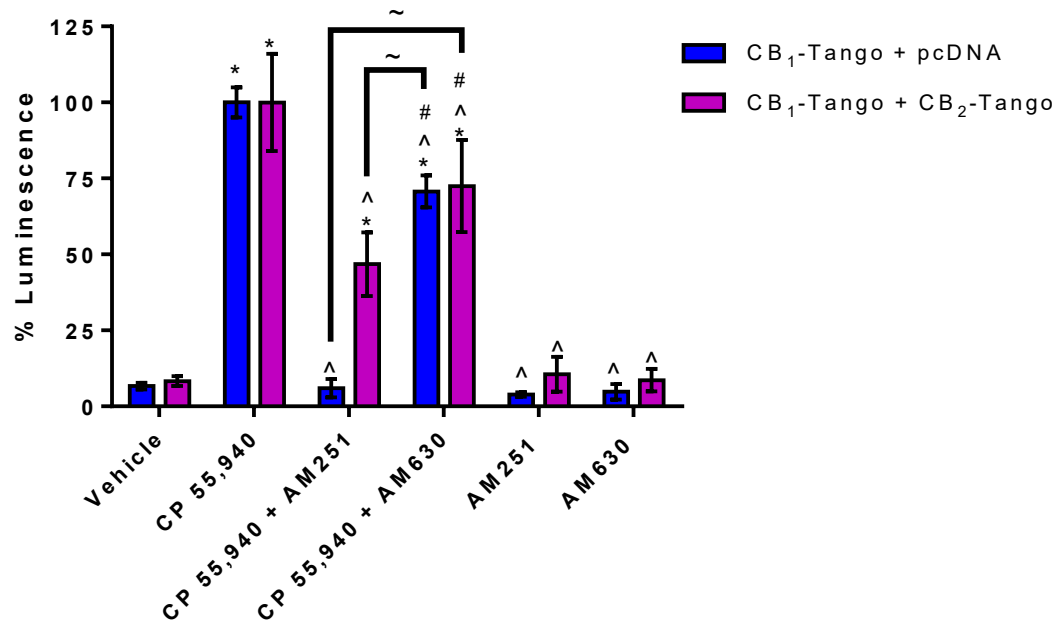
% Luminescence
125
100
75
50
25
0
Vehicle
CP 55,940
CP 55,940 + AM251
CP 55,940 + AM630
AM251
AM630
CB1-Tango + pcDNA
CB1-Tango + CB2-Tango

B

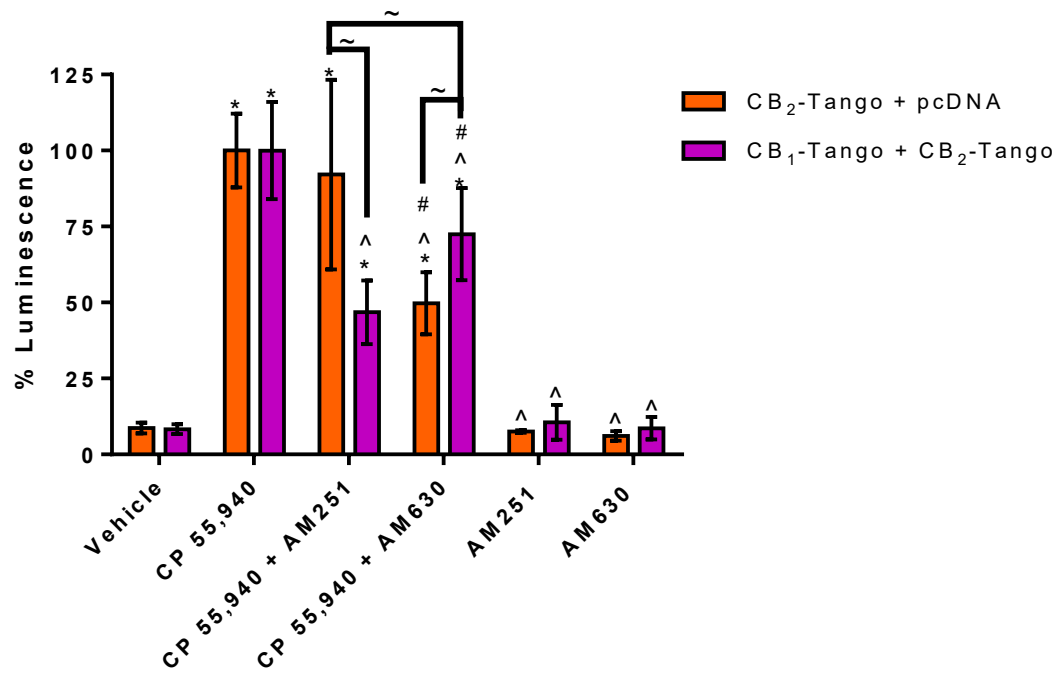
% Luminescence
125
100
75
50
25
0
Vehicle
CP 55,940
CP 55,940 + AM251
CP 55,940 + AM630
AM251
AM630
CB2-Tango + pcDNA
CB1-Tango + CB2-Tango

Figure 3.35. The Effect of Antagonism on CP 55,940-Dependant β-arrestin Recruitment in Co-Transfected Tango/Non-Tango Cells

Histograms represent β-arrestin2 mobilization in HTLA cells treated with 125 nM CP 55,940 alone or in combination with 500 nM AM251 or AM630. Controls included cells treated with vehicle (OptiMEM I SFM with 0.1% MeOH and 0.1% DMSO) or 500 nM AM251 or AM630 alone. HTLA cells were transiently transfected with either 25 ng CB_1-Tango, 25 ng each of CB_1-Tango and 3xHA-CB_2 cDNA **(A),** 25 ng CB_2-Tango, or oCB_2-Tango and CB_1_pcDNA cDNA **(B)**. Cells were pre-treated with antagonist for 30 min before incubation with CP 55,940 and indicated antagonist. Differences in % Luminescence values between treatment groups were evaluated using two-way ANOVA with Tukey's post hoc test of significance. Data are presented as mean and SD. n=3 independent experiments carried out on 3 different days. * indicates $p < 0.05$ compared to vehicle treated cells; ^ indicates $p < 0.05$ compared to cells treated with 125 nM CP 55,940 only; # indicates $p < 0.05$ compared to cells treated with 125 nM CP 55,940 and 500 nM AM251; ~ indicates $p < 0.05$ between the indicated groups.

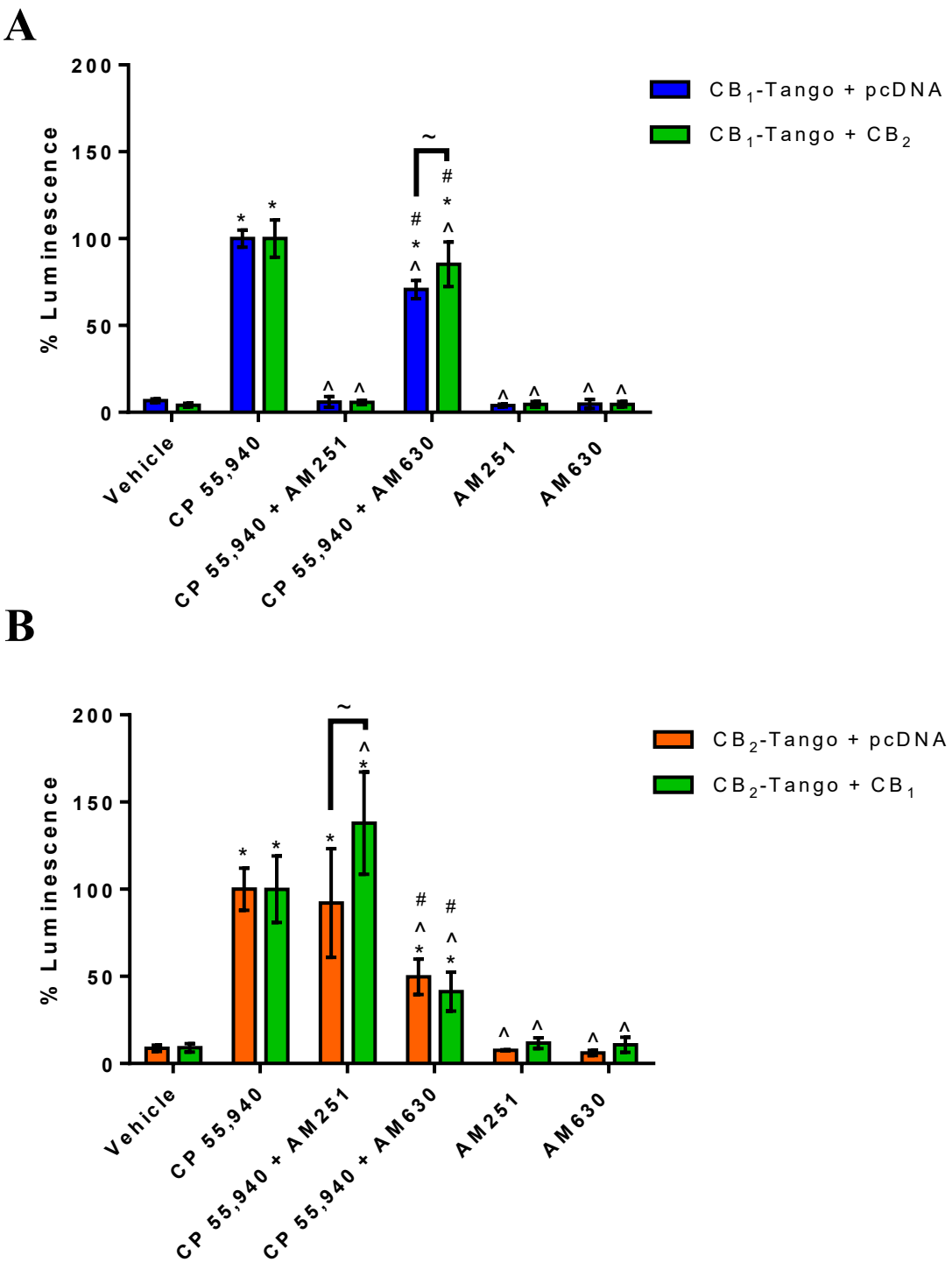
A
200
150
100
50
0
% Luminescence
CB1-Tango + pcDNA
CB1-Tango + CB2
Vehicle
CP 55,940
CP 55,940 + AM251
CP 55,940 + AM630
AM251
AM630
B
200
150
100
50
0
% Luminescence
CB2-Tango + pcDNA
CB2-Tango + CB1
Vehicle
CP 55,940
CP 55,940 + AM251
CP 55,940 + AM630
AM251
AM630

CHAPTER 4: DISCUSSION

4.1 Summary

The goal of this research was to test whether alterations in cell signalling observed in cells co-expressing CB_1 and CB_2 was a result of changes in the interaction between these individual receptors with β-arrestin following receptor activation when both receptors were present. We started by optimizing the conditions necessary to use the Tango-reporter assay to detect interactions between CB_1 or CB_2 and β-arrestin when both receptors were expressed and quantify the dose-dependent effect of agonist on this interaction. Allosteric interactions between CB_1 and CB_2 were detected when these receptors were co-expressed. Specifically, we noted an allosteric inhibition in β-arrestin2 recruitment to CB_1 following non-selective agonism in the presence of CB_2. Similarly, we observed inhibition in β-arrestin2 recruitment to CB_2 following non-selective agonism in the presence of CB_1. Selective antagonism of either CB_1 or CB_2 resulted in an apparent potentiation in β-arrestin2 to recruitment to the other co-expressed receptor. This data supports the published evidence of CB_1/CB_2 heteromer formation and alterations in cannabinoid receptor pharmacology of CB_1/CB_2 heteromers relative to the activity of singly expressed cannabinoid receptors (Callén *et al.* 2012; Sierra *et al.* 2015; Navarro, Borroto-Escuela, *et al.* 2018).

4.2 Lipofectamine®3000 Transfection Reduced CB_1- and CB_2-Tango Assay Sensitivity Relative to PEI Transfection

The Tango β-Arrestin2 recruitment *luc* reporter assay has classically been used in medium to high throughput assays to test a wide range of compounds against different receptors to screen for novel drug targets (Kroeze *et al.* 2015; Dogra *et al.* 2016). The published use of the Tango assay to detect GPCR heteromer-dependant changes in β-

arrestin2 recruitment has been a recent development and data are limited (Ang *et al.* 2018; Gao *et al.* 2018; Mores *et al.* 2019). To our knowledge there have been no published studies documenting the use of the Tango assay to detect changes in β-arrestin2 recruitment to the CB_1/CB_2 heteromer. Firstly, by testing agonist incubation times of 6, 8, and 18 hr with CP 55,940, it was evident that agonist incubation time was an essential factor to consider when measuring dose-dependant, saturable tTA-dependant luciferase reporter gene transcription. Secondly, we found that the transfection reagent used had a significant effect on Tango assay sensitivity. Lastly, before combining replicate data from independent experiments, we found that standardizing data to a predefined dose was important to help reduce inter-plate variability due to differences in RLU.

The finding that time-dependant luciferase expression was not the same between CB_1-Tango and CB_2-Tango following CP 55,940 activation is an important detail when using the Tango β-arrestin2 reporter assay to study heteromer interactions. For example, an agonist incubation time of 6 hr was sufficient to generate a saturable CP 55,940 dose-response curve in cells transfected with CB_2-Tango cDNA, but not CB_1-Tango. This finding was consistent with the reported receptor-dependant variability in GPCR-Tango receptor activity within the Tango assay (Kroeze *et al.* 2015). Despite achieving saturable, dose-dependant luciferase expression following incubation with CP 55,940, our early pilot experiments showed low fold-change activity over vehicle stimulated cells that correlated with poor assay sensitivity, as indicated by Z' factor calculations. Low assay sensitivity was not improved by serum starvation but was significantly improved by changing our transfection medium from the lipid based Lipofectamine® 3000 to the polymeric PEI reagent. Upon further consideration, we believe that the lipid-based

profile of Lipofectamine® 3000 may interfere with cannabinoid-Tango receptor activity. Endocannabinoids are uncharged lipophilic transmitters that diffuse within and across the plasma membrane down a concentration gradient (Zou and Kumar 2018). We propose here that the use of the lipofectamine reagent may be interfering with the lipid concentration gradient in a way that affects cannabinoid drugs from activating the CB_1 and CB_2 receptors. Furthermore, it has been documented that cannabinoid receptors, especially CB_1, commonly exhibit intracellular localization in endosomal or lysosomal compartments in addition to expression on the plasma membrane (Brailoiu *et al.* 2011). This distribution corresponded to CB_1 and CB_2 immunostaining of cells co-transfected with both receptors. With this logic in mind, it would follow that reducing the ability for CP 55,940 to pass the plasma membrane would decrease CB_r-Tango activation and impede Tango assay *luc* reporter activity. Switching transfection methods to a non-lipid-based reagent such as PEI could therefore explain the difference in assay sensitivity. Of course, it is possible that Lipofectamine is affecting the HTLA cells in some way that we have not considered, as Lipofectamine has been shown to lead to potentially unintended signaling and phenotype changes in certain cell types (Guo *et al.* 2019). It is important to note that the findings in this section were not part of our original hypothesis or experimental plan, and experiments would require repeated testing with more thoughtful planning to confirm the findings and theories regarding the effect of Lipofectamine on cannabinoid receptor activity.

4.3 CB_1 and CB_2 Co-Localize Following Transient Transfection in HEK293T Cells

We showed qualitative evidence, through dual immunostaining, that CB_1 and CB_2 co-localized at the cell membrane following transient plasmid transfection in HEK293T

cells. Co-localization following transient transfection in HEK293T cells has been documented and was shown through BRET to coincide to CB_1/CB_2 heteromer formation (Callén *et al.* 2012). In addition to published CB_1/CB_2 heteromer formation in SH-SY5Y cells, Pinealocyte cells, nucleus accumbens and globus pallidus slices (Callén *et al.* 2012), cultured and primary microglia (Navarro *et al.* 2018), Pallidothalamic projection neurons, and Globus pallidus slices (Sierra *et al.* 2015), we feel confident in using co-localization as the minimum required evidence to indicate CB_1/CB_2 heteromer formation. Of note, we also showed that co-transfection does not always lead to co-expression of the desired receptors, and even in co-expressing cells the receptors are not always co-localized. We feel that this is a noteworthy detail that is not currently addressed in the literature. More specifically, heteromer studies appear to commonly assume heteromer formation in all cells following co-transfection, and often present data to support this claim. For example, Callén *et al.* (2012) showed that antagonism of CB_1 or CB_2 in SH-SY5Y cells endogenously expressing CB_1 and transiently transfected with CB_2 was able to maximally inhibit pAkt signaling through the partner receptor, which suggests that antagonising one receptor causes complete loss of signaling from the partner receptor. Furthermore, this data would imply that they achieved 100% transfection efficiency following PEI transfection of this cell line. Based on our immunostaining, we propose that populations of transiently transfected cells are more likely made up of CB_1 or CB_2 or CB_1/CB_2 expressing cells, and that cells co-expressing both receptors express a mixed population of receptor monomers, homomers, and heteromers.

4.4 CB_1 and CB_2 Display Negative Allosteric Modulation of β-arrestin2 Recruitment in Co-Transfected HTLA Cells Following CP 55,940 Agonism

Following agonist-mediated cannabinoid receptor activation, β-arrestin2 is rapidly mobilized to promote receptor desensitization and internalization via clathrin-coated endocytosis (Ibsen *et al.* 2019). Receptor endocytosis and desensitization mark the cessation of G-protein-dependant signaling, in addition to the transduction of β-arrestin-dependant signaling cascades (DeFea, 2011). The dynamic balance between β-arrestin-dependant signal modulation, adjustment of receptor surface density, and receptor sequestration is an important process in cell homeostasis and function (Kovacs *et al.* 2009). Non-selective agonism of cannabinoid receptor heteromers, such as the CB_1/D_{2L} heteromer, results in changes in β-arrestin2 recruitment relative to agonism of either receptor partner alone (Bagher *et al.* 2017). Cells co-expressing CB_1 and CB_2 exhibit different signaling patterns than cells expressing CB_1 or CB_2 alone, which has been attributed to heteromer formation (Callén *et al.* 2012; Navarro *et al.* 2018; Navarro *et al.* 2020). To date, there has been no published data which directly compared β-arrestin2 recruitment in cells co-expressing CB_1 and CB_2 relative to cells expressing either receptor alone. Here, we found that non-selective agonism with CP 55,940 in HTLA cells co-transfected with CB_1 and CB_2 cDNA (at a 1:1 ratio) lead to a significant reduction in β-arrestin2 recruitment to both receptors, relative to the transfection of either receptor alone. The reduction in β-arrestin2 recruitment was unique to cells transfected with CB_1 and CB_2 cDNA and was not noted in cells transfected with combinations of plasmid DNA encoding the same receptor (ie. CB_1-Tango and CB_1, or CB_2-Tango and CB_2) under the same conditions (Fig. 4.1/ Fig. 4.2). This effect appeared to be dependant on the relative mass of transfected plasmids. Combining CB_1-Tango and CB_2-Tango plasmids did not

change CP 55,940-induced luminescence relative to cells transfected with CB_1-Tango alone, but roughly doubled luminescence relative to cells transfected with CB_2-Tango alone (Fig. 4.3). Because the noted decreases in β-arrestin2 recruitment was unique to cells transfected with CB_1 and CB_2 plasmids, and the summative luminescence from cells transfected with CB_1-Tango and CB_2-Tango was less than expected by adding luminescence from cells expressing CB_1-Tango and CB_2-Tango alone, we believe that decreases in β-arrestin2 recruitment are due to specific allosteric interactions between CB_1 and CB_2. Importantly, we are unable to determine if the functional units forming the heteromer are monomeric receptors or homomers (Fig. 4.1A/ Fig. 4.2A). Homomer formation is documented with the CB_1 receptor (Bagher 2017), and CB_1 can form higher order oligomeric structures with D_{2L}, composed of CB_1 and D_{2L} homomers. CB_2 homomers have detected by mass spectroscopy and homo-bifunctional crosslinking (Filppula *et al.* 2004; Singh *et al.* 2012) but have not been confirmed using direct biophysical methods.

Negative allostery following non-selective receptor agonism of CB_1 and CB_2 has been documented, albeit not with respect to β-arrestin2 recruitment. This form of negative allostery, whereby agonist treatment of both receptors leads to a decrease in functional activity, has been termed negative crosstalk and evidence of this interaction between CB_1 and CB_2 has been measured as changes in the accumulation of secondary messengers and altered phosphorylation of signalling proteins down stream of receptor activation. Negative cross talk occurs in the pAKT pathway and affects neurite outgrowth in SH-SY5Y cells using the CB_1 selective agonist ACEA and CB_2 selective agonist JWH133 (Callén *et al.* 2012). The cAMP and pERK1/2 pathways are affected by

negative crosstalk in resting (but not M1) N9 and primary striatal microglia following combined ACEA and JWH133 treatment, and treatment with the endocannabinoids 2-AG or AEA, respectively (Navarro *et al.* 2018). Similarly, negative crosstalk affects the $G_{\alpha i}$-dependant cAMP pathway following THC treatment in HEK293T cells (Navarro *et al.* 2018). β-arrestin1/2 recruitment can directly or indirectly modulate pAkt, pERK1/2, and cAMP signaling (Kovacs *et al.* 2009; Jean-Charles *et al.* 2017; van Gastel *et al.* 2018). In active (M1) microglia, co-agonism of CB_1 and CB_2 has been shown to potentiate $G_{\alpha i}$ signalling to further decrease cAMP and increase G-protein dependant, early pERK1/2 activity (Navarro *et al.* 2018). Based on the relationship between β-arrestin1/2 and G-protein signalling (that is, β-arrestin1/2 effectively stops G-protein activity following mobilization to the activated receptor), this observation fits with our finding. Essentially, our observed decrease in β-arrestin2 recruitment, could explain previously documented increases in $G_{\alpha i}$ signalling under similar conditions. Interestingly, this relationship was not noted in resting microglia, where co-agonism negatively modulated $G_{\alpha i}$-dependant reductions in cAMP and early pERK1/2 activity (Navarro *et al.* 2018). While these results appear contradictory, it is important to remember that CB_2 protein expression is significantly upregulated following microglial activation to the M1 phenotype (Ashton and Glass 2007), which implies that cannabinoid receptor stoichiometry may influence CB_1/CB_2 heteromer dependant signaling paradigms. Interestingly, we did not find any significant difference in β-arrestin2 recruitment to either CB_1 or CB_2 following non-selective agonism in cells transfected with 5:1 CB_1-Tango and CB_2, or CB_2-Tango and CB_1 cDNA. It is important to note that in our case, the Tango assay measured the summative accumulation of luciferase from cumulative β-arrestin2 recruitment over 18

hr, and we cannot rule out that low level expression did not lead to small differences in β-arrestin2 recruitment that were below our detection limits. Unexpectedly, there was a significant decrease in β-arrestin2 recruitment to CB_2-Tango when transfected 1:2 with CB_2. While it is tempting to rule this out as an artifact, allostery between receptors in GPCR homomers has been proposed (Smith and Milligan 2010) and we cannot rule out the possibility of stoichiometric and/or conformation-dependant induction of CB_2/CB_2 homomers with properties distinct from CB_2 monomers. We also propose that if both receptors recruit β-arrestin2 following heteromer formation, that the formation of a CB_1/CB_2 heterotetramer, composed of CB_1 and CB_2 homomers is possible.

4.5 CB_1/CB_2 Heteromers Display Atypical Antagonism Following AM251 and AM630 Treatment.

GPCR heteromers can display cross-antagonism. Cross antagonism occurs when selective antagonism of one receptor partner within a heteromer effectively inhibits activation of its partner receptor (Smith and Milligan 2010). We found that in cells co-transfected with CB_1-Tango and CB_2-Tango cDNA, AM251 appeared less efficacious at inhibiting β-arrestin2 recruitment relative to CB_1-Tango only cells, and AM630 was less efficacious relative to CB_2-Tango only cells (Table 4.1). While this decreased effect could be reasonably be explained by the presence of another Tango receptor which was also activated by CP 55,940, we also measured the effect of antagonism in cells co-transfected with CB_1-Tango and CB_2, and CB_2-Tango and CB_1. Under these conditions, pre-incubation with AM630 in cells co-transfected with CB_1-Tango and CB_2 lead to a moderate, but significant increase in arrestin recruitment to CB_1-Tango (Fig. 4.4A), relative to cells transfected with CB_1-Tango alone and treated with AM630. Similarly, pre-incubation with AM251 in cells transfected with CB_2-Tango and CB_1 resulted in

a significant increase in β-arrestin2 recruitment to CB_2-Tango (Fig. 4.4B) relative to AM251 treatment in cells transfected with CB_2-Tango only, where AM251 had no effect. This AM251-dependant increase in β-arrestin2 recruitment to CB_2-Tango was likewise significantly higher than cells treated with CP 55,940 alone. In short, it appears that antagonism of either CB_1 or CB_2 in heteromer, acts to block the reduction in β-arrestin2 recruitment to either receptor following their co-activation, or may potentiate β-arrestin2 recruitment to the partner receptor (Fig. 4.4). To our knowledge, no studies have published data examining the effect of selective antagonism of β-arrestin2 recruitment in CB_1/CB_2 heteromers, although patterns of cross antagonism have been documented in the pAkt pathway and neurite outgrowth in SH-SY5Y cells, and in the early pERK1/2 pathway in rat globus pallidus slices (Callén *et al.* 2012); and the cAMP and pERK1/2 pathways in resting and pro-inflammatory N9 and primary striatal microglia (Navarro *et al.* 2018). While this data creates a very complicated story, and highlights some very complex pharmacology, we do propose a few theories behind this puzzling interaction. Firstly, we must address our antagonists, their relationship with cannabinoid receptors, and their relationship to our agonist CP 55,940. As expected, AM251 was able to selectively inhibit CP 55,940-dependant agonism in CB_1-Tango transfected cells, while having no effect on CP 55,940 activation of CB_2-Tango. What we cannot resolve, however, is how AM251 is achieving this outcome. Radioligand binding studies using (^{3}H)CP 55,940 and (^{123}I)AM251 indicate that CP 55,940 and AM251 likely occupy distinct binding locations on CB_1, as the IC_{50} of cannabinoid ligands such as methanamide, WIN 55212-2, and non-labeled CP 55,940 to displace the radiolabelled ligands was significantly different between the two (Gatley *et al.* 1997). If it is true that

CP 55,940 and AM251 interact with different regions of the CB_1 receptor, then it is possible that we are observing an effect of ligand-dependant allostery, on top of heteromer-dependant allostery. The relative selectivity of AM630 was low and AM630 produced significant inhibition of CP 55,940-dependant β-arrestin2 recruitment to CB_1-Tango. It is possible that AM630 is binding allosterically to the CB_1 receptor. Theoretically, allosteric binding might make AM630 appear selective to CB_2, as it may not displace a radiolabelled reference ligand which was binding to the orthosteric pocket. Under such conditions, it could still having efficacy towards inhibition of β-arrestin2 recruitment, as noted in the Tango assay. In addition, AM630 has been identified as a protean ligand, whereby its actions are highly dependent on its chemical and cellular environment (Bolognini *et al.* 2012). We therefore cannot rule out that AM630 itself exerts actions on the CP 55,940 activated CB_1/CB_2 heteromer that are distinctly different than its actions on CB_1 or CB_2 alone. Furthermore, it is possible that we have revealed a novel mechanism of the CB_1/CB_2 heteromer, whereby antagonism of one receptor enhances the effect of agonist activation in the partner receptor. While this has not been documented within the CB_1/CB_2 heteromer, this has been noted within the CXCR2/ΔOR heteromer (Parenty *et al.* 2008).

4.6 Limitations of This Study

Heterologous Expression

The use of heterologous expression systems in HEK293T has a number of limitations that limit extrapolation our results to an endogenous system. Firstly, transient transfection results in three cell population including: 1) cells that successfully express both receptors, 2) cells that only express one receptor, and 3) cells that do not express either receptor. While cells that did not express any receptor would be silent within the

mixed population with respect to the Tango reporter, cells expressing only one Tango receptor despite co-transfection would act in the same manner as cells transfected with only one Tango plasmid. This could result in an alteration in the noted CP 55,940-induced change in β-arrestin2 recruitment in cells co-expressing CB_1 and CB_2 than that expected if all cells had been co-transfected and expressed all receptors of interest. While we are hesitant to fully accept that all cells co-express CB_1 and CB_2 in regions where CB_1/CB_2 heteromers form, we cannot discount this possibility, or ignore the potential differences between this scenario and the data presented in this thesis. Furthermore, it is important to highlight those findings from our modified plasmids, in modified HEK293T cells, may not be the same in different cell lines, or in a fully functioning biological system, as has been shown when comparing signalling in HEK293T and SH-SY5Y cell lines (Alberts *et al.* 2000). We do not, however, feel that this fact undermines the validity of our findings, or the importance of the added benefit of control in experimental cell-based research.

Dual Immunofluorescence

Transfection of plasmids into HEK293T cells was carried out using PEI. Because These experiments were not repeated (n=1), quantified, or mirrored using Lipofectamine3000, our ability to infer anything from this qualitative data is inherently limited. Furthermore, dual immunofluorescence was carried out using non-tango plasmids, and may not be a true reflection of the expression patterns of the Tango plasmids. While they are all controlled by the CMV promoter, the Tango receptors are FLAG- and Tango-tagged, while non-tango plasmids are either untagged (CB_1) or 3xHA-tagged (CB_2). These differences would logically result in plasmids of different sizes for

each receptor of interest, and plasmid size has been identified as an important factor in transfection efficiency (Pezzoli *et al.* 2017).

Tango

Tango plasmids encode for receptors with C-terminal tail modifications, which allow for the transcription of luciferase (Kroeze *et al.*2015). These modifications include replacement of the cognate receptor tail with the C-terminal of the V_2 receptor, which is known to recruit β-arrestin2 more robustly than CB_1 or CB_2 (Ibsen *et al.* 2019). This modification may exaggerate the reported differences in β-arrestin2 recruitment in the experiments presented in this thesis.

4.7 Significance and Future Directions

Heteromer formation is a beautiful example of evolutionary parsimony in action. Instead of the biological cost of expansion of unique receptor types, the combination of entropy, natural selection, and time has allowed for the interaction between pre-existing protein receptors to create novel pathways and responses in different cell populations and in response to physiological and pathological state. Our research adds to the body of literature supporting the observations that CB_1/CB_2 heteromers have unique pharmacology compared to individual receptors. The observation that these receptors negatively regulate β-arrestin recruitment provides a mechanism to understand the change in signalling cells co-expressing both receptors. Without experiments to link β-arrestin recruitment and signaling, we reasonably limit our extrapolations of the physiological significance of this interaction. What we can say is that the current literature has shown that the CB_1/CB_2 heteromer is more abundant in neuronal and non-neuronal populations of the CNS, specifically in regions of the basal ganglia *in vivo* (Sierra *et al.* 2015;

Navarro *et al.* 2018) and that there is potential for changes in the distribution of heteromers and response to ligands under such conditions. While much research is yet to be done to understand the precise function of the CB_1/CB_2 heteromer, it is not a stretch to say that its limited distribution may one day provide a more specific target for cannabinoid therapy in the CNS than can be currently offered through targeting the CB_1, which is widely expressed in the CNS.

Future directions in the study of the CB_1/CB_2 heteromer using Tango will investigate the effect of potent and selective agonism on β-arrestin2 recruitment to CB_1 and CB_2 in co-transfected cells. In addition, we feel that the use of selective, neutral antagonists would allow us to better interpret the effect of cross-antagonism at the CB_1/CB_2 heteromer. In addition, biophysical methods such as $BRET^2$ or Bi-fluorescence complementation should be used to study ligand and/or time-dependant patterns of cannabinoid heteromer formation. These methods can test interactions between fluorescent-labeled receptors over a shorter time than Tango and can be expanded to include protein interactions between the CB_1/CB_2 heteromer and G-proteins, β-arrestin1 and/or β-arrestin2. We also feel that the use of cells stably expressing CB_1 or CB_2 would be of great benefit. Our dual immunostaining demonstrated that transient co-transfection does not always lead to co-expression of your proteins of interest. Stably transfected cells would provide a much higher likelihood that all cells in culture were, at minimum, expressing the stably transfected receptor. Using stably transfected cells, we could use western blotting or quantitative immunofluorescence (On/In-Cell Western^{TM}; Li-Cor Biosciences, USA) to detect changes in cAMP, early and late pERK1/2, and cellular localization of CB_1 and CB_2 proteins following co-transfection. Furthermore, we could

understand how these functional aspects of heteromer behavior change depending on the use of different drugs, and over time. We could likewise transfect BRET-based plasmids to study heteromer formation and signaling in the same cell types. As cannabinoid receptor function has been shown to be highly dynamic based on the cell being studied (Shenglong Zou and Ujendra Kumar 2018), we feel that the only way to truly compare protein interactions and signaling events is by studying them in the same cell type.

Figure 4.1. Protein-Protein Allostery Reduces β-Arrestin2 Recruitment to CB_1 Following Non-Selective CP 55,940 Agonism

CP 55,940 agonism in HTLA cells transfected with CB_1-Tango only was used as the primary reference point for β-arrestin2 recruitment to CB_1. The Tango assay cannot differentiate from receptors acting as monomers, or homomers, so this must be considered while interpreting results **(A)**. Co-transfection of CB_1-Tango and CB_1 did not result in any change in β-arrestin2 recruitment to CB_1-Tango following CP 55,940 agonism **(B)**. Co-transfection of CB_1-Tango and CB_2 resulted in an approximate 25% reduction in β-arrestin2 recruitment to CB_1-Tango following non-selective CP 55,940 agonism **(C)**. '+ signs' indicate strength of luciferase expression and intensity of β-arrestin2-dependant luminescence output following CP 55,940-induced receptor activation.

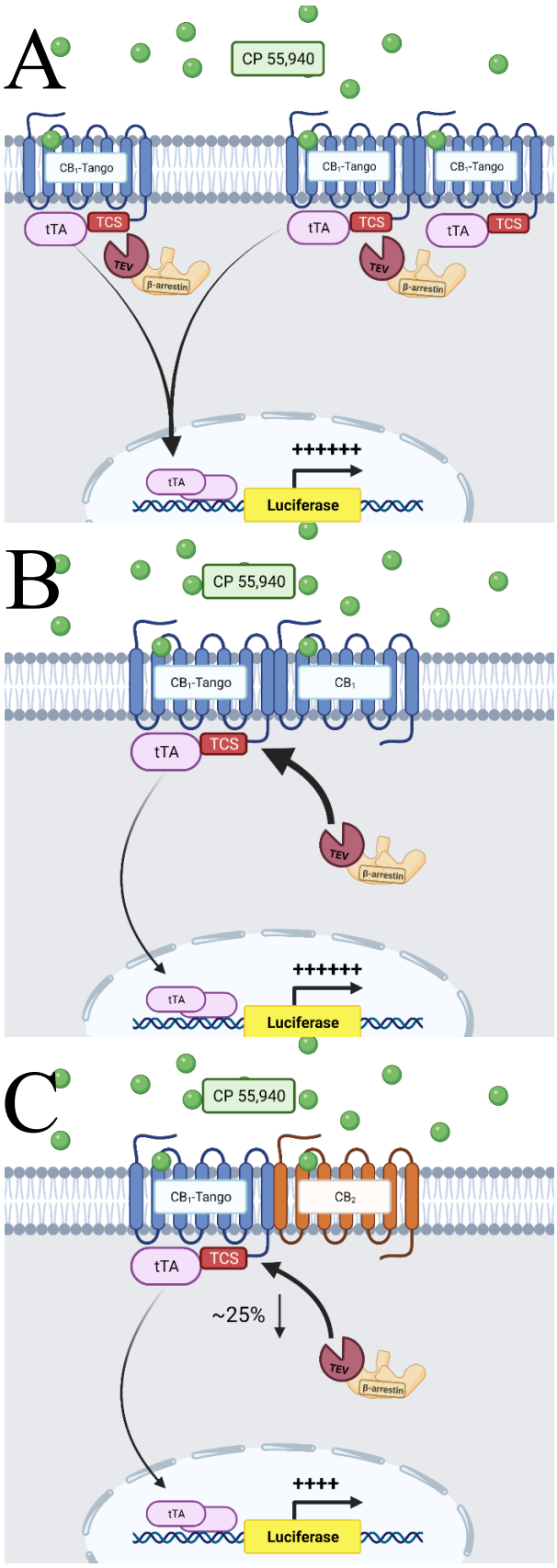
A
CP 55,940
CB1-Tango
tTA
TCS
TEV
β-arrestin
++++++
Luciferase
B
CP 55,940
CB1-Tango
CB1
C
CP 55,940
CB1-Tango
CB2
~25%
++++
Luciferase

Figure 4.2. Protein-Protein Allostery Between Cannabinoid Receptors Reduces β-Arrestin2 Recruitment to CB_2 Following Non-Selective CP 55,940 Agonism

CP 55,940 agonism in HTLA cells transfected with CB_2-Tango only was used as the primary reference point for β-arrestin2 recruitment to CB_2. The Tango assay cannot differentiate from receptors acting as monomers, or homomers, so this must be considered while interpreting results **(A)**. Co-transfection of CB_2-Tango and CB_2 did not result in any change in β-arrestin2 recruitment to CB_2-Tango following CP 55,940 agonism **(B)**. Co-transfection of CB_2-Tango and CB_1 resulted in an approximate 25% reduction in β-arrestin2 recruitment to CB_2-Tango following non-selective CP 55,940 agonism **(C)**. '+ signs' indicate strength of luciferase expression and intensity of β-arrestin2-dependant luminescence output following CP 55,940-induced receptor activation.

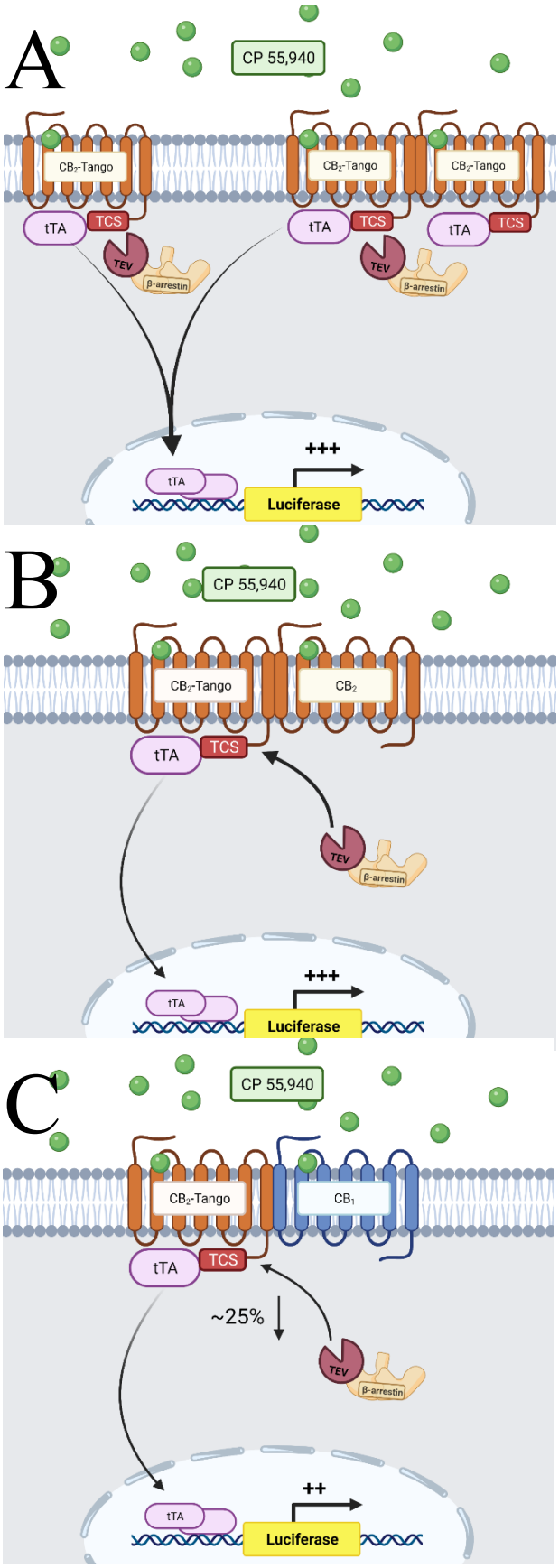
A
CP 55,940
CB2-Tango
tTA
TCS
TEV
β-arrestin
+++
Luciferase
B
CP 55,940
CB2-Tango
CB2
C
CP 55,940
CB2-Tango
CB1
~25%
++

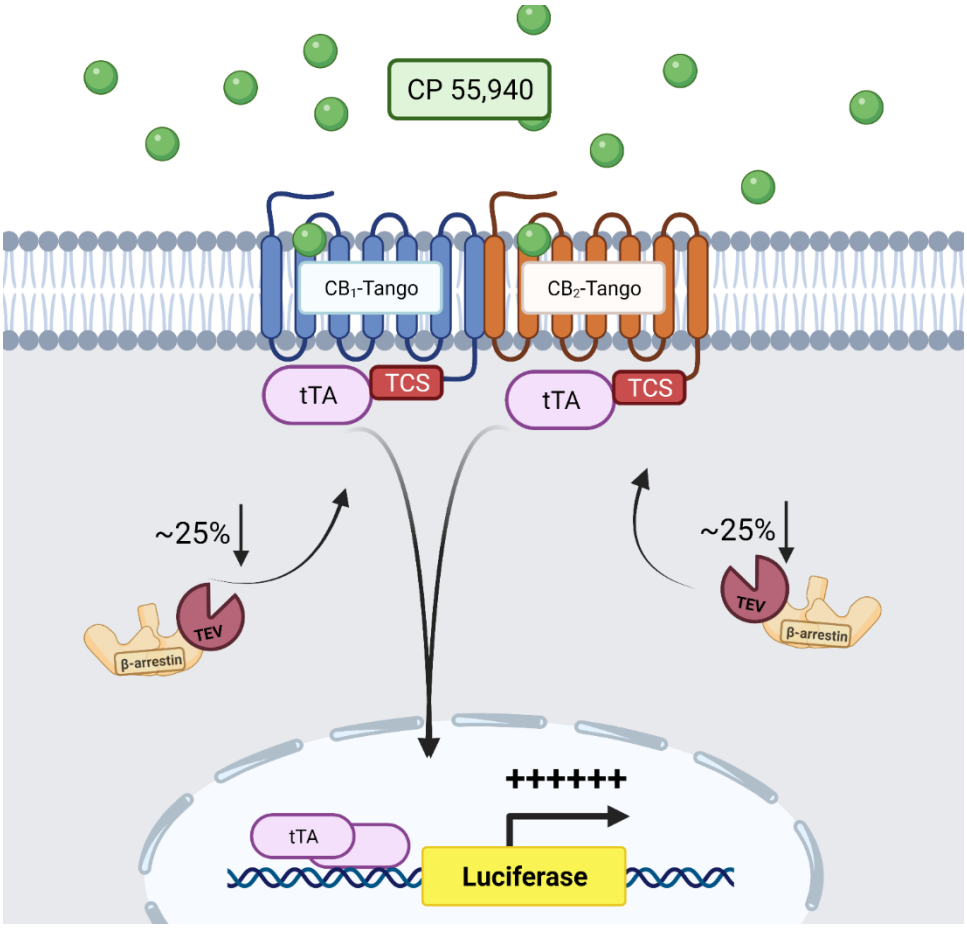

Figure 4.3. Protein-Protein Allostery Between Cannabinoid Receptors Reduces β-Arrestin2 Recruitment Following Non-Selective Agonism

CP 55,940 agonism in HTLA cells transfected with CB_1-Tango and CB_2-Tango resulted in lower luminescence than the summation of luminescence from cells expressing CB_1-Tango or CB_2-Tango alone. Luminescence intensity was no different than cells expressing CB_1-Tango alone, and two times as intense as cells expressing CB_2-Tango alone. We propose that CB_1 and CB_2 both recruit β-Arrestin2 while in complex following non-selective agonism. Protein allostery, however, reduces the relative efficacy of CP 55,940 to promote β-Arrestin2 to either receptor by approximately 25%.

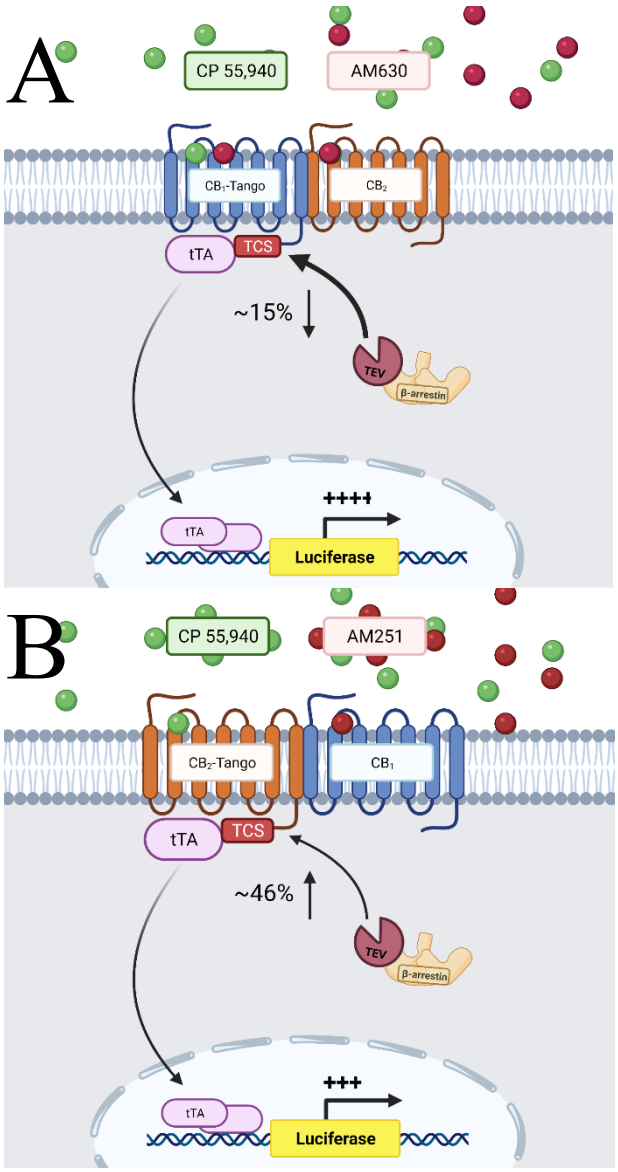

Figure 4.4. Protein-Protein Allostery Between CB_1 and CB_2 Increases β-arrestin2 Recruitment to Cannabinoid Receptors Following Antagonism

AM630 treatment in cells co-transfected with CB_1-Tango and CB_2 leads to a 15% reduction in β-arrestin2 recruitment relative to CP 55,940 treatment. In cells transfected with CB_1-Tango alone, AM630 treatment reduced β-arrestin2 recruitment by ~29%. AM630 may compete with CP 55,950 binding at the orthosteric site or bind to an allosteric ligand binding pocket. AM630 treatment increased β-arrestin2 recruitment to CB_1-Tango when co-expressed with CB_2 **(A)**. AM251 treatment in cells co-expressing CB_2-Tango and CB_1 increased β-arrestin2 recruitment to CB_2-Tango by ~46% relative to CP 55,950 treatment. AM251 had no effect on CP 55,940-induced β-arrestin2 recruitment to CB_2-Tango in the nanomolar range. AM630 treatment increased β-arrestin2 recruitment to CB_2-Tango when co-expressed with CB_1 **(B).**

Table 4.1 Comparison of β-arrestin2 Mobilization Between Transfection Groups and Drug Treatments Used in This Thesis

Comparison of the effects of drug treatments between transfection groups. '+ signs' correspond to approximate strength of β-arrestin2-induced luminescence. n/a indicates that luminescence was not different than vehicle treated cells.

Transfection Condition	Drug Treatment	β-arrestin2 Recruitment
CB_1-Tango	CP 55,940	++++++
	CP 55,940 + AM251	n/a
	CP 55,940 + AM630	++++
CB_1-Tango + CB_1	CP 55,940	++++++
CB_1-Tango + CB_2	CP 55,940	++++
	CP 55,940 + AM251	n/a
	CP 55,940 + AM630	+++
CB_2-Tango	CP 55,940	+++
	CP 55,940 + AM251	+++
	CP 55,940 + AM630	+
CB_2-Tango + CB_2	CP 55,940	+++
CB_2-Tango + CB_1	CP 55,940	++
	CP 55,940 + AM251	+++
	CP 55,940 + AM630	+
CB_1-Tango + CB_2-Tango	CP 55,940	++++++
	CP 55,940 + AM251	+++
	CP 55,940 + AM630	++++

BIBLIOGRAPHY

Ahn S, Shenoy SK, Wei H, Lefkowitz RJ. 2004. Differential Kinetic and Spatial Patterns of β-Arrestin and G Protein-mediated ERK Activation by the Angiotensin II Receptor. J Biol Chem. 279(34):35518–35525. doi:10.1074/jbc.M405878200.

Albayram Ö, Passlick S, Bilkei-Gorzo A, Zimmer A, Steinhäuser C. 2016. Physiological impact of CB1 receptor expression by hippocampal GABAergic interneurons. Pflüg Arch - Eur J Physiol. 468(4):727–737. doi:10.1007/s00424-015-1782-5.

Alberts GL, Pregenzer JF, Bin Im W. 2000. Advantages of heterologous expression of human D2long dopamine receptors in human neuroblastoma SH-SY5Y over human embryonic kidney 293 cells. British J Pharmacol. 131(2): 514-520.

Albizu L, Moreno JL, González-Maeso J, Sealfon SC. 2010. Heteromerization of G Protein-Coupled Receptors: Relevance to Neurological Disorders and Neurotherapeutics. CNS Neurol Disord Drug Targets. 9(5):636–650.

Ang Z, Xiong D, Wu M, Ding JL. 2018. FFAR2-FFAR3 receptor heteromerization modulates short-chain fatty acid sensing. FASEB J. 32(1):289–303. doi:10.1096/fj.201700252RR.

Ashton JC, Glass M. 2007. The Cannabinoid CB2 Receptor as a Target for Inflammation-Dependent Neurodegeneration. Curr Neuropharmacol. 5(2):73–80.

Ayoub MA, Pfleger KDG. 2010. Recent advances in bioluminescence resonance energy transfer technologies to study GPCR heteromerization. Curr Opin Pharmacol. 10(1):44–52. doi:10.1016/j.coph.2009.09.012.

Bagher AM. 2017. Allosteric Interactions Within Cannabinoid Receptor 1 (CB1) and Dopamine Receptor 2 Long (D2L) Heteromers [Thesis].https://DalSpace.library.dal.ca//handle/10222/73150.

Bagher AM, Laprairie RB, Kelly ME, Denovan-Wright EM. 2016 Jan 1. Antagonism of dopamine receptor 2 long (D2L) affects cannabinoid receptor 1 (CB1) signaling in a cell culture model of striatal medium spiny projection neurons. Mol Pharmacol. doi:10.1124/mol.116.103465.

Bagher AM, Laprairie RB, Toguri JT, Kelly Melanie E.M., Denovan-Wright EM. 2017. Bidirectional allosteric interactions between cannabinoid receptor 1 (CB 1) and dopamine receptor 2 long (D 2L) heterotetramers. Eur J Pharmacol. 813:66–83. doi:10.1016/j.ejphar.2017.07.034.

Bagher AM, Laprairie RB, Toguri JT, Kelly Melanie E. M., Denovan-Wright EM. 2017. Bidirectional allosteric interactions between cannabinoid receptor 1 (CB1) and dopamine receptor 2 long (D2L) heterotetramers. Eur J Pharmacol. 813:66–83. doi:10.1016/j.ejphar.2017.07.034.

Balenga NA, Martínez-Pinilla E, Kargl J, Schröder R, Peinhaupt M, Platzer W, Bálint Z, Zamarbide M, Dopeso-Reyes IG, Ricobaraza A, *et al.* 2014. Heteromerization of GPR55 and cannabinoid CB $_2$ receptors modulates signalling: Heteromerization of GPR55 and CB $_2$ receptors. Br J Pharmacol. 171(23):5387–5406. doi:10.1111/bph.12850.

Bari M, Battista N, Fezza F, Gasperi V, Maccarrone M. 2006. New Insights into Endocannabinoid Degradation and its Therapeutic Potential. Mini-Rev Med Chem. 6(3):257–268. doi:10.2174/138955706776073466.

Bari M, Battista N, Valenza M, Mastrangelo N, Malaponti M, Catanzaro G, Centonze D, Finazzi-Agrò A, Cattaneo E, Maccarrone M. 2013. *In vitro* and *in vivo* models of Huntington's disease show alterations in the endocannabinoid system. FEBS J. 280(14):3376–3388. doi:10.1111/febs.12329.

Barrie N, Manolios N. 2017. The endocannabinoid system in pain and inflammation: Its relevance to rheumatic disease. Eur J Rheumatol. 4(3):210–218. doi:10.5152/eurjrheum.2017.17025.

Blázquez C, Chiarlone A, Sagredo O, Aguado T, Pazos MR, Resel E, Palazuelos J, Julien B, Salazar M, Börner C, *et al.* 2011. Loss of striatal type 1 cannabinoid receptors is a key pathogenic factor in Huntington's disease. Brain J Neurol. 134(Pt 1):119–136. doi:10.1093/brain/awq278.

Bolognini D, Cascio MG, Parolaro D, Pertwee RG. 2012. AM630 behaves as a protean ligand at the human cannabinoid CB2 receptor. Br J Pharmacol. 165(8):2561–2574. doi:10.1111/j.1476-5381.2011.01503.x.

Borroto-Escuela DO, Carlsson J, Ambrogini P, Narváez M, Wydra K, Tarakanov AO, Li X, Millón C, Ferraro L, Cuppini R, *et al.* 2017. Understanding the Role of GPCR Heteroreceptor Complexes in Modulating the Brain Networks in Health and Disease. Front Cell Neurosci. 11. doi:10.3389/fncel.2017.00037.

Brailoiu GC, Oprea TI, Zhao P, Abood ME, Brailoiu E. 2011. Intracellular Cannabinoid Type 1 (CB1) Receptors Are Activated by Anandamide. J Biol Chem. 286(33):29166–29174. doi:10.1074/jbc.M110.217463.

Bushlin I, Gupta A, Stockton SD, Miller LK, Devi LA. 2012. Dimerization with Cannabinoid Receptors Allosterically Modulates Delta Opioid Receptor Activity during Neuropathic Pain. PLoS ONE. 7(12). doi:10.1371/journal.pone.0049789.

Cadas H, Gaillet S, Beltramo M, Venance L, Piomelli D. 1996. Biosynthesis of an Endogenous Cannabinoid Precursor in Neurons and its Control by Calcium and cAMP. J Neurosci. 16(12):3934–3942. doi:10.1523/JNEUROSCI.16-12-03934.1996.

Callén L, Moreno E, Barroso-Chinea P, Moreno-Delgado D, Cortés A, Mallol J, Casadó V, Lanciego JL, Franco R, Lluis C, *et al.* 2012. Cannabinoid Receptors CB $_1$ and

CB $_2$ Form Functional Heteromers in Brain. J Biol Chem. 287(25):20851–20865. doi:10.1074/jbc.M111.335273.

Canals M, Marcellino D, Fanelli F, Ciruela F, de Benedetti P, Goldberg SR, Neve K, Fuxe K, Agnati LF, Woods AS, *et al.* 2003. Adenosine A2A-Dopamine D2 Receptor-Receptor Heteromerization: Qualitative and Quantitative Assessments by Fluorescence and Bioluminescence Energy Transfer. J Biol Chem. 278(47):46741–46749. doi:10.1074/jbc.M306451200.

Carriba P, Ortiz O, Patkar K, Justinova Z, Stroik J, Themann A, Müller C, Woods AS, Hope BT, Ciruela F, *et al.* 2007. Striatal Adenosine A2A and Cannabinoid CB1 Receptors Form Functional Heteromeric Complexes that Mediate the Motor Effects of Cannabinoids. Neuropsychopharmacology. 32(11):2249–2259. doi:10.1038/sj.npp.1301375.

Castillo PE, Younts TJ, Chávez AE, Hashimotodani Y. 2012. Endocannabinoid signaling and synaptic function. Neuron. 76(1):70–81. doi:10.1016/j.neuron.2012.09.020.

Chen D, Gao M, Gao F, Su Q, Wu J. 2017. Brain cannabinoid receptor 2: expression, function and modulation. Acta Pharmacol Sin. 38(3):312–316. doi:10.1038/aps.2016.149.

Chen X, Zheng C, Qian J, Sutton SW, Wang Z, Lv J, Liu C, Zhou N. 2014. Involvement of β-arrestin-2 and clathrin in agonist-mediated internalization of the human cannabinoid CB2 receptor. Curr Mol Pharmacol. 7(1):67–80. doi:10.2174/1874467207666140714115824.

Cravatt BF, Giang DK, Mayfield SP, Boger DL, Lerner RA, Gilula NB. 1996. Molecular characterization of an enzyme that degrades neuromodulatory fatty-acid amides. Nature. 384(6604):83–87. doi:10.1038/384083a0.

DeFea KA. 2011. Beta-arrestins as regulators of signal termination and transduction: how do they determine what to scaffold? Cell Signal. 23(4):621–629. doi:10.1016/j.cellsig.2010.10.004.

Denovan-Wright EM, Robertson HA. 2000. Cannabinoid receptor messenger RNA levels decrease in a subset of neurons of the lateral striatum, cortex and hippocampus of transgenic Huntington's disease mice. Neuroscience. 98(4):705–713. doi:10.1016/S0306-4522(00)00157-3.

Devane WA, Hanus L, Breuer A, Pertwee RG, Stevenson LA, Griffin G, Gibson D, Mandelbaum A, Etinger A, Mechoulam R. 1992. Isolation and structure of a brain constituent that binds to the cannabinoid receptor. Science. 258(5090):1946–1949. doi:10.1126/science.1470919.

Di Marzo V. 2006. Endocannabinoids: synthesis and degradation. In: Reviews of Physiology Biochemistry and Pharmacology. Vol. 160. Berlin, Heidelberg:

Springer Berlin Heidelberg. (Reviews of Physiology, Biochemistry and Pharmacology). p. 1–24.

Di Marzo V. 2008. Targeting the endocannabinoid system: to enhance or reduce? Nat Rev Drug Discov. 7(5):438–455. doi:10.1038/nrd2553.

Dinh TP, Carpenter D, Leslie FM, Freund TF, Katona I, Sensi SL, Kathuria S, Piomelli D. 2002. Brain monoglyceride lipase participating in endocannabinoid inactivation. Proc Natl Acad Sci. 99(16):10819–10824. doi:10.1073/pnas.152334899.

Dogra S, Sona C, Kumar A, Yadav PN. 2016. Tango assay for ligand-induced GPCR-β-arrestin2 interaction: Application in drug discovery. Methods Cell Biol. 132:233–254. doi:10.1016/bs.mcb.2015.11.001.

Eishingdrelo H, Kongsamut S. 2013. Minireview: Targeting GPCR Activated ERK Pathways for Drug Discovery. Curr Chem Genomics Transl Med. 7:9–15. doi:10.2174/2213988501307010009.

El Khamlichi C, Reverchon-Assadi F, Hervouet-Coste N, Blot L, Reiter E, Morisset-Lopez S. 2019. Bioluminescence Resonance Energy Transfer as a Method to Study Protein-Protein Interactions: Application to G Protein Coupled Receptor Biology. Molecules. 24(3). doi:10.3390/molecules24030537.

Ellis J, Pediani JD, Canals M, Milasta S, Milligan G. 2006. Orexin-1 Receptor-Cannabinoid CB1 Receptor Heterodimerization Results in Both Ligand-dependent and -independent Coordinated Alterations of Receptor Localization and Function. J Biol Chem. 281(50):38812–38824. doi:10.1074/jbc.M602494200.

Farrens DL, Altenbach C, Yang K, Hubbell WL, Khorana HG. 1996. Requirement of Rigid-Body Motion of Transmembrane Helices for Light Activation of Rhodopsin. Science. 274(5288):768–770. doi:10.1126/science.274.5288.768.

Ferré S, Franco R. 2010. Oligomerization of G protein-coupled receptors: A reality. Curr Opin Pharmacol. 10(1):1–5. doi:10.1016/j.coph.2009.11.002.

Filppula S, Yaddanapudi S, Mercier R, Xu W, Pavlopoulos S, Makriyannis A. 2004. Purification and mass spectroscopic analysis of human CB2 cannabinoid receptor expressed in the baculovirus system. J Pept Res Off J Am Pept Soc. 64(6):225–236. doi:10.1111/j.1399-3011.2004.00188.x.

Fonseca BM, Costa MA, Almada M, Correia-da-Silva G, Teixeira NA. 2013. Endogenous cannabinoids revisited: A biochemistry perspective. Prostaglandins Other Lipid Mediat. 102–103:13–30. doi:10.1016/j.prostaglandins.2013.02.002.

Fowler CJ. 2013. Transport of endocannabinoids across the plasma membrane and within the cell. FEBS J. 280(9):1895–1904. doi:10.1111/febs.12212@10.1002

Franco R, Martínez-Pinilla E, Lanciego JL, Navarro G. 2016. Basic Pharmacological and Structural Evidence for Class A G-Protein-Coupled Receptor Heteromerization. Front Pharmacol. 7:76. doi:10.3389/fphar.2016.00076.

Franco R, Villa M, Morales P, Reyes-Resina I, Gutiérrez-Rodríguez A, Jiménez J, Jagerovic N, Martínez-Orgado J, Navarro G. 2019 Feb 7. Increased expression of cannabinoid CB2 and serotonin 5-HT1A heteroreceptor complexes in a model of newborn hypoxic-ischemic brain damage. Neuropharmacology. doi:10.1016/j.neuropharm.2019.02.004.

Fuxe K, Agnati LF, Benfenati F, Celani M, Zini I, Zoli M, Mutt V. 1983. Evidence for the existence of receptor--receptor interactions in the central nervous system. Studies on the regulation of monoamine receptors by neuropeptides. J Neural Transm Suppl. 18:165–179.

Gaitonde SA, González-Maeso J. 2017. Contribution of heteromerization to G protein-coupled receptor function. Curr Opin Pharmacol. 32:23–31. doi:10.1016/j.coph.2016.10.006.

Gao X, Albee LJ, Volkman BF, Gaponenko V, Majetschak M. 2018. Asymmetrical ligand-induced cross-regulation of chemokine (C-X-C motif) receptor 4 by α1-adrenergic receptors at the heteromeric receptor complex. Sci Rep. 8. doi:10.1038/s41598-018-21096-4.

García Lopez MA, Aguado Martínez A, Lamaze C, Martínez-A. C, Fischer T. 2009. Inhibition of dynamin prevents CCL2-mediated endocytosis of CCR2 and activation of ERK1/2. Cell Signal. 21(12):1748–1757. doi:10.1016/j.cellsig.2009.07.010.

García-Gutiérrez MS, García-Bueno B, Zoppi S, Leza JC, Manzanares J. 2012. Chronic blockade of cannabinoid CB2 receptors induces anxiolytic-like actions associated with alterations in GABAA receptors. Br J Pharmacol. 165(4):951–964. doi:https://doi.org/10.1111/j.1476-5381.2011.01625.x.

van Gastel J, Hendrickx JO, Leysen H, Santos-Otte P, Luttrell LM, Martin B, Maudsley S. 2018. β-Arrestin Based Receptor Signaling Paradigms: Potential Therapeutic Targets for Complex Age-Related Disorders. Front Pharmacol. 9. doi:10.3389/fphar.2018.01369.

Gatley SJ, Lan R, Pyatt B, Gifford AN, Volkow ND, Makriyannis A. 1997. Binding of the non-classical cannabinoid CP 55,940, and the diarylpyrazole AM251 to rodent brain cannabinoid receptors. Life Sci. 61(14):PL191–PL197. doi:10.1016/S0024-3205(97)00690-5.

Gilman AG. 1987. G Proteins: Transducers of Receptor-Generated Signals. Annu Rev Biochem. 56(1):615–649. doi:10.1146/annurev.bi.56.070187.003151.

Glass M, Faull RLM, Dragunow M. 1997. Cannabinoid receptors in the human brain: a detailed anatomical and quantitative autoradiographic study in the fetal, neonatal and adult human brain. Neuroscience. 77(2):299–318. doi:10.1016/S0306-4522(96)00428-9.

Glass M, Felder CC. 1997. Concurrent Stimulation of Cannabinoid CB1 and Dopamine D2 Receptors Augments cAMP Accumulation in Striatal Neurons: Evidence for a G $_s$ Linkage to the CB1 Receptor. J Neurosci. 17(14):5327–5333. doi:10.1523/JNEUROSCI.17-14-05327.1997.

Gomes I, Ayoub MA, Fujita W, Jaeger WC, Pfleger KDG, Devi LA. 2016a. G Protein–Coupled Receptor Heteromers. Annu Rev Pharmacol Toxicol. 56:403–425. doi:10.1146/annurev-pharmtox-011613-135952.

Gomes I, Ayoub MA, Fujita W, Jaeger WC, Pfleger KDG, Devi LA. 2016b. G Protein–Coupled Receptor Heteromers. Annu Rev Pharmacol Toxicol. 56:403–425. doi:10.1146/annurev-pharmtox-011613-135952.

Gomes I, Jordan BA, Gupta A, Trapaidze N, Nagy V, Devi LA. 2000. Heterodimerization of μ and δ Opioid Receptors: A Role in Opiate Synergy. J Neurosci. 20(22):RC110. doi:10.1523/JNEUROSCI.20-22-j0007.2000.

Guo X, Wang H, Li Y, Leng X, Huang W, Ma Y, Xu T, Qi X. 2019. Transfection reagent Lipofectamine triggers type I interferon signaling activation in macrophages. Immunol Cell Biol. 97(1):92–96. doi:https://doi.org/10.1111/imcb.12194.

Gurevich VV, Gurevich EV. 2019. GPCR Signaling Regulation: The Role of GRKs and Arrestins. Front Pharmacol. 10. doi:10.3389/fphar.2019.00125.

Haack KKV, McCarty NA. 2011. Functional Consequences of GPCR Heterodimerization: GPCRs as Allosteric Modulators. Pharmaceuticals. 4(3):509–523. doi:10.3390/ph4030509.

Haga K, Haga T. 1992. Activation by G protein beta gamma subunits of agonist- or light-dependent phosphorylation of muscarinic acetylcholine receptors and rhodopsin. J Biol Chem. 267(4):2222–2227.

Hanuš L, Breuer A, Tchilibon S, Shiloah S, Goldenberg D, Horowitz M, Pertwee RG, Ross RA, Mechoulam R, Fride E. 1999. HU-308: A specific agonist for CB2, a peripheral cannabinoid receptor. Proc Natl Acad Sci. 96(25):14228–14233. doi:10.1073/pnas.96.25.14228.

Harden TK, Waldo GL, Hicks SN, Sondek J. 2011. Mechanism of Activation and Inactivation of Gq/Phospholipase C-β Signaling Nodes. Chem Rev. 111(10):6120. doi:10.1021/cr200209p.

Herkenham M, Lynn AB, Johnson MR, Melvin LS, Costa B de, Rice KC. 1991. Characterization and localization of cannabinoid receptors in rat brain: a

quantitative in vitro autoradiographic study. J Neurosci. 11(2):563–583. doi:10.1523/JNEUROSCI.11-02-00563.1991.

Hillard CJ, Manna S, Greenberg MJ, DiCamelli R, Ross RA, Stevenson LA, Murphy V, Pertwee RG, Campbell WB. 1999. Synthesis and Characterization of Potent and Selective Agonists of the Neuronal Cannabinoid Receptor (CB1). J Pharmacol Exp Ther. 289(3):1427–1433.

Hoffman AF, Laaris N, Kawamura M, Masino SA, Lupica CR. 2010. Control of Cannabinoid CB1 Receptor Function on Glutamate Axon Terminals by Endogenous Adenosine Acting at A1 Receptors. J Neurosci. 30(2):545–555. doi:10.1523/JNEUROSCI.4920-09.2010.

Hojo M, Sudo Y, Ando Y, Minami K, Takada M, Matsubara T, Kanaide M, Taniyama K, Sumikawa K, Uezono Y. 2008. μ-Opioid Receptor Forms a Functional Heterodimer With Cannabinoid CB1 Receptor: Electrophysiological and FRET Assay Analysis. J Pharmacol Sci. 108(3):308–319. doi:10.1254/jphs.08244FP.

Hopkins AL, Groom CR. 2002. The druggable genome. Nat Rev Drug Discov. 1(9):727–730. doi:10.1038/nrd892.

Howlett AC. 2002. International Union of Pharmacology. XXVII. Classification of Cannabinoid Receptors. Pharmacol Rev. 54(2):161–202. doi:10.1124/pr.54.2.161.

Hua T, Vemuri K, Nikas SP, Laprairie RB, Wu Y, Qu L, Pu M, Korde A, Jiang S, Ho J-H, *et al.* 2017. Crystal structures of agonist-bound human cannabinoid receptor CB 1. Nature. 547(7664):468–471. doi:10.1038/nature23272.

Hua T, Vemuri K, Pu M, Qu L, Han GW, Wu Y, Zhao S, Shui W, Li S, Korde A, *et al.* 2016. Crystal Structure of the Human Cannabinoid Receptor CB1. Cell. 167(3):750-762.e14. doi:10.1016/j.cell.2016.10.004.

Hudson BD, Hébert TE, Kelly ME. 2010. Physical and functional interaction between CB $_1$ cannabinoid receptors and β $_2$ -adrenoceptors: CB $_1$ /β $_2$ AR interactions. Br J Pharmacol. 160(3):627–642. doi:10.1111/j.1476-5381.2010.00681.x.

Ibsen MS, Connor M, Glass M. 2017. Cannabinoid CB1 and CB2 Receptor Signaling and Bias. Cannabis Cannabinoid Res. 2(1):48–60. doi:10.1089/can.2016.0037.

Ibsen MS, Finlay DB, Patel M, Javitch JA, Glass M, Grimsey NL. 2019. Cannabinoid CB1 and CB2 Receptor-Mediated Arrestin Translocation: Species, Subtype, and Agonist-Dependence. Front Pharmacol. 10. doi:10.3389/fphar.2019.00350.

Iiri T, Farfel Z, Bourne HR. 1998. G-protein diseases furnish a model for the turn-on switch. Nature. 394(6688):35–38. doi:10.1038/27831.

Jean-Charles P-Y, Kaur S, Shenoy SK. 2017. GPCR signaling via β-arrestin-dependent mechanisms. J Cardiovasc Pharmacol. 70(3):142–158. doi:10.1097/FJC.0000000000000482.

Jin W, Brown S, Roche JP, Hsieh C, Celver JP, Kovoor A, Chavkin C, Mackie K. 1999. Distinct domains of the CB1 cannabinoid receptor mediate desensitization and internalization. J Neurosci Off J Soc Neurosci. 19(10):3773–3780.

Jordan BA, Devi LA. 1999. G-protein-coupled receptor heterodimerization modulates receptor function. Nature. 399(6737):697–700. doi:10.1038/21441.

Kargl J, Balenga N, Parzmair GP, Brown AJ, Heinemann A, Waldhoer M. 2012. The Cannabinoid Receptor CB1 Modulates the Signaling Properties of the Lysophosphatidylinositol Receptor GPR55. J Biol Chem. 287(53):44234–44248. doi:10.1074/jbc.M112.364109.

Kearn CS. 2005. Concurrent Stimulation of Cannabinoid CB1 and Dopamine D2 Receptors Enhances Heterodimer Formation: A Mechanism for Receptor Cross-Talk? Mol Pharmacol. 67(5):1697–1704. doi:10.1124/mol.104.006882.

Kendall DA, Yudowski GA. 2017. Cannabinoid Receptors in the Central Nervous System: Their Signaling and Roles in Disease. Front Cell Neurosci. 10. doi:10.3389/fncel.2016.00294.

Kim MW, Wang W, Sanchez MI, Coukos R, von Zastrow M, Ting AY. Time-gated detection of protein-protein interactions with transcriptional readout. eLife. 6. doi:10.7554/eLife.30233.

Kirilly E, Hunyady L, Bagdy G. 2013. Opposing local effects of endocannabinoids on the activity of noradrenergic neurons and release of noradrenaline: relevance for their role in depression and in the actions of CB1 receptor antagonists. J Neural Transm. 120(1):177–186. doi:10.1007/s00702-012-0900-1.

Kohout TA, Lin F-T, Perry SJ, Conner DA, Lefkowitz RJ. 2001. β-Arrestin 1 and 2 differentially regulate heptahelical receptor signaling and trafficking. Proc Natl Acad Sci. 98(4):1601–1606. doi:10.1073/pnas.98.4.1601.

Komorowska-Müller JA, Schmöle A-C. 2020. CB2 Receptor in Microglia: The Guardian of Self-Control. Int J Mol Sci. 22(1). doi:10.3390/ijms22010019.

Kovacs JJ, Hara MR, Davenport CL, Kim J, Lefkowitz RJ. 2009. Arrestin Development: Emerging Roles for β-arrestins in Developmental Signaling Pathways. Dev Cell. 17(4):443–458. doi:10.1016/j.devcel.2009.09.011.

Krishna Kumar K, Shalev-Benami M, Robertson MJ, Hu H, Banister SD, Hollingsworth SA, Latorraca NR, Kato HE, Hilger D, Maeda S, *et al.* 2019. Structure of a Signaling Cannabinoid Receptor 1-G Protein Complex. Cell. 176(3):448-458.e12. doi:10.1016/j.cell.2018.11.040.

Kroeze WK, Sassano MF, Huang X-P, Lansu K, McCorvy JD, Giguere PM, Sciaky N, Roth BL. 2015. PRESTO-TANGO: an open-source resource for interrogation of the druggable human GPCR-ome. Nat Struct Mol Biol. 22(5):362–369. doi:10.1038/nsmb.3014.

Kruk-Slomka M, Dzik A, Budzynska B, Biala G. 2017. Endocannabinoid System: the Direct and Indirect Involvement in the Memory and Learning Processes—a Short Review. Mol Neurobiol. 54(10):8332–8347. doi:10.1007/s12035-016-0313-5.

Laprairie RB, Kelly MEM, Denovan-Wright EM. 2013. Cannabinoids increase type 1 cannabinoid receptor expression in a cell culture model of striatal neurons: Implications for Huntington's disease. Neuropharmacology. 72:47–57. doi:10.1016/j.neuropharm.2013.04.006.

Laroche G, Giguère PM. 2019. Measurement of β-Arrestin Recruitment at GPCRs Using the Tango Assay. In: Tiberi M, editor. G Protein-Coupled Receptor Signaling. Vol. 1947. New York, NY: Springer New York. (Methods in Molecular Biology). p. 257–267.

Lau T, Schloss P. 2008. The cannabinoid CB1 receptor is expressed on serotonergic and dopaminergic neurons. Eur J Pharmacol. 578(2):137–141. doi:10.1016/j.ejphar.2007.09.022.

Lavoie C, Mercier J-F, Salahpour A, Umapathy D, Breit A, Villeneuve L-R, Zhu W-Z, Xiao R-P, Lakatta EG, Bouvier M, *et al.* 2002. β1/β2-Adrenergic Receptor Heterodimerization Regulates β2-Adrenergic Receptor Internalization and ERK Signaling Efficacy. J Biol Chem. 277(38):35402–35410. doi:10.1074/jbc.M204163200.

van der Lee MMC, Blomenröhr M, van der Doelen AA, Wat JWY, Smits N, Hanson BJ, van Koppen CJ, Zaman GJR. 2009. Pharmacological Characterization of Receptor Redistribution and β-Arrestin Recruitment Assays for the Cannabinoid Receptor 1. J Biomol Screen. 14(7):811–823. doi:10.1177/1087057109337937.

Lefkowitz RJ, Shenoy SK. 2005. Transduction of Receptor Signals by ß-Arrestins. Science. 308(5721):512–517. doi:10.1126/science.1109237.

Lefkowitz RJ, Whalen EJ. 2004. β-arrestins: traffic cops of cell signaling. Curr Opin Cell Biol. 16(2):162–168. doi:10.1016/j.ceb.2004.01.001.

Li X, Hua T, Vemuri K, Ho J-H, Wu Y, Wu L, Popov P, Benchama O, Zvonok N, Locke K, *et al.* 2019. Crystal Structure of the Human Cannabinoid Receptor CB2. Cell. 176(3):459-467.e13. doi:10.1016/j.cell.2018.12.011.

Liu H, Tian Y, Ji B, Lu H, Xin Q, Jiang Y, Ding L, Zhang J, Chen J, Bai B. 2016. Heterodimerization of the kappa opioid receptor and neurotensin receptor 1 contributes to a novel β-arrestin-2–biased pathway. Biochim Biophys Acta BBA - Mol Cell Res. 1863(11):2719–2738. doi:10.1016/j.bbamcr.2016.07.009.

Liu X, Xu X, Hilger D, Aschauer P, Tiemann JKS, Du Y, Liu H, Hirata K, Sun X, Guixà-González R, *et al.* 2019. Structural Insights into the Process of GPCR-G Protein Complex Formation. Cell. 177(5):1243-1251.e12. doi:10.1016/j.cell.2019.04.021.

Lovinger DM. 2008. Presynaptic Modulation by Endocannabinoids. In: Südhof TC, Starke K, editors. Pharmacology of Neurotransmitter Release. Berlin, Heidelberg: Springer. (Handbook of Experimental Pharmacology). p. 435–477.

Luttrell LM, Daaka Y, Della Rocca GJ, Lefkowitz RJ. 1997. G Protein-coupled Receptors Mediate Two Functionally Distinct Pathways of Tyrosine Phosphorylation in Rat 1a Fibroblasts. J Biol Chem. 272(50):31648–31656. doi:10.1074/jbc.272.50.31648.

Lutz B. 2002. Molecular biology of cannabinoid receptors. Prostaglandins Leukot Essent Fat Acids PLEFA. 66(2–3):123–142. doi:10.1054/plef.2001.0342.

Mafi A, Kim S-K, Goddard WA. 2020. Mechanism of β-arrestin recruitment by the μ-opioid G protein-coupled receptor. Proc Natl Acad Sci. 117(28):16346–16355. doi:10.1073/pnas.1918264117.

Margeta-Mitrovic M, Jan YN, Jan LY. 2000. A Trafficking Checkpoint Controls GABAB Receptor Heterodimerization. Neuron. 27(1):97–106. doi:10.1016/S0896-6273(00)00012-X.

Martínez-Pinilla E, Reyes-Resina I, Oñatibia-Astibia A, Zamarbide M, Ricobaraza A, Navarro G, Moreno E, Dopeso-Reyes IG, Sierra S, Rico AJ, *et al.* 2014. CB1 and GPR55 receptors are co-expressed and form heteromers in rat and monkey striatum. Exp Neurol. 261:44–52. doi:10.1016/j.expneurol.2014.06.017.

Marzo VD, Bifulco M, Petrocellis LD. 2004. The endocannabinoid system and its therapeutic exploitation. Nat Rev Drug Discov. 3(9):771–784. doi:10.1038/nrd1495.

Masters SB, Miller RT, Chi MH, Chang FH, Beiderman B, Lopez NG, Bourne HR. 1989. Mutations in the GTP-binding site of GS alpha alter stimulation of adenylyl cyclase. J Biol Chem. 264(26):15467–15474.

Mato S, Del Olmo E, Pazos A. 2003. Ontogenetic development of cannabinoid receptor expression and signal transduction functionality in the human brain: Ontogeny of CB_1 receptors in human brain. Eur J Neurosci. 17(9):1747–1754. doi:10.1046/j.1460-9568.2003.02599.x.

Matsuda LA, Lolait SJ, Brownstein MJ, Young AC, Bonner TI. 1990. Structure of a cannabinoid receptor and functional expression of the cloned cDNA. Nature. 346(6284):561–564. doi:10.1038/346561a0.

McAllister SD, Rizvi G, Anavi-Goffer S, Hurst DP, Barnett-Norris J, Lynch DL, Reggio PH, Abood ME. 2003. An Aromatic Microdomain at the Cannabinoid CB $_1$ Receptor Constitutes an Agonist/Inverse Agonist Binding Region. J Med Chem. 46(24):5139–5152. doi:10.1021/jm0302647.

Mecha M, Carrillo-Salinas FJ, Feliú A, Mestre L, Guaza C. 2016. Microglia activation states and cannabinoid system: Therapeutic implications. Pharmacol Ther. 166:40–55. doi:10.1016/j.pharmthera.2016.06.011.

Moreno E, Chiarlone A, Medrano M, Puigdellívol M, Bibic L, Howell LA, Resel E, Puente N, Casarejos MJ, Perucho J, *et al.* 2018. Singular Location and Signaling Profile of Adenosine A 2A -Cannabinoid CB 1 Receptor Heteromers in the Dorsal Striatum. Neuropsychopharmacology. 43(5):964–977. doi:10.1038/npp.2017.12.

Mores KL, Cassell RJ, van Rijn RM. 2019. Arrestin recruitment and signaling by G protein-coupled receptor heteromers. Neuropharmacology. 152:15–21. doi:10.1016/j.neuropharm.2018.11.010.

Munro S, Thomas KL, Abu-Shaar M. 1993. Molecular characterization of a peripheral receptor for cannabinoids. Nature. 365(6441):61–65. doi:10.1038/365061a0.

Murphy T, Le Foll B. 2020. Targeting the Endocannabinoid CB1 Receptor to Treat Body Weight Disorders: A Preclinical and Clinical Review of the Therapeutic Potential of Past and Present CB1 Drugs. Biomolecules. 10(6). doi:10.3390/biom10060855.

Navarrete F, Pérez-Ortiz JM, Manzanares J. 2012. Cannabinoid CB2 receptor-mediated regulation of impulsive-like behaviour in DBA/2 mice. Br J Pharmacol. 165(1):260–273. doi:https://doi.org/10.1111/j.1476-5381.2011.01542.x.

Navarro G, Borroto-Escuela D, Angelats E, Etayo Í, Reyes-Resina I, Pulido-Salgado M, Rodríguez-Pérez AI, Canela EI, Saura J, Lanciego JL, *et al.* 2018. Receptor-heteromer mediated regulation of endocannabinoid signaling in activated microglia. Role of CB1 and CB2 receptors and relevance for Alzheimer's disease and levodopa-induced dyskinesia. Brain Behav Immun. 67:139–151. doi:10.1016/j.bbi.2017.08.015.

Navarro G, Carriba P, Gandí J, Ciruela F, Casadó V, Cortés A, Mallol J, Canela EI, Lluis C, Franco R. 2008. Detection of Heteromers Formed by Cannabinoid CB $_1$, Dopamine D $_2$, and Adenosine A $_{2A}$ G-Protein-Coupled Receptors by Combining Bimolecular Fluorescence Complementation and Bioluminescence Energy Transfer. Sci World J. 8:1088–1097. doi:10.1100/tsw.2008.136.

Navarro G, Morales P, Rodríguez-Cueto C, Fernández-Ruiz J, Jagerovic N, Franco R. 2016. Targeting Cannabinoid CB2 Receptors in the Central Nervous System. Medicinal Chemistry Approaches with Focus on Neurodegenerative Disorders. Front Neurosci. 10. doi:10.3389/fnins.2016.00406.

Navarro G, Reyes-Resina I, Rivas-Santisteban R, Sánchez de Medina V, Morales P, Casano S, Ferreiro-Vera C, Lillo A, Aguinaga D, Jagerovic N, *et al.* 2018. Cannabidiol skews biased agonism at cannabinoid CB1 and CB2 receptors with smaller effect in CB1-CB2 heteroreceptor complexes. Biochem Pharmacol. 157:148–158. doi:10.1016/j.bcp.2018.08.046.

Navarro G, Varani K, Lillo A, Vincenzi F, Rivas-Santisteban R, Raïch I, Reyes-Resina I, Ferreiro-Vera C, Borea PA, Sánchez de Medina V, *et al.* 2020. Pharmacological data of cannabidiol- and cannabigerol-type phytocannabinoids acting on cannabinoid CB1, CB2 and CB1/CB2 heteromer receptors. Pharmacol Res. 159:104940. doi:10.1016/j.phrs.2020.104940.

Noor N, Patel CB, Rockman HA. 2011. β-arrestin: a signaling molecule and potential therapeutic target for heart failure. J Mol Cell Cardiol. 51(4):534–541. doi:10.1016/j.yjmcc.2010.11.005.

de Oliveira Alvares L, Pasqualini Genro B, Vaz Breda R, Pedroso MF, Costa Da Costa J, Quillfeldt JA. 2006. AM251, a selective antagonist of the CB1 receptor, inhibits the induction of long-term potentiation and induces retrograde amnesia in rats. Brain Res. 1075(1):60–67. doi:10.1016/j.brainres.2005.11.101.

Pandey R, Mousawy K, Nagarkatti M, Nagarkatti P. 2009. Endocannabinoids and immune regulation. Pharmacol Res Off J Ital Pharmacol Soc. 60(2):85–92. doi:10.1016/j.phrs.2009.03.019.

Parenty G, Appelbe S, Milligan G. 2008. CXCR2 chemokine receptor antagonism enhances DOP opioid receptor function via allosteric regulation of the CXCR2–DOP receptor heterodimer. Biochem J. 412(Pt 2):245–256. doi:10.1042/BJ20071689.

Paronis CA, Nikas SP, Shukla VG, Makriyannis A. 2012. Δ(9)-Tetrahydrocannabinol acts as a partial agonist/antagonist in mice. Behav Pharmacol. 23(8):802–805. doi:10.1097/FBP.0b013e32835a7c4d.

Perry SJ, Baillie GS, Kohout TA, McPhee I, Magiera MM, Ang KL, Miller WE, McLean AJ, Conti M, Houslay MD, *et al.* 2002. Targeting of Cyclic AMP Degradation to β2-Adrenergic Receptors by β-Arrestins. Science. 298(5594):834–836. doi:10.1126/science.1074683.

Pertwee R, Griffin G, Fernando S, Li X, Hill A, Makriyannis A. 1995. AM630, a competitive cannabinoid receptor antagonist. Life Sci. 56(23):1949–1955. doi:10.1016/0024-3205(95)00175-6.

Pertwee RG. 2005. Pharmacological Actions of Cannabinoids. In: Pertwee Roger G., editor. Cannabinoids. Vol. 168. Berlin/Heidelberg: Springer-Verlag. p. 1–51.

Pertwee RG. 2006. The pharmacology of cannabinoid receptors and their ligands: an overview. Int J Obes. 30(1):S13–S18. doi:10.1038/sj.ijo.0803272.

Pertwee RG. 2015. Endocannabinoids and Their Pharmacological Actions. In: Pertwee RG, editor. Endocannabinoids. Vol. 231. Cham: Springer International Publishing. p. 1–37.

Pertwee RG, Howlett AC, Abood ME, Alexander SPH, Di Marzo V, Elphick MR, Greasley PJ, Hansen HS, Kunos G, Mackie K, *et al.* 2010. International Union of Basic and Clinical Pharmacology. LXXIX. Cannabinoid Receptors and Their Ligands: Beyond CB1 and CB2. Pharmacol Rev. 62(4):588–631. doi:10.1124/pr.110.003004.

Pezzoli D, Guipponi E, Mantovani D, Candiani G. 2017. Size matters for *in vitro* gene delivery: investigating the relationships among complexation protocol, transfection medium, size and sedimentation. *Sci Rep* **7,** 44134. doi:10.1038/srep44134

Pierce KL, Lefkowitz RJ. 2001. Classical and new roles of β-arrestins in the regulation of G-Protein Coupled receptors. Nat Rev Neurosci. 2(10):727–733. doi:10.1038/35094577.

Pierce KL, Premont RT, Lefkowitz RJ. 2002. Seven-transmembrane receptors. Nat Rev Mol Cell Biol. 3(9):639–650. doi:10.1038/nrm908.

Pirkmajer S, Chibalin AV. 2011. Serum starvation: *caveat emptor*. Am J Physiol-Cell Physiol. 301(2):C272–C279. doi:10.1152/ajpcell.00091.2011.

Przybyla JA, Watts VJ. 2010. Ligand-Induced Regulation and Localization of Cannabinoid CB1 and Dopamine D2L Receptor Heterodimers. J Pharmacol Exp Ther. 332(3):710–719. doi:10.1124/jpet.109.162701.

Pertwee RP. 1999. Pharmacology of Cannabinoid Receptor Ligands. Current Medicinal Chemistry. Bentham Science Publishers. (6):635-664

Ramírez BG, Blázquez C, del Pulgar TG, Guzmán M, de Ceballos ML. 2005. Prevention of Alzheimer's Disease Pathology by Cannabinoids: Neuroprotection Mediated by Blockade of Microglial Activation. J Neurosci. 25(8):1904–1913. doi:10.1523/JNEUROSCI.4540-04.2005.

Recent Advances in Structure-Based Drug Design Targeting Class A G Protein-Coupled Receptors Utilizing Crystal Structures and Computational Simulations | Journal of Medicinal Chemistry.

Receptor-receptor interactions in the central nervous system. A new integrative mechanism in synapses - Fuxe - 1985 - Medicinal Research Reviews - Wiley Online Library.

Repele A, Manu. 2019. Robust Normalization of Luciferase Reporter Data. Methods Protoc. 2(3). doi:10.3390/mps2030062.

Rios C, Gomes I, Devi LA. 2009. μ opioid and CB1 cannabinoid receptor interactions: reciprocal inhibition of receptor signaling and neuritogenesis: Opioid-cannabinoid interactions. Br J Pharmacol. 148(4):387–395. doi:10.1038/sj.bjp.0706757.

Rodríguez JJ, Mackie K, Pickel VM. 2001. Ultrastructural Localization of the CB1 Cannabinoid Receptor in μ-Opioid Receptor Patches of the Rat Caudate Putamen Nucleus. J Neurosci. 21(3):823–833. doi:10.1523/JNEUROSCI.21-03-00823.2001.

Ross RA, Brockie HC, Stevenson LA, Murphy VL, Templeton F, Makriyannis A, Pertwee RG. 1999. Agonist-inverse agonist characterization at CB1 and CB2 cannabinoid receptors of L759633, L759656 and AM630. Br J Pharmacol. 126(3):665–672. doi:https://doi.org/10.1038/sj.bjp.0702351.

Rozenfeld R, Devi LA. 2007. Receptor heterodimerization leads to a switch in signaling: β-arrestin2-mediated ERK activation by μ-δ opioid receptor heterodimers. FASEB J Off Publ Fed Am Soc Exp Biol. 21(10):2455–2465. doi:10.1096/fj.06-7793com.

Rozenfeld R, Gupta A, Gagnidze K, Lim MP, Gomes I, Lee-Ramos D, Nieto N, Devi LA. 2011. AT1R–CB1R heteromerization reveals a new mechanism for the pathogenic properties of angiotensin II. EMBO J. 30(12):2350–2363. doi:10.1038/emboj.2011.139.

Sánchez-Zavaleta R, Cortés H, Avalos-Fuentes JA, García U, Segovia Vila J, Erlij D, Florán B. 2018. Presynaptic cannabinoid CB2 receptors modulate [3 H]-Glutamate release at subthalamo-nigral terminals of the rat. Synap N Y N. 72(11):e22061. doi:10.1002/syn.22061.

Schurman LD, Lichtman AH. 2017. Endocannabinoids: A Promising Impact for Traumatic Brain Injury. Front Pharmacol. 8:69. doi:10.3389/fphar.2017.00069.

Seifert R, Wenzel-Seifert K. 2002. Constitutive activity of G-protein-coupled receptors: cause of disease and common property of wild-type receptors. Naunyn Schmiedebergs Arch Pharmacol. 366(5):381–416. doi:10.1007/s00210-002-0588-0.

Seyedabadi M, Ghahremani MH, Albert PR. 2019. Biased signaling of G protein coupled receptors (GPCRs): Molecular determinants of GPCR/transducer selectivity and therapeutic potential. Pharmacol Ther. 200:148–178. doi:10.1016/j.pharmthera.2019.05.006.

Sharkey KA, Darmani NA, Parker LA. 2014. Regulation of nausea and vomiting by cannabinoids and the endocannabinoid system. Eur J Pharmacol. 722. doi:10.1016/j.ejphar.2013.09.068.

Shenglong Zou, Ujendra Kumar. 2018. Cannabinoid Receptors and the Endocannabinoid System: Signaling and Function in the Central Nervous System. Int J Mol Sci. 19(3):833. doi:10.3390/ijms19030833.

Showalter M, Compton R, Martin A, Abood E. 1996. Evaluation of Binding in a Transfected Cell Line Expressing a Peripheral Cannabinoid Receptor (CB2): Identification of Cannabinoid Receptor Subtype Selective Ligands. 278:11.

Sierra S, Gupta A, Gomes I, Fowkes M, Ram A, Bobeck EN, Devi LA. 2019. Targeting Cannabinoid 1 and Delta Opioid Receptor Heteromers Alleviates Chemotherapy-Induced Neuropathic Pain. ACS Pharmacol Transl Sci. 2(4):219–229. doi:10.1021/acsptsci.9b00008.

Sierra S, Luquin N, Rico AJ, Gómez-Bautista V, Roda E, Dopeso-Reyes IG, Vázquez A, Martínez-Pinilla E, Labandeira-García JL, Franco R, *et al.* 2015. Detection of cannabinoid receptors CB1 and CB2 within basal ganglia output neurons in macaques: changes following experimental parkinsonism. Brain Struct Funct. 220(5):2721–2738. doi:10.1007/s00429-014-0823-8.

Singh J, Song Z-H, Reggio PH. 2012. Structure of a Cannabinoid Receptor Subtype 2 Homodimer Determined by Cysteine and Homobifunctional Crosslinking Experiments Combined with Computational Studies. Biophys J. 102(3):244a. doi:10.1016/j.bpj.2011.11.1344.

Smith NJ, Milligan G. 2010. Allostery at G Protein-Coupled Receptor Homo- and Heteromers: Uncharted Pharmacological Landscapes. Pharmacol Rev. 62(4):701–725. doi:10.1124/pr.110.002667.

Sorkin A, Zastrow M von. 2002. Signal transduction and endocytosis: close encounters of many kinds. Nat Rev Mol Cell Biol. 3(8):600–614. doi:10.1038/nrm883.

Sriram K, Insel PA. 2018. G Protein-Coupled Receptors as Targets for Approved Drugs: How Many Targets and How Many Drugs? Mol Pharmacol. 93(4):251–258. doi:10.1124/mol.117.111062.

Stella N, Schweitzer P, Piomelli D. 1997. A second endogenous cannabinoid that modulates long-term potentiation. Nature. 388(6644):773–778. doi:10.1038/42015.

Stempel AV, Stumpf A, Zhang H-Y, Özdoğan T, Pannasch U, Theis A-K, Otte D-M, Wojtalla A, Rácz I, Ponomarenko A, *et al.* 2016. Cannabinoid Type 2 Receptors Mediate a Cell Type-Specific Plasticity in the Hippocampus. Neuron. 90(4):795–809. doi:10.1016/j.neuron.2016.03.034.

Sugiura T, Kondo S, Sukagawa A, Nakane S, Shinoda A, Itoh K, Yamashita A, Waku K. 1995. 2-Arachidonoylglycerol: a possible endogenous cannabinoid receptor ligand in brain. Biochem Biophys Res Commun. 215(1):89–97. doi:10.1006/bbrc.1995.2437.

Suzuki N, Hajicek N, Kozasa T. 2009. Regulation and Physiological Functions of G12/13-Mediated Signaling Pathways. Neurosignals. 17(1):55–70. doi:10.1159/000186690.

Syrovatkina V, Alegre KO, Dey R, Huang X-Y. 2016. Regulation, Signaling and Physiological Functions of G-proteins. J Mol Biol. 428(19):3850–3868. doi:10.1016/j.jmb.2016.08.002.

Szabo B, Siemes S, Wallmichrath I. 2002. SHORT COMMUNICATION Inhibition of GABAergic neurotransmission in the ventral tegmental area by cannabinoids. Eur J Neurosci. 15(12):2057–2061. doi:https://doi.org/10.1046/j.1460-9568.2002.02041.x.

Taussig R, Iniguez-Lluhi JA, Gilman AG. 1993. Inhibition of adenylyl cyclase by Gi alpha. Science. 261(5118):218–221. doi:10.1126/science.8327893.

Manira AE, Kyriakatos. 2010. The Role of Endocannabinoid Signaling in Motor Control. Physiology (Bethesda). 25(4):230-8. doi:10.1152/physiol.00007.2010.

Trifilieff P, Rives M-L, Urizar E, Piskorowski RA, Vishwasrao HD, Castrillon J, Schmauss C, Slättman M, Gullberg M, Javitch JA. 2011. Detection of antigen interactions ex vivo by proximity ligation assay: endogenous dopamine D2-adenosine A2A receptor complexes in the striatum. BioTechniques. 51(2):111–118. doi:10.2144/000113719.

Tzavara ET, Davis RJ, Perry KW, Li X, Salhoff C, Bymaster FP, Witkin JM, Nomikos GG. 2003. The CB1 receptor antagonist SR141716A selectively increases monoaminergic neurotransmission in the medial prefrontal cortex: implications for therapeutic actions. Br J Pharmacol. 138(4):544–553. doi:10.1038/sj.bjp.0705100.

Van Sickle MD. 2005. Identification and Functional Characterization of Brainstem Cannabinoid CB2 Receptors. Science. 310(5746):329–332. doi:10.1126/science.1115740.

Viñals X, Moreno E, Lanfumey L, Cordomí A, Pastor A, de La Torre R, Gasperini P, Navarro G, Howell LA, Pardo L, *et al.* 2015. Cognitive Impairment Induced by Delta9-tetrahydrocannabinol Occurs through Heteromers between Cannabinoid CB1 and Serotonin 5-HT2A Receptors. Nestler EJ, editor. PLOS Biol. 13(7):e1002194. doi:10.1371/journal.pbio.1002194.

Vischer HF, Watts AO, Nijmeijer S, Leurs R. 2011. G protein-coupled receptors: walking hand-in-hand, talking hand-in-hand? Br J Pharmacol. 163(2):246–260. doi:10.1111/j.1476-5381.2011.01229.x.

Viscomi MT, Oddi S, Latini L, Pasquariello N, Florenzano F, Bernardi G, Molinari M, Maccarrone M. 2009. Selective CB2 Receptor Agonism Protects Central Neurons

from Remote Axotomy-Induced Apoptosis through the PI3K/Akt Pathway. J Neurosci. 29(14):4564–4570. doi:10.1523/JNEUROSCI.0786-09.2009.

Waksman Y, Olson JM, Carlisle SJ, Cabral GA. 1999. The Central Cannabinoid Receptor (CB1) Mediates Inhibition of Nitric Oxide Production by Rat Microglial Cells. J Pharmacol Exp Ther. 288(3):1357–1366.

Wallmichrath I, Szabo B. 2002. Cannabinoids inhibit striatonigral GABAergic neurotransmission in the mouse. Neuroscience. 113(3):671–682. doi:10.1016/S0306-4522(02)00109-4.

Wang T, Li Z, Cvijic ME, Krause C, Zhang L, Sum CS. 2004. Measurement of β-Arrestin Recruitment for GPCR Targets. In: Markossian S, Sittampalam GS, Grossman A, Brimacombe K, Arkin M, Auld D, Austin CP, Baell J, Caaveiro JMM, Chung TDY, *et al.*, editors. Assay Guidance Manual. Bethesda (MD): Eli Lilly & Company and the National Center for Advancing Translational Sciences.

Ward RJ, Pediani JD, Milligan G. 2011. Heteromultimerization of Cannabinoid CB1 Receptor and Orexin OX1 Receptor Generates a Unique Complex in Which Both Protomers Are Regulated by Orexin A. J Biol Chem. 286(43):37414–37428. doi:10.1074/jbc.M111.287649.

Wettschureck N, Offermanns S. 2005. Mammalian G Proteins and Their Cell Type Specific Functions. Physiol Rev. 85(4):1159–1204. doi:10.1152/physrev.00003.2005.

White JH, Wise A, Main MJ, Green A, Fraser NJ, Disney GH, Barnes AA, Emson P, Foord SM, Marshall FH. 1998. Heterodimerization is required for the formation of a functional GABA(B) receptor. Nature. 396(6712):679–682. doi:10.1038/25354.

Wisler JW, Rockman HA, Lefkowitz RJ. 2018. Biased G protein-coupled receptor signaling: Changing the paradigm of drug discovery. Circulation. 137(22):2315–2317. doi:10.1161/CIRCULATIONAHA.117.028194.

Yang Z, Yang F, Zhang D, Liu Z, Lin A, Liu C, Xiao P, Yu X, Sun J-P. 2017. Phosphorylation of G Protein-Coupled Receptors: From the Barcode Hypothesis to the Flute Model. Mol Pharmacol. 92(3):201–210. doi:10.1124/mol.116.107839.

Yin J, Chen K-YM, Clark MJ, Hijazi M, Kumari P, Bai X-C, Sunahara RK, Barth P, Rosenbaum DM. 2020. Structure of a D2 dopamine receptor-G-protein complex in a lipid membrane. Nature. 584(7819):125–129. doi:10.1038/s41586-020-2379-5.

Zhang null, Chung null, Oldenburg null. 1999. A Simple Statistical Parameter for Use in Evaluation and Validation of High Throughput Screening Assays. J Biomol Screen. 4(2):67–73. doi:10.1177/108705719900400206.

Zhang J-H, Oldenburg KR. 2009. Z-Factor. In: Schwab M, editor. Encyclopedia of Cancer. Berlin, Heidelberg: Springer. p. 3227–3228.

Zou S, Somvanshi RK, Kumar U. 2017. Somatostatin receptor 5 is a prominent regulator of signaling pathways in cells with coexpression of Cannabinoid receptors 1. Neuroscience. 340:218–231. doi:10.1016/j.neuroscience.2016.10.056.